AN EXPERIMENTAL STUDY OF COHESION AND FRICTION DURING CREEP IN SATURATED CLAY

By

Robert Glenn Bea

A Thesis Presented to the Graduate Council of the University of Florida
in Partial Fulfillment of the Requirements for the Degree of
Master of Science in Engineering

UNIVERSITY OF FLORIDA

June, 1960

Abstract of Thesis Presented to the Graduate Council in Partial Fulfillment of the Requirements for the Degree of Master of Science in Engineering

AN EXPERIMENTAL STUDY OF COHESION AND FRICTION DURING CREEP IN SATURATED CLAY

By

Robert Glenn Bea

June, 1960

This thesis undertakes a study of the creep phenomenon and its influence on the strength of saturated clay. Saturated clay specimens were first ~~triaxially~~ hydrostatically consolidated and then, permitting no further drainage, were subjected to constant loads. Subsequently the samples were tested to determine the effect of creep on the cohesion-friction-strain behavior.

The experimental results show that during creep there is a transfer of stress to the frictional component of strength. Evidence is collected which suggests that a clay may exhibit an apparent negative cohesion.

ACKNOWLEDGMENTS

The writer wishes to express his sincere appreciation to Professor John H. Schmertmann for suggesting this thesis problem and for supervising the study. He is indebted to Professor Schmertmann for his interest in the investigation, timely advice and encouragement, and for generously providing the writer with the experimental procedures and testing equipment which were essential to this study.

The writer is grateful to all those persons who aided him in the conduct of this investigation and who offered suggestions for the preparation of this manuscript. The help of Mr. John R. Hall, Jr., graduate research assistant in the University of Florida Soil Mechanics Research Laboratory, in the preparation of the clay samples and in mastering the testing technique is gratefully acknowledged.

Appreciation is expressed to Dr. F. E. Richart, Jr., Professor W. H. Zimpfer, and to the members of the Graduate Supervisory Committee for their interest and helpful suggestions.

TABLE OF CONTENTS

LIST OF FIGURES

LIST OF TABLES

NOTATIONS

c - Cohesion, as defined in this paper

c_ϵ - Cohesion at strain ϵ

u - Pore water pressure, as measured by a piezometer

t_c - Time allowed for consolidation

ϵ - Axial compressive strain

σ - Normal stress

$\bar{\sigma}$ - Normal intergranular stress

σ_h - Triaxial cell pressure

σ_1 - Major principal stress

$\bar{\sigma}_1$ - Major principal intergranular stress

σ_3 - Minor principal stress

$\bar{\sigma}_3$ - Minor principal intergranular stress

σ_d - Deviator stress, applied axially by piston

$\bar{\sigma}_{pct}$ - Hydrostatic, triaxial preconsolidation pressure

τ - Shear stress

ϕ - Angle of internal friction, as defined in this paper

ϕ_ϵ - Angle of internal friction at strain ϵ

SECTION I

INTRODUCTION

The almost imperceptible movement of soil down slopes, the gradual increase in pressure on tunnel and retaining walls, the secondary compression of soils, and the variation of stress distribution in a soil with time are a few of the instances in which the phenomenon of creep requires serious consideration in foundation engineering and design. Consequently, it is important for the engineer to have knowledge of the creep characteristics and their influence on the soils with which he has to work.

The phenomenon of creep, which is the slow movement or change in the shape of a material in the direction of a constant or varying stress which is applied over a long period of time, is very common. When a piece of steel is subjected to a stress over a long period of time and at elevated temperature it will slowly flow or deform. When concrete is subjected to high compressive stress it tends to creep and thus relieve the stress. The thickening of large glass store-fronts at the bottom and the slow bending or flow of wax candles during hot summer days are additional illustrations of creep action.

True creep is viscous in nature; thus, the movement or change in shape will not only be a function of the stresses applied but also a function of time, the material characteristics, and the environment.

Plastic flow and relaxation are other types of creep action. If a plastic substance is subjected to a shearing strain which is then held constant the shearing stresses slowly diminish. This is the phenomenon of relaxation. Plastic flow is merely a short-time creep action.

Since creep is primarily viscous in nature, it is the clays and clay-soils which exhibit the creep phenomenon. The creep characteristics of these soils are important in many phases of soil mechanics and foundation engineering; however, little work has been done to determine these characteristics or their influence on the strength of the soil. Some theoretical and experimental investigations into the creep, plastic flow, and relaxation phenomena in clays have been made; the bulk of the research having been done in the fields of rheology and ceramics. Terzaghi (53)* has stated that because of the remarkable diversity of creep phenomena and their practical implications, creep research is a very promising field, and thus far the field has hardly been explored.

Purpose of This Investigation

In an attempt to supplement the limited information on creep action and its influence on cohesive soils, this investigation was undertaken. A review is given of the work done to the present time (1960) on the creep action in soils and in some of the other common engineering materials.

The experimental study is divided into three parts: First

---

*Numbers in parentheses refer to references listed at the end of this paper.

and primarily, it is a study of how creep action will influence the strength components, cohesion and friction, of a near saturated clay; the second and third phases of the investigation are concerned with the creep characteristics and the pore water pressure variation during creep.

Scope of This Investigation

Two different clay soils and two types of samples were used in this investigation. These included both remolded and undisturbed samples of Boston Blue Clay as well as remolded samples of Kaolinite Clay. The testing samples were 8.00 cm in height and 3.59 cm in diameter.

The research equipment basically consists of a triaxial compression testing machine, associated pore pressure measuring equipment, a bank of triaxial cell chambers, and a bank of creep-loading racks.

The experimental program was divided into two groups of tests. The first group consists of a series of tests to determine the variation of cohesion and friction with strain in the samples not subjected to creep action. These tests will be termed standard CFS-tests. The separation of the strength components was accomplished by using a recently developed laboratory technique, the CFS-test (47), which will be discussed and described in the following sections of this paper. The details of this standard series of tests and the figures in which the experimental data are shown are given in Table 1.

The second group of tests consists of what will be termed creep-strength tests. During the first phase of this test, the creep phase, the hydrostatically consolidated sample was subjected to a constant load,

permitting no drainage, for a given period of time. Measurements were taken of axial compression, pore water pressure and time. All of the creep tests were performed at constant water content. No attempt was made to alter pore water pressure so as to maintain constant volume. In the second phase, the strength phase, the sample was tested using the CFS-test technique. This was done to determine the influence of creep action on the cohesion-friction-strain (CFS) characteristics of the sample.

The creep-strength tests generally were performed on a group of three specimens. These groups will be given test series designations: A, B, C, D, and E. The details of the test series and the figures in which the experimental data are shown are given in Table 2.

TABLE 1

STANDARD CFS-TEST SUMMARY

Test	Sample Type	Sample No.	Strain Rate 10^{-3} mm/min	$\bar{\sigma}$ pct	Test Time min	Figure No.
B-1	DWEPK	751	5	3.65	1,461	page (71) 15
H-13	DWEPK	799	5	3.65	1,560	(73) 16
B-5	BBC	521	5	3.65	740	(76) 20
H-22	BBC	539	5	3.65	1,565	(77) 21
B-18	BBC	532	1.5	3.65	11,340	(83) 26
B-12	BBC	528	1.5	3.65	770	(81) 25
S-91	U-BBC	R-4	5	4.00	906	(86) 30

failure observed on open drainage secondary ?

TABLE 2

CREEP--STRENGTH TEST SUMMARY

Test Series	Test No.	Sample Type	Creep Load kg	Creep Period days	Experimental Data Figures			
					Stress-Strain & Comp. Results		Creep Curves	u/t Curves
	B-2	DWEPK	11.0	9	17	73		
A	B-3	DWEPK	16.6	10	18	79	36	40
	B-4	DWEPK	20.0	11	19	75		
	B-6	BBC	11.0	19	22	78		
B	B-7	BBC	16.6	19	23	79	37	42
	B-8	BBC	19.0	19	24	80		
	B-9	BBC	19.2	18	27	83		
C	B-10	BBC	19.2	2	28	84	38	43
	B-11	BBC	19.2	9	29	85		
D	B-13	U-BBC	19.2	11	31	87	39	44
	B-14	U-BBC	19.2	3	32	88		
	B-15	BBC	38.3	17	33	89		
E	B-16	BBC	26.3	19	34	90	40	45
	B-17	DWEPK	36.2	19	35	91		

SECTION II

REVIEW OF PREVIOUS WORK

A considerable amount of research has been done to determine the creep characteristics of metals, concrete, and other engineering materials. This review will not only summarize what is known concerning the creep phenomenon in soils but also our present knowledge of the creep characteristics of metals, concrete, and plastics. The reason for briefly studying these other materials lies in the fact that this knowledge can act as a good guide for possible further study of the creep phenomenon in soils. As this review is developed it will be noted that there are many striking similarities in the creep behavior and characteristics of these different materials.

The Creep Characteristics of Metals

A large amount of research has been done to determine the creep characteristics of metals at elevated temperatures. McVetty (29) describes creep as the gradual deformation or flow of a material in the direction of an applied stress usually over a long period of time and at elevated temperature. This definition embodies four important considerations: Plastic deformation, stresses which are usually considerably below the yield strength, long period of time, and elevated temperatures.

The creep test of a metal specimen consists of subjecting the

specimen to a constant stress and an elevated temperature. The resulting deformations are measured as a function of time. Thus, there are four variables to be considered in the creep test: Stress, strain, time, and temperature.

While studying the results of the usual tensile creep test of a metal there are two basic processes to be kept in mind: The first is the strain hardening of the metal due to plastic strains; the second is the removal of this hardening due to the elevated temperatures acting over a long period of time. The strain hardening phenomenon in metals is believed due to the orientation of the grains in a position more favorable for resisting the applied stresses. Thus, the strain hardening is due to a plastic deformation of the material; but, in all cases where part of the material undergoes plastic deformation it becomes harder and its ductility is greatly reduced. Strain hardening has the effect of inducing residual stresses in the crystals of the material so that if the stress is reversed these residual stresses combine with the reversed stress and produce a premature yielding. This reduction of the ability of the material to resist loads in the reversed direction is known as the "Bauschinger Effect" (31).

When a plot is made of the data obtained in a tensile creep test, as shown in Figure 1, page 16, it is readily noted that the creep curve is divided into three main stages. The first stage, termed the initial elastic adjustment stage, is characterized by a very high time-rate of straining. However, this rate soon decreases due to the strain hardening effect and continues to decrease until the second

stage is reached. During this second stage, termed the visco-plastic stage, the rate of creep remains almost constant. This is believed to be due to the balance between the strain hardening and temperature effects, i.e., the hardening effect is destroyed at a uniform rate by the softening effect of the high temperature. This second stage continues at essentially a constant rate depending on the stress and temperature. As soon as the third stage is reached the specimen necks down and there is a greatly increased strain rate until fracture. In this third stage of creep action the grain boundaries gradually break up because of the effects of the long period of loading at high temperature. During a compression creep test the failure or third stage of creep generally is not obtained due to the increase in cross section of the specimen with strain.

A strong metal may creep for several years at a constant rate; thus, the time required for performing a creep test over these three stages is often very great. In order to make data on new materials readily available various extrapolation procedures have been devised for short-time creep test results. One of the simplest and one that is generally satisfactory is suggested by McVetty (29). He recommends that each creep curve in the second stage be replaced for the purpose of extrapolation by a straight line having the equation: $E = Eo + Vt$, where E is the final plastic deformation at the time t, Eo is the initial adjustment, and V is the creep rate or slope of the line in the second stage of creep action. Using this procedure, if the initial elastic adjustment and the second stage creep rate are

determined in a short-time test, it will then be possible for any given time to estimate the magnitude of the final plastic strain. This is based on the assumption that the third or accelerated creep rate stage is not reached.

From the preceding discussion it can be seen that the viscous behavior of the grain boundary material at high temperature is very important in the magnitude and rate of creep obtained. The ratio of the volume of the boundary material to the volume of crystals for a given metal will depend on the crystal size. A fine grained metal will have a greater ratio than a coarse grained metal and therefore a greater proportion of boundary material. As a result, a coarse grained material will be more resistant to creep at elevated temperatures even though the fine grained material will have greater strength at normal temperatures. This conclusion is confirmed by test data; however, this data indicates that the grain size is not the only variable affecting creep. Other factors include the carbon content and distribution of non-metallic materials. These will affect the boundary material and the composition of the grains.

The Creep Characteristics of Concrete and Plastics

In concrete creep is considered as a non-elastic deformation which results from sustained loads acting over a long period of time. The creep of concrete is believed to involve any or all three types of yielding: Crystalline flow or slippage along the crystal planes, seepage of water due to applied forces and evaporation, and viscous

flow involving a movement of the particles one over the other (23). At this time there is no conclusive experimental evidence as to the exact mechanism of creep in concrete. It seems to be a function of many different factors. The main ones appear to be the type and gradation of the aggregate, the water-cement ratio, and the moisture conditions. Neville (34) concludes that the quantity commonly referred to as creep in concrete is a combination of true creep, which is viscous in nature, and shrinkage, which is essentially the result of seepage due to evaporation. Variations in humidity, temperature, and curing conditions do not affect creep but will affect shrinkage.

In plastics it is possible by various heat treatments to change the basic structure of the material. The structure may be changed from crystalline, to intermediate (commercial grade), to amorphous. In the crystalline form the atoms are arranged in a definite geometrical pattern and tend to deform simultaneously in a series of slips. The amorphous form is characterized by no specific arrangement of atoms and a smooth continuous deformation. It was observed in a recent series of tests (9) that the greatest amount of creep will occur in the amorphous structure and the least in the crystalline structure. Both the time-independent, or elastic strains, and the time-dependent, or creep strains, were much larger in the amorphous structure.

Again as in steel and concrete, there is no one single factor which entirely dominates the creep processes. The creep characteristics vary widely with the different plastics and with the different chemical

and heat treatments. However, the structure and characteristics of the boundary material still appear to be the main factors.

The Creep Phenomenon in Soils

The slopes of a soil mass are constantly subjected to forces which tend to decrease its slope. Terzaghi (51) defines the creep of slopes as a movement in which the center of gravity of the moving mass advances in a downward and outward direction. This movement is at a very slow rate. In a soft plastic clay the slopes will tend to deform in a continuous and progressive manner. The deforming forces in this case are the shear stresses which are due to the force of gravity. The deformations will reach a finite limit only if the slope is fully retained or the slope significantly reduced. In general, creep does not involve the failure of a slope but it may be one of the contributing factors leading to such a failure.

The load at which creep begins is commonly called the fundamental or creep strength. As long as the shear stresses are less than this creep strength, the material will deform almost instantaneously under load but will not flow. Terzaghi (55) notes that if the shearing stress in a clay is increased to a value greater than one-half the total shearing strength, the clay is likely to creep at a constant shearing stress. Peck (41) states that the ratio between the creep strength and the ultimate shearing resistance for insensitive clays is as low as 0.3 and as high as 0.8 for brittle clays. Vialov and Skibitsky (58) found in their direct shear tests on dense clays that

there is a certain limiting shearing stress, which they call the ultimate continuous resistance of a dense clay, which if exceeded the deformations lead to failure. For the Tertiary clay of the beidellite-montmorillonite type this critical shear stress was approximately 0.9 of the standard strength of the clay as measured by conventional short duration tests. In the course of the 2.5 months' observations the deformation of the test specimens either stopped (0.3, 0.5, and 0.7 of the standard strength) or resulted in failure (0.9 of the standard strength). The failure noted in this study occurred at approximately 35 days from the time of loading.

When an attempt is made to retain slopes composed of or underlain by cohesive soils the creep characteristics must be considered. The deformation conditions of a retaining wall are a basic consideration in its design. It is the development of shearing resistance in the soil due to the wall movement which causes a reduction in soil pressure. If the wall retains a cohesive soil and if the induced shearing stresses exceed the fundamental strength of this material the stresses will undergo a slow relaxation and the soil will tend to creep toward the wall. Thus, the shearing stresses tend to decrease while the lateral pressures increase. Peck (42) notes that the creep of a clay beneath and adjacent to retaining walls is a common cause of failure. This consideration indicates that it is feasible to design a retaining wall on the basis of active pressure only if a continuous yield can occur. Since this is not practical for permanent construction it is considered advisable to design the wall for the earth pressure at rest.

Secondary compression is the additional compression beyond that as determined by the consolidation theory. It is described as the gradual adjustment of the soil structure to stress and increases with activity and is reduced by remoulding (52). Terzaghi (54) notes that the creep phenomena may be responsible for part of the secondary settlement of structures located above thick clay deposits; further, that the secondary time influences are probably due to the fact that the compression of a clay layer is accompanied by direct slippage between the clay particles.

At the beginning of the consolidation process the entire stress increase on the clay mass is carried by the excess hydrostatic pressure. As the water moves from the highly stressed regions to the lower stressed regions, the load is gradually transferred from the water to the soil particles. These soil particles attempt to distribute the load and thus the load is taken up by the water films which surround the particles. These water films gradually relax and transfer the load to the solid contacts. As long as there are excessive stresses in these water films the void ratio will continue to decrease. As the rate of movement of the particles decreases the resistance due to the viscosity between water films combines with another supplementary resistance, thixotropic stiffening. This is believed to be due to the building up of molecular bonds within the adsorbed layers of water surrounding the particles. The settlement that is inherent in this void ratio decrease due to relaxation of the water films is called secondary compression. This is essentially the explanation of the

secondary compression phenomenon in clays as given by Terzabhi (44).

Lambe (19) in his recent paper on the structure of clay, states that creep is probably due to particle realignment and greater inter-particle spacing. He later notes that the secondary compression results from changes in particle orientation and spacings as the layers of adsorbed water on a particle are moved past those on other particles or as some of this water is forced from the contact areas. Rowe (45) proposes that the secondary compression could be due to the creep of the cohesive bonds due to the redundancy of the soil structure.

In a series of tests by Casagrande and Wilson (6) the creep-strength tests were performed on various clays and shales at constant water content. The results of one of these tests is shown in Figure 2, page 16. The test shown is a "consolidated-quick triaxial creep-strength test" in which the specimen is consolidated under a given hydrostatic pressure and then, permitting no further consolidation, is subjected to a sustained load. From their results it is apparent that this time deformation curve for a clay soil is divided into three major stages, just as was the case for metals, concrete, and plastics. The first portion of the curve is probably that due to the adjustment of the material. This adjustment is also exhibited on release of the load (11). Next, the deformation rate shows a sharp decrease. This corresponds to the strain hardening phase in metals. This strain hardening in soils, which is an increase in resistance to deformation with strain, probably results from particle and double

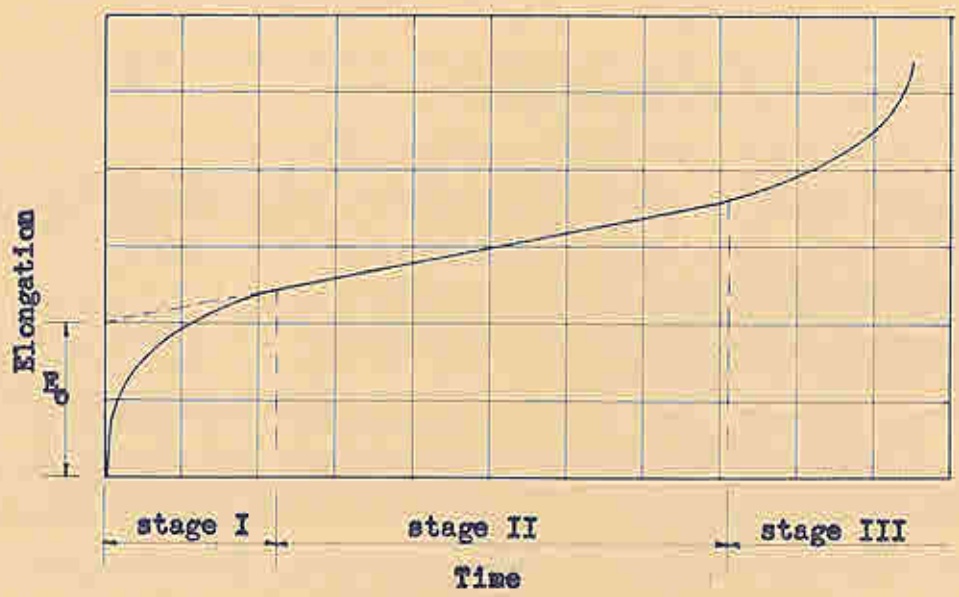

Figure 1.-Idealized Creep Curve

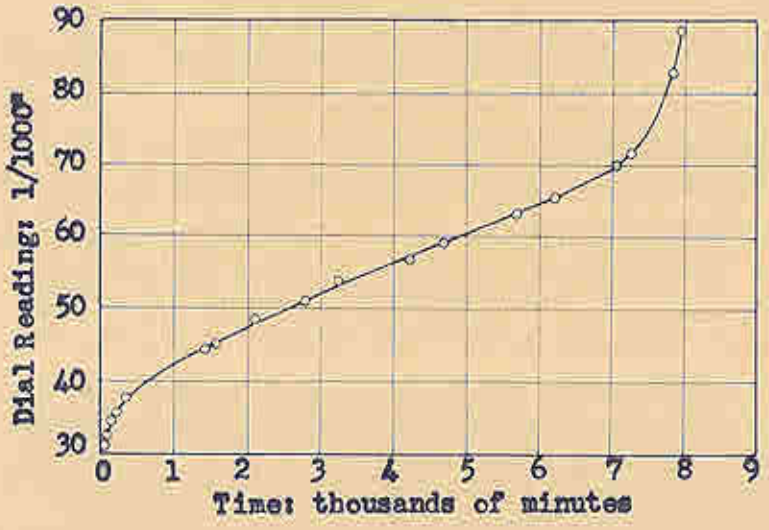

Figure 2.-A Creep Curve for a Cucaracha Clay-Shale
(After Casagrande and Wilson)

layer water reorientation. The second portion of the curve, the visco-plastic portion, is characterized by an almost constant rate of strain until the third portion is reached. During the third portion there is a continuous deformation at an increasing rate until complete failure. The range of results from this series of tests for the creep-strength at constant water content gave from 80 to 40 per cent reduction in shear strength in periods ranging from 5 to 30 days.

The Mechanism of Creep in Cohesive Soils

In order to understand the probable mechanism of creep in cohesive soils the processes involved in and the results of the deformation of the soil structure must be considered.

A clay may be regarded as a first approximation as a colloid with close interparticle spacing. These particles are almost completely dominated by surface forces. The clay particles are generally not in direct contact for they are separated by water films of varying thickness. Since the clay particles are believed to carry a net negative charge (19), the water which is a dipolar material is strongly attracted to it. On the basis of this attractive force the water in the clay can be divided into three general types: adsorbed water, double layer water, and free water.

The adsorbed water and double layer water are electrically attracted to the soil particle while the free water is not. Therefore, their behavior is believed to be different from that of the free water, this being due to the molecular interaction between the

solid and water. It is imagined that this water behaves in a viscous manner, the viscosity decreasing with increasing distance from the soil particles. Due to this viscous action between the water layers there is going to be a time lag between the application of the force and the deformation of the soil structure.

Bloor (4) states that the plastic deformation or creep can take place mainly because of the distortion or shearing of the outside layers of viscous liquid in the moisture phase of the soil. This is to say that first the moisture films are stressed and then relaxed by the viscous flow. A relaxation of the pore water pressure in the clay will result in an increase in the magnitude and a change in the direction of the intergranular stresses. It is this transfer, change in magnitude, and change in direction that results in the flow of a clay.

In his hypothesis for normally loaded clays at equilibrium, Rowe (45) states that his initial experiments on remolded clays suggests that the cohesion is possibly unstressed at equilibrium and that as long as the stress is applied to the cohesion a rate of flow will occur. The rate of creep is believed to depend on the consolidation pressure and mobilization of the cohesion. Rowe concludes that structures which resist creep movements will be subjected to a gradual increase in pressure, the ultimate pressure being that due to a soil having only true friction.

SECTION III

EXPERIMENTAL EQUIPMENT AND SAMPLES

Experimental Equipment Used in This Study

The Triaxial Testing Equipment.- The triaxial equipment which was used during this study was developed at the Norwegian Geotechnical Institute, Oslo-Blindern, Norway. Two of these modern triaxial testing units have been installed in the Soil Mechanics Research Laboratory of the University of Florida. A photograph of these testing units is shown in Figure 3. A detailed description of this equipment and its operation is to be found in Publication Nr. 21 by the Norwegian Geotechnical Institute (1).

The major components of the equipment consist of several triaxial cell chambers, control valves, constant pressure cells, pore pressure instruments, a loading press and proving rings, Bourdon gages and mercury-water manometers. The principal modifications of this equipment include the use of an aluminum tube and SR-4 strain gages to replace the proving rings (13), the use of Harvard ball-bearing pistons for several of the triaxial cells, and two independent pore pressure devices instead of one. These modifications and their advantages are described in detail in reference (47).

The measurements of pore water pressure in the samples during creep were obtained with the pore pressure instrument of the triaxial

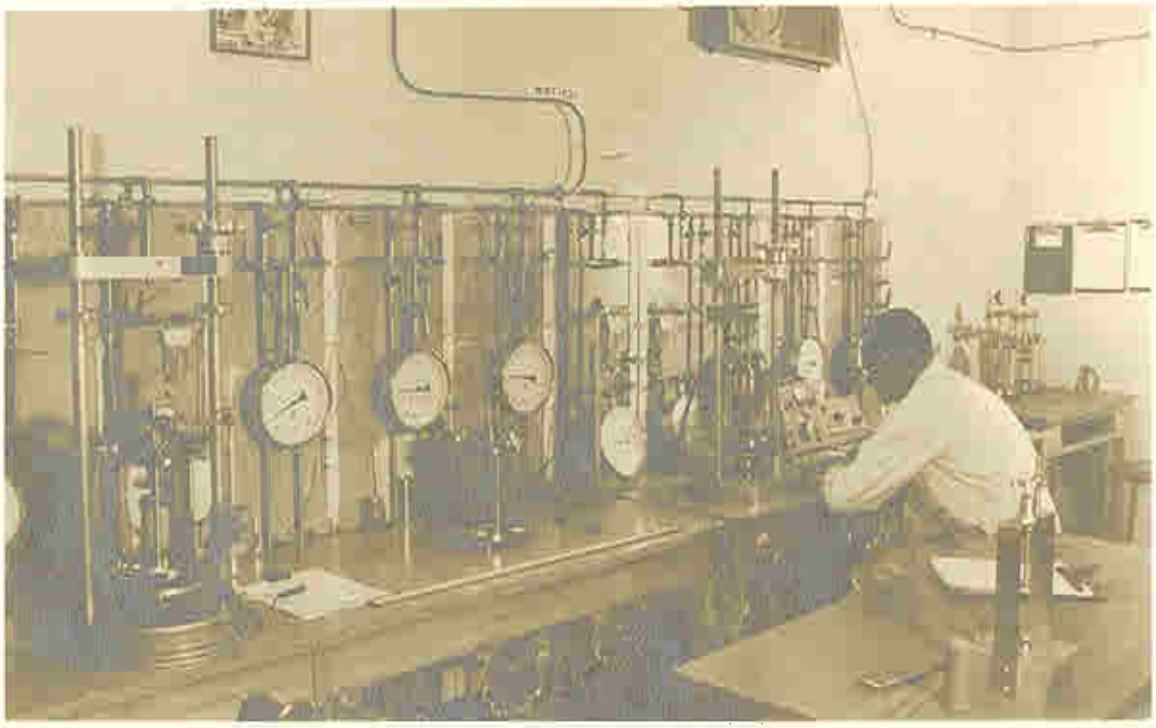

Figure 3. The Triaxial Testing Equipment

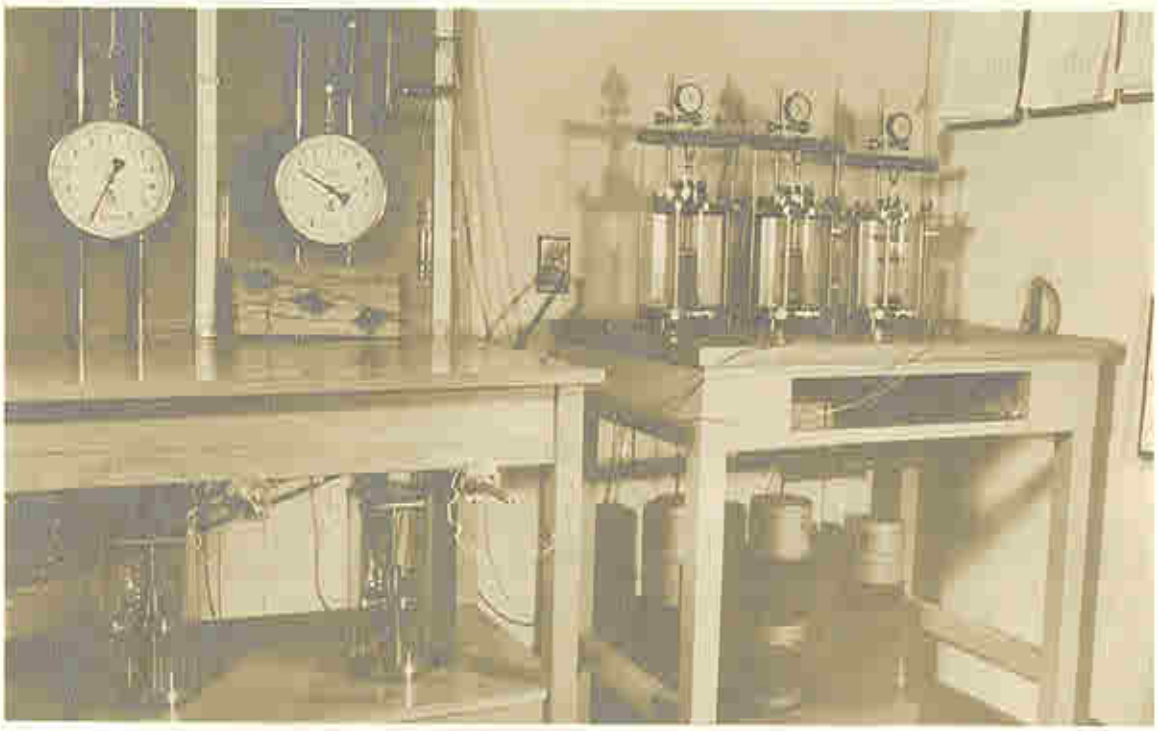

Figure 4. The Creep Test Equipment

equipment. This device is basically a U-tube filled with mercury. One side of the U is connected to the sample drainage outlet and the other side to a manometer and screw control. The screw control is a metal cylinder filled with water and is capable of developing either pressure or a vacuum within the system. The drainage outlet for each of the samples was connected to a central valve system which permitted the use of a single pore pressure instrument in measuring the pore water pressure in any one of the samples. Saran tubing, 1/4 inch outside diameter and 1/8 inch inside diameter, was used to connect the drainage outlets to the pore pressure device. This tubing showed a negligible volume change for the range of pressures used in this study. The valves in this system were piston or slide valves supplied by the Norwegian Geotechnical Institute. These valves are constructed so as to cause a negligible volume change during their operation.

The Creep Test Equipment.- A laboratory table, mounted on rubber pads, was prepared to accommodate a bank of three triaxial cells and loading racks. The pressure for this bank of cells was obtained from a pressure cell unit on the adjacent triaxial equipment. Individual connections to the cells were made with a special series of valves placed on this last pressure cell unit.

In order to subject the samples to a constant load for long periods of time during the creep test, a special loading system was devised for the triaxial cells. The loading system consisted of two horizontal yokes connected by two vertical rods. The loading platforms

were attached to the bottom yoke with a single vertical rod. A ball bearing was placed between the bearing head of the top yoke and the triaxial cell piston to eliminate horizontal forces on the piston. The axial deformation was measured at a platform on the top yoke by means of a dial gage, graduated in 0.002 mm divisions, attached to the triaxial cell mounting post. The arrangement of the creep test equipment may be seen in Figure 4.

Preparation of Remolded Samples Used in This Study

Vac-Aire Extrusion Machine.- The majority of samples used in this investigation were remolded samples prepared by extrusion from a "Vac-Aire" extruder. With this mechanical extruder, which is manufactured by the International Clay Machinery Company, it is possible to prepare a large number of remolded samples of uniform quality and structure with a high degree of saturation and with any desired cross-section (27).

The extruder is comprised of two augers mounted in series which pass through a feed chamber and a vacuum chamber. The prepared clay is placed in the feed chamber and transported by means of the first auger to the second chamber. The second chamber is sealed and held under a vacuum of approximately 27 inches of mercury. The material is forced out of the vacuum chamber by the second auger through a die to produce the desired shape of sample.

Sample Preparation.- The prepared material was passed several times through the extruder to give a thorough mixing and high degree

of uniformity. Then in a continuous series the samples were cut into 10 cm lengths and immediately waxed. The samples used in this study were extruded in a circular bar 3.58 cm in diameter. After the first layer of wax dried, the samples were numbered and a second layer of wax applied. The samples, preserved and sealed, were then stored until ready for use. During sample preparation periodic samples were taken to determine the water content of the extruded samples. The maximum variation in the water content of a series of 50 samples was 2.6 per cent.

The Samples Used in This Investigation

Remolded Kaolinite Clay Samples.- The first series of tests, B-1 through B-4, and B-17 were performed on remolded Kaolinite Clay samples, designated as DWEPK. The Kaolinite used was a commercially prepared powder manufactured by the Edgar Plastic Kaolin Company of Edgar, Florida. In preparation for extrusion the dry material was thoroughly mixed with a predetermined amount of distilled water and passed several times through the extruder to assure thorough mixing. After extrusion, a period of about two months elapsed before testing was begun. The average water content, degree of saturation, and void ratio for this series of samples were 4.72 per cent, 99.5 per cent, and 1.097, respectively. This clay has a specific gravity of 2.61, a liquid limit of 52, and a plasticity index of 21.

Remolded Boston Blue Clay Samples.- The remainder of the tests in this study with the exception of tests B-13 and B-14 were performed on remolded Boston Blue Clay samples, designated as BBC. The clay for

these samples was obtained from a clay pit in Cambridge, Massachusetts, by Professor Schmertmann, who prepared these samples. This material was first machine remolded and allowed to dry so as to permit extrusion. After gaining sufficient strength this material was extruded and handled in the same manner as the Kaolinite samples. A period of approximately ten months elapsed between extrusion and testing of this series of samples. The average water content, degree of saturation, and void ratio for this series of samples were 26.18 per cent, 98.4 per cent, and 0.747, respectively. This clay has a specific gravity of 2.81, a liquid limit of 38, and a plasticity index of 19.

Undisturbed Boston Blue Clay Samples.- Tests B-13 and B-14 were performed on undistrubed samples of Boston Blue Clay, designated as U-BBC. The sample was obtained by Dr. F. E. Richart from Hewes Clay Pit in Cambridge, Massachusetts. The individual samples were carefully separated from the main sample and trimmed to the same dimensions as the extruded samples. The experiments on the undistrubed samples were performed with the objective of comparing test results on undistrubed and remolded samples of the same type of clay, thus gaining an indication of the influence of structure. The average water content, degree of saturation, and void ratio for these samples were 34.91 per cent, 99.9 per cent, and 0.982, respectively. This material has a specific gravity of 2.81, a liquid limit of 35, and a plasticity index of 15.

A summary of the properties of these soils is given in Table 3 and the index properties for each of the samples used in this study are to be found in Table 4.

TABLE 3

PROPERTIES OF THE SOILS USED IN THIS STUDY

Sample Type	Designation	Extruded	Tested	LL	PI	G	Data for Grain Size Analysis	
							% -200 Sieve	% -2μ
Remolded Kaolinite	DWEPK	10/59	1/60	52	21	2.61	100	70
Remolded Boston Blue Clay	BBC	3/59	2-3/60	38	19	2.81	98	43
Undisturbed Boston Blue Clay	U-BBC	-	2-3/60	35	15	2.81	100	46

TABLE 4

TEST SUMMARY

Test No.	Sample Type	Sample No.	Consol. Period min	CFS-Test Comp. Rate 10^{-3} mm/min	As Extruded e	As Extruded s %	As Extruded w %	After Consol. e	After Consol. w %	After CFS-Test e	After CFS-Test s %	After CFS-Test w %	Δe Due to CFS-Test
B-1	DWEPK	751	1,000	5	1,098	99.4	41.67	0.913	34.59	0.900	100.7	34.53	-0.003
B-2	DWEPK	752	1,300	5	1.098	99.7	41.95	0.908	34.69	0.911	98.9	34.54	+0.006
B-3	DWEPK	755	1,200	5	1,104	99.4	42.05	0.895	35.18	0.900	89.0	34.25	+0.008
B-4	DWEPK	757	1,000	5	1.089	99.8	41.65	0.898	34.32	0.895	99.7	34.18	+0.012
B-5	BBC	523	1,100	5	0.757	98.7	26.60	0.650	22.80	0.677	98.5	23.71	+0.003
B-6	BBC	519	1,200	5	0.754	97.8	26.25	0.637	22.08	0.645	98.1	22.51	+0.007
B-7	BBC	520	1,300	5	0.732	97.6	25.41	0.640	22.11	0.667	97.7	23.19	+0.009
B-8	BBC	521	1,200	5	0.745	98.4	26.09	0.640	22.32	0.658	99.1	23.20	+0.017
B-9	BBC	525	6,800	1.5	0.750	98.6	26.30	0.630	22.03	0.650	98.4	22.76	+0.005
B-10	BBC	526	6,800	1.5	0.740	99.8	26.28	0.620	21.97	0.678	99.7	24.05	+0.009
B-11	BBC	527	6,800	1.5	0.746	97.7	25.94	0.625	21.64	0.653	97.8	22.75	+0.002
B-12	BBC	528	6,800	1.5	0.752	98.9	26.47	0.626	21.99	0.687	96.6	23.61	-0.001
B-13	U-BBC	R-2	1,500	1.5	0.985	100.4	35.19	0.800	28.60	0.834	98.5	29.22	+0.007
B-14	U-BBC	R-3	1,300	1.5	0.979	99.4	34.62	0.831	29.34	0.883	96.9	30.44	+0.000
B-15	BBC	529	1,400	1.5	0.753	98.9	26.51	0.633	22.23	0.645	100.5	23.08	+0.002
B-16	BBC	530	1,400	1.5	0.745	98.1	26.00	0.620	21.54	0.648	98.7	22.77	+0.003
B-17	DWEPK	759	1,300	1.5	1.096	98.3	41.30	0.883	33.15	0.870	100.6	33.53	+0.012
B-18	BBC	532	6,800	1.5	0.748	98.0	26.09	0.625	21.70	0.635	100.5	23.82	+0.011
H-13	DWEPK	799	1,200	5	1.064	99.8	40.70	0.888	33.60	0.891	99.6	34.01	+0.003
H-22	BBC	539	1,200	5	0.744	96.9	26.41	0.641	22.45	0.649	100.0	22.43	+0.004
S-91	U-BBC	R-4	1,300	5	0.965	99.7	34.25	0.820	28.81	0.828	98.0	28.88	+0.005

SECTION IV

EXPERIMENTAL PROCEDURE

Preparation of Sample for Testing

This first phase of the experimental procedure is concerned with the preparation of the sample and its mounting in the triaxial cell chamber. First, the wax cover surrounding the extruded sample was carefully removed. This was accomplished by using a razor blade to remove the ends and to make a longitudinal cut in the wax cover. Both edges of the cut were then peeled back and the specimen removed. The undisturbed samples used in this study were carefully trimmed to the same dimensions as the extruded samples by using a trimming frame and wire saw. The extruded and undisturbed samples were subsequently treated in the same manner.

In order to obtain better distribution and measurement of the pore water pressure during the experiment, wool yarn was placed longitudinally in the sample. The number of these drains, which are very useful in the performance of the CFS-test, will depend on the permeability of the sample. A system of three symmetrically placed drains were used in the BBC and U-BBC samples and a single axial drain was used in the DWEPK samples. The procedure for placing these drains is described in detail in reference (47).

After placement of the internal drainage system, the specimen

was placed in an 8 cm miter box and the ends trimmed and squared. The sample was then carefully weighed, measured, and placed on the mounting pedestal of the triaxial chamber. A Whatman #54 filter paper cap was used at the top and bottom of the sample to facilitate drainage and to prevent erosion of the sample at the bottom porous stone. In addition to this, longitudinal filter paper drainage strips were used on the exterior of the sample.

The sample was enclosed with two rubber membranes. "Shiek" brand prophylactics were used as membranes. These were placed over the sample using a special mounting cylinder. A heavy uniform layer of type M Apiezon grease was applied to the exterior of the first membrane before placement of the second membrane. Two rubber sealing rings were placed at the top and bottom of the membranes, which were secured to the bottom pedestal and loading head. The upper head of the triaxial chamber was placed over the mounted sample, the wing bolts secured, and the chamber filled with water. The pore water pressure system was connected and saturated.

Consolidation

The next phase of sample preparation was hydrostatic consolidation. A burette, graduated in 0.1 ml divisions, was used to measure the water expelled from the sample during consolidation. To initiate consolidation the desired pressure in the triaxial chamber was developed, and the burette valve opened. A record was made of the initial burette reading and the time consolidation was initiated. At given intervals readings were taken of time, burette volume, and axial

shortening.

All samples except that in test S-91 were consolidated to a pressure of 3.65 kg per cm^2. (The sample in test S-91 was consolidated to a pressure of 4.00 kg per cm^2.) The majority of samples were consolidated for a period of about twenty hours, after which time they were well into the secondary compression stage. One series of samples was consolidated for about 115 hours to determine the influence of the long periods of consolidation on the creep-strength characteristics. Figure 46, page 102, shows a typical consolidation curve for each of the soil types used in this investigation.

The Creep Test

Upon completion of hydrostatic consolidation, the burette was disconnected and the connecting line sealed. The pore water system was then thoroughly flushed to remove any air. The valve system which connected the triaxial cells to the pore pressure measuring device was previously saturated and tested under a pressure of 8.0 kg per cm^2 to assure no leakage would take place through the valves.

Next, the loading frame was assembled and placed on the triaxial cell piston. It was necessary to dead-load the loading frame so as to just balance the uplift of the triaxial cell piston. The axial compression dial was mounted and the pore pressure measuring device activated. The sample was loaded by placing weights on the loading frame shelves. Loads were placed at intervals of about ten minutes so as to make the total loading time in all cases sixty minutes. Readings of the axial compression and pore water pressure

were taken during the initial loading period.

After placement of the total creep load, readings were taken of time, axial compression, and pore water pressure. These readings were recorded on a printed form arranged for this purpose. All of the experimental data for a given sample were kept on a separate clip board, which was located on a wall adjacent to the bank of triaxial cells. Each triaxial cell was given a position number and then all associated equipment clearly marked with this number. A photograph of the arrangement of the equipment for the creep test is shown in Figure 4.

Measurement of the Pore Water Pressure.- Since the measurement of the pore water pressure in the sample during creep was an important phase of this test, it will be described in greater detail. As noted earlier, all of the drainage outlets to the samples were connected to a central valve system which permitted the use of a single pore pressure instrument for measuring the pore water pressure in any one of the samples. Before the valve to a cell was opened, a pressure equal to or slightly greater than that expected in the sample was placed on the pore pressure measuring system.

When the valve was opened the screw control was used to increase or decrease the back pressure to keep the mercury level in the U tube at the same elevation, thus preventing pore water movement. The pressure required to hold the mercury column in the U tube level was therefore equal to the pore water pressure in the sample. Equilibrium, which was obtained by making the necessary pressure adjustments to keep the level of mercury at the same elevation, was

generally obtained in 10 to 15 minutes depending on the magnitude of the pressure being measured. When equilibrium was reached, the pore water pressure reading was taken and recorded.

After the pore water pressure reading for a sample was obtained, the valve leading to that sample was closed and the same procedure repeated for the other samples. When all pore pressure readings were completed a back-pressure greater than the highest measured pressure was placed in the pore pressure measuring system. This was done to assure that no leakage would take place from the samples. As an additional precaution, the main valve to the pore pressure system was closed. Thus, between readings each sample had two closed piston valves between it and a pore pressure measuring device always kept at a higher pressure.

Triaxial Cell Transfer.- Upon completion of the creep test it was necessary to transfer the triaxial cell from the creep loading table to the loading press of the triaxial machine. Before the cell was to be transferred, readings were taken of the pore water pressure and axial compression. Then the weights were removed from the loading frame and the triaxial cell moved immediately to the loading press where the load was again placed and maintained on the sample. The moving process usually took about ten minutes. This transfer was made from 18 to 20 hours before the CFS-test was to be initiated. This was done to allow the sample to fully recover from the influence of the short time unloading-loading procedure. The subsequent measurements of pore water pressure and axial compression indicated

the moving process had negligible or only small effects on these values.

The Cohesion-Friction-Strain Test

After completion of the creep test, the cohesion-friction-strain (CFS) test was performed to determine the influence of the creep action on the cohesion-friction-strain behavior of the near saturated clays used in this investigation. Similar tests were performed to determine the CFS-behavior, before creep, of the soils used in this study.

CFS-Test Development.- It is important both from a theoretical and practical standpoint to know not only the creep characteristics and how creep action will affect the total strength of a clay, but also how creep will influence the cohesion and friction components comprising the total strength. Until recently (1960) it has not been possible to accomplish in the laboratory a satisfactory separation of the cohesion and friction comprising the total strength of a sample. Professor John H. Schmertmann, director of this experimental study, has developed a laboratory technique by means of which the defined cohesion and friction components may be accurately separated. The development and theory of the testing procedure is presented in detail in reference (47). Two important concepts form the basis of this test: The first is the working definitions of cohesion and friction; and the second is the concept of using the pore water pressure as a test control.

Cohesion-Friction Definitions.- The working definitions of cohesion and friction utilized in the development of the CFS-test are quoted from reference (47) as follows:

> Cohesion (c).- The cohesion of a soil, at any strain, is the shear stress developed on the plane of Mohr envelope tangency at that strain if the intergranular stress on that plane could be reduced to zero without significant change in soil structure.
>
> Angle of Internal Friction (ϕ).- The angle of internal friction, at any strain, is the angle whose tangent is the ratio of the change in shear stress to the change in normal intergranular stress occurring on the plane of Mohr envelope tangency at that strain, during a stress change occurring without significant change in soil structure.

Thus, the cohesion is the strength component which is independent of intergranular pressure, and friction is the component which is a function of intergranular pressure. The intergranular pressure is defined as the total stress minus the pore water pressure. It is the control of the intergranular pressure by regulation of the pore water pressure that is the basic technique used in this test.

General CFS-Test Procedure.- In preparation for the CFS-test, the pore water pressure necessary to obtain the first desired intergranular pressure was imposed on the sample. This was done approximately twenty minutes before initiating compression so that when the test was begun the sample had almost reached equilibrium at the desired intergranular pressure and no time was lost in obtaining the first data points.

The remainder of the CFS-test consists of regulating the

pore water pressure so as to move alternately back and forth between two pre-selected values of intergranular pressure while the sample is being strained at a constant rate. After equilibrium at the imposed pore water pressure is obtained, readings are taken of the time, axial compression, axial load on the sample, and the volume change. The detailed procedure for this test is given in reference (47).

After completion of the CFS-test, the sample was carefully dismounted from the triaxial cell chamber, weighed, and measured with vernier calipers. The sample was then placed in a drying oven and after 2 to 3 days the final dry weight was obtained. The index properties for each of the samples after the CFS-test are given in Table 4.

Range of Intergranular Pressure.- The two values of intergranular pressure generally used in this test were 3.41 and 2.69 kg per cm^2. These values were selected after a study (47) showed that a range of about 75 to 100 per cent of the preconsolidation pressure produced strength changes that can be interpreted with sufficient accuracy and yet cause only small void ratio changes. The volume change measurements taken during this series of tests indicate that this change is usually on the order of 1 per cent of the initial void ratio. This is presently considered minor in the interpretation of the results.

The Constant Compression Rates.- At the beginning of this study the constant compression rate used was 0.005 mm/min, or

approximately 0.4 per cent axial compressive strain per hour for the 8.0 cm initial height of the specimens used. This rate is slow enough to allow the experimenter to obtain enough data points with sufficient pore water pressure uniformity and yet reach 4 or 5 per cent strain in a testing day.

After the first series of tests was performed at this rate, it was found desirable to reduce the compression rate so as to be able to define the cohesion-friction characteristics at a very low value of strain. For this reason, the strain rate was reduced to 0.0015 mm/min or about 0.1 per cent axial compressive strain per hour. This allowed the sample to reach about 1 to 1 1/2 per cent axial strain in a testing day. In several instances tests were performed at this and the previous rate over a period of 2 to 5 days to give some indication of the cohesion-friction behavior at very high strains. The strain rate used in each test may be found in Table 4.

It should be noted here that in its present stage of development, the influence of the different values of these very slow strain rates on the CFS-test results has not been evaluated.

CFS-Test Data Analysis

Experimental Data.- The experimental data, which consist basically of time, load, axial compression, pore water pressure, and volume change readings, are used to compute the values of axial strain and corresponding axial stress for the two computed values of intergranular pressure. Appropriate corrections for the measured and calibrated volume changes, increase in the area of the sample,

and compression of the loading device are applied to the axial stress and compression data.

Stress-Strain Curves.- Two stress-strain curves, one for each value of intergranular pressure, were prepared from the computed data (Figure 15). At selected values of strain which were close to experimental points on both curves, the axial compressive stress was obtained from each curve. These values of axial stress together with the computed values of intergranular pressure at that strain (the numbers adjacent to the data points on the CFS-tests) comprise the data with which it is possible to compute the cohesion and friction angle at that given strain.

Computation of Cohesion and Friction Angle.- With one of the values of intergranular pressure and the minor principal stress it is possible to construct a Mohr circle of stress at that strain. Another Mohr circle may be constructed with the other value of intergranular pressure and minor principal stress. This gives two Mohr circles of stress at a given strain. If a common tangent is drawn to these circles the slope of this tangent is the tangent of the angle of internal friction and the vertical intercept of the tangent is the cohesion, both at the given value of strain. Using this same procedure for a number of other values of strain it is possible to determine the variation of cohesion and friction angle with strain.

This is the basic theory which underlies the mathematical extrapolation technique which was used. This has proven to be superior to the circle-tangent technique. The basic development of this

procedure is given in Figure 5. The basic assumption in this extrapolation technique is that the Coulomb-Hvorslev equation is valid at any compressive strain. Schmertmann (47) has shown experimentally that this is a valid assumption for the test conditions used in this study.

From the Coulomb-Hvorslev failure criterion and the geometrical relationships of the Mohr stress circle it is possible, as shown in Figure 5, to obtain equation 2. This can be interpreted as a straight line on a plot of $\sigma_a/2$ as the ordinate and $\bar{\sigma}_3$, as the abscissa. As explained previously, the CFS-test stress-strain curves will give values of σ_a and $\bar{\sigma}_3$ at any axial compressive strain; thus, with the experimental data it is possible to define a straight line. This line is computed mathematically and with the resulting values the cohesion and friction angle at a given strain are determined by means of equations 3 and 4. The results of the computations are presented as a plot of the variation of cohesion and friction angle with strain.

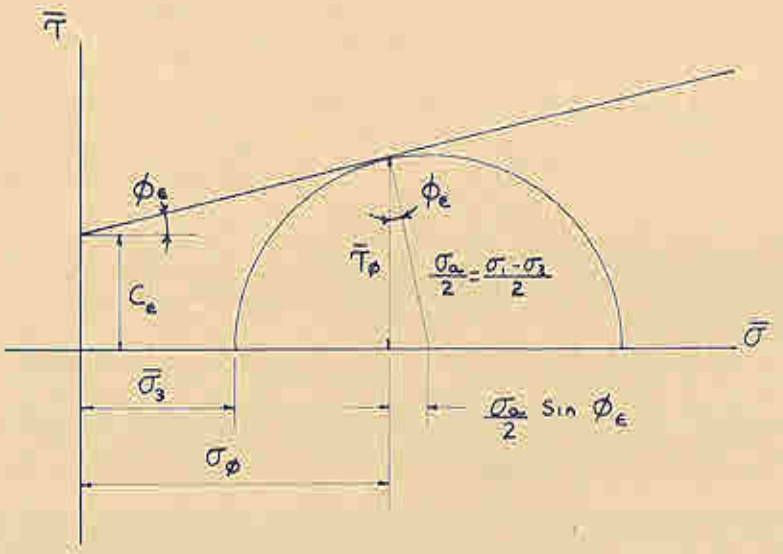

If it is assumed that the Coulomb-Hvorslev equation governing the failure criteria of homogeneous clay is valid at any axial compressive strain ϵ, then:

$$\bar{\tau}_\phi = C_\epsilon + \bar{\sigma}_\phi \tan \phi_\epsilon \qquad (1)$$

From the geometrical relationship of the Mohr circle shown above:

$$\tau_\phi = \frac{\sigma_a}{2} \cos \phi_\epsilon$$

$$\bar{\sigma}_\phi = \bar{\sigma}_3 + \frac{\sigma_a}{2} - \frac{\sigma_a}{2} \sin \phi_\epsilon$$

Inserting the expressions for $\bar{\tau}_\phi$ and $\bar{\sigma}_\phi$ into equation (1) and simplifying gives:

$$\frac{\sigma_a}{2} = \left(\frac{\sin \phi_\epsilon}{1 - \sin \phi_\epsilon}\right) \bar{\sigma}_3 + C_\epsilon \left(\frac{\cos \phi_\epsilon}{1 - \sin \phi_\epsilon}\right) \qquad (2)$$

This is the expression for a straight line 1-2, with slope m and intercept b, as shown below.

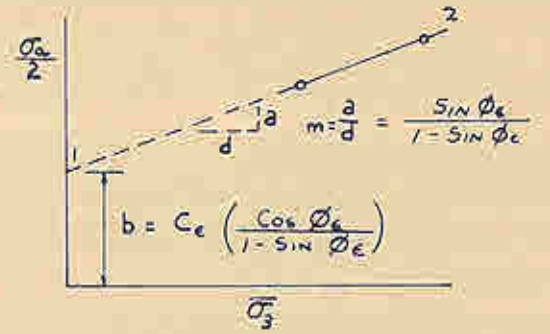

$$\phi_\epsilon = \sin^{-1} \frac{a}{d + a} \qquad (3)$$

$$C_\epsilon = b \frac{1 - \sin \phi_\epsilon}{\cos \phi_\epsilon} \qquad (4)$$

Reference (47)

Figure 5.-Method of Extrapolation For ϕ_ϵ and C_ϵ From Results of CFS-Test

SECTION V

PRESENTATION OF EXPERIMENTAL DATA AND RESULTS

The Cohesion-Friction-Strain Characteristics; Without Creep

As noted earlier there were three types of soils used in this study: Remolded Kaolinite Clay (DWEPK), remolded Boston Blue Clay (BBC), and undisturbed Boston Blue Clay (U-BBC). There were seven tests performed to determine the cohesion-friction-strain behavior of these soils before creep. The experimental data for these tests is included in the Appendix; Table 1 gives a summary of these tests and the figures in which the data may be found.

The experimental data is presented in the form of plots of axial stress and strain for the two standard intergranular pressures (Figure 15). The computed value of intergranular pressure is shown adjacent to each data point. The strains at which cohesion and friction were computed are shown on these curves as vertical dashed lines. The computed results are presented in the form of plots of the variation of cohesion and friction angle with axial compressive strain. The experimental data and computed results are presented in the same figure.

The Effect of Creep on the CFS Characteristics

There were fourteen tests performed in the course of this study to determine the influence of creep on the cohesion-friction-strain behavior of the DWEPK, BBC, and U-BBC samples. The experimental

data and results are presented as described in the preceding section and are contained in the Appendix. Table 2 gives a summary of these tests and the figures in which the data may be found.

The circled point at the beginning of the stress-strain curves (Figure 17) is the stress and corresponding strain of the sample at the end of the creep test. The figure adjacent to the point is the intergranular pressure of the sample at the end of the creep test. The vertical dashed line on the computed results indicates the strain at the beginning of the CFS-test.

In order to allow a convenient comparison of the effects of creep on the CFS behavior of a given soil composite plots of the CFS-coordinates are presented in Figures 6 through 11. To avoid confusion, only the resulting curves are plotted without presenting the data points which are to be found in the Appendix. The variation of the defined cohesion is shown as a solid line while the variation of the defined friction angle is shown as a dashed line. The vertical line (Figure 6) connecting the corresponding friction angle and cohesion curves indicates the strain at which the CFS-test was begun. For comparison the CFS-characteristics of the soil before creep are shown as heavy-lined curves on the same figure.

The short dashed lines (Figure 6) at the beginning of the friction and cohesion curves represent computed extrapolations of the behavior of the soil at the extremely small strains. These extrapolations were necessary since the first computed cohesion and friction points could not be obtained until about 0.5 per cent CFS-test strain.

To arrive at each of these extrapolations two sets of computations were performed using equation 2, Figure 5. First, a graphical extrapolation was made of the friction curve to zero CFS-test strain, and then using the known values of axial stress and minor principal stress it was possible to compute the cohesion required to satisfy equation 2. The second computation was made on the assumption of zero initial cohesion and the required friction angle computed from equation 2. In only three cases did the first computation produce reasonable results; these were tests B-10, B-13, and B-14. This extrapolation and its ramifications will be discussed in the following section.

The Creep Characteristics of the Soils Used in This Study

The experimental data for the creep characteristics of the soils used in this study are presented as plots of the variation of the axial deformation of the sample with time. This data is included in the Appendix and is presented in Figures 36 through 40. For ease of comparison, the creep characteristics of both BBC and U-BBC are shown in Figure 14. Figure 13 shows a comparison of the creep characteristics of BBC and DWEPK for the same set of loads and testing conditions. The detailed information for each of the creep tests may be found in Tables 1 and 5.

The Pore Water Pressure Characteristics During Creep

The experimental data on the pore water pressure characteristics during creep is presented as plots of the variation of pore water pressure with time. This data is included in the

Appendix and is shown in Figures 41 through 45. The peak and final pore water pressures for each creep test are given in Table 5.

TABLE 5

CREEP TEST SUMMARY

Test No.	Sample Type	Initial Adjustment %	Second Stage Creep Rate mm/day	Strain During Creep at end %	Peak Pore Water Pressure Kg/cm^2	At End of Creep Test Kg/cm^2		
						u	σ_a	$\bar{\sigma}_1$
B-2	DWEPK	0.60	0.008	0.71	0.77	0.50	1.12	4.27
B-3	DWEPK	1.73	0.005	1.82	1.85	1.50	1.69	3.84
B-4	DWEPK	4.75	0.012	5.00	2.56	1.51	1.96	4.10
B-6	BBC	0.52	0.009	0.82	0.76	0.14	1.12	4.63
B-7	BBC	2.68	0.005	2.82	2.15	1.96	1.64	3.33
B-8	BBC	6.14	0.011	6.30	2.60	1.57	1.82	3.90
B-9	BBC	2.30	0.006	2.77	1.80	0.12	1.89	5.42
B-10	BBC	2.22	--	2.37	2.08	2.03	1.90	3.52
B-11	BBC	1.45	0.015	1.58	1.90	1.62	1.91	3.94
B-13	U-BBC	2.21	0.022	2.51	1.90	1.90	2.02	3.77
B-14	U-BBC	1.80	--	1.97	1.78	1.78	2.00	3.87
B-15	BBC	13.63	--	19.09	2.62	2.05	3.09	4.69
B-16	BBC	11.90	--	18.82	2.58	2.25	3.04	4.44
B-17	DWEPK	4.90	--	6.09	2.54	0.90	3.54	6.29

SECTION VI

DISCUSSION OF EXPERIMENTAL RESULTS

General

When a saturated clay soil is stressed and left undrained, how will it deform with time; how will the pore water pressure vary with time; and how is the stress proportioned between the cohesive and frictional components of strength? The answers to these questions were the major objectives of this investigation and each will be discussed in the light of experimental evidence obtained during this study.

The Cohesion-Friction-Strain Characteristics; Without Creep

The Development of c and ϕ with Strain.- This group of tests, which were performed to show the strain-rate development of cohesion and friction in the soils before they had been subjected to creep action, generally indicated that the cohesion develops to a maximum value at low compressive strains while the friction angle requires much greater strains to reach its maximum value. The cohesion reaches its maximum value at about 1 per cent strain.

The Influence of the Period of Consolidation.- Several tests in this group were performed on samples which had consolidated 6,800 minutes rather than the usual 1,200 to 1,300 minutes. The samples consolidated 1,200 to 1,300 minutes showed a friction angle of about 4 degrees at the strain of the maximum cohesion. However, the

samples consolidated 6,800 minutes showed a much higher friction angle, 10 to 14 degrees at the same strain. The variation of cohesion was essentially the same as that noted in the other tests.

Thus, the period of secondary consolidation had a marked influence on the development of friction with strain. The greater period of consolidation, which resulted in the formation of high frictional strengths at low strains, probably allowed the sample to adjust more structurally. A mechanical picture such as that offered by Terzaghi (54) could explain the increased frictional resistance.

The Influence of Structure.- An indication of the influence of structure on the CFS behavior may be obtained by a comparison of tests S-91 (Figure 30) and B-5 (Figure 20), on U-BBC and BBC, respectively. No direct comparison should be made of the relative values of maximum cohesion since test S-91 was consolidated at a pressure of 4.00 kg per cm^2 while all other tests were consolidated at 3.65 kg per cm^2. It has been shown experimentally (47) that the peak cohesion is dependent on the preconsolidation pressure. It has been suggested that this peaking effect, noted in BBC and U-BBC and absent in DWEPK, increases as the amount of coarse particles in the clay increases (47).

Duplicability of Results.- A comparison of the CFS-test results for the same soil under the same conditions but performed by different investigators shows the excellent duplicability of this testing technique. This is evident in a comparison of tests B-1 and H-13 on DWEPK (Figures 15 and 16) and on tests B-5 and H-22 on BBC

(Figures 20 and 21). The tests performed by the author are designated B, while those performed by Mr. J. R. Hall, Jr., and Professor J. H. Schmertmann are designated H and S, respectively.

The Effect of Creep on the Cohesion-Friction-Strain Characteristics

Test Series A.- This series of tests, shown in Figure 6, for the remolded Kaolinite Clay samples clearly indicates the influence that creep action has had on the CFS characteristics. Initially the friction angle is much greater and the cohesion much less than that found in the standard tests. With the increased strain rate of the CFS-test the friction angle quickly decreases, reaches a minimum value, and then begins to build up at the higher strains along the same line as the standard test. The cohesion, on the other hand, increases very rapidly at the low strains as was noted in the standard tests. At the higher strains the cohesion generally follows the same lines as the standard tests. The stepping action noted in test B-4 and which probably would have been noted in tests H-13 and B-1, had more detailed data been obtained at these high strains, is thought to be due to the formation of failure planes in the sample.

Test Series B.- These tests, shown in Figure 7, on remolded Boston Blue Clay were performed under the same conditions as those in test series A. The same striking behavior of friction and cohesion at low strains is noted; a high initial value of friction which decreases with strain and a low initial value of cohesion which quickly increases with the CFS-test strain. A difference is noted in the cohesion-friction behavior at the high CFS-test strains in these two

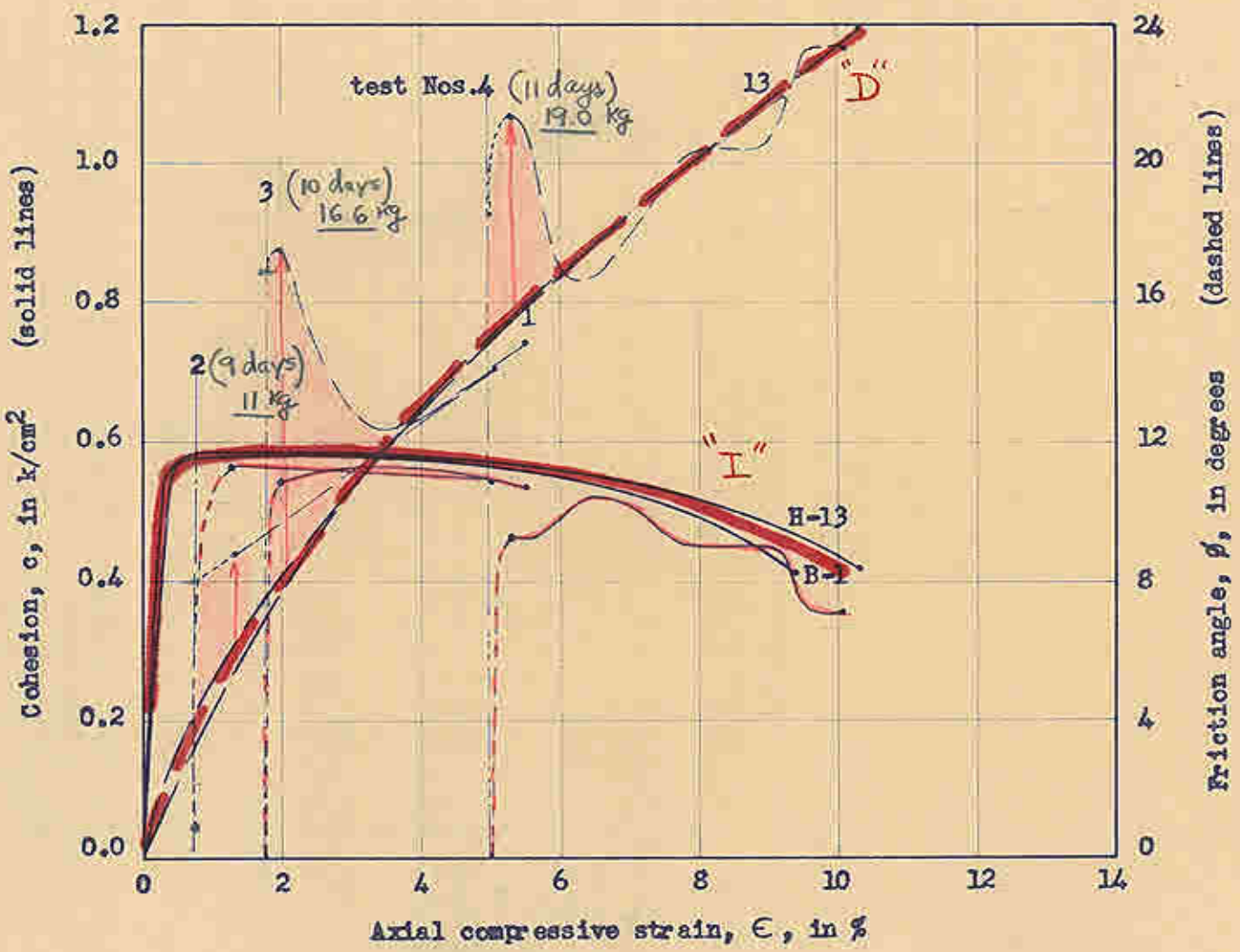

Figure 6.- Computed results of CFS-tests on DWEPK samples

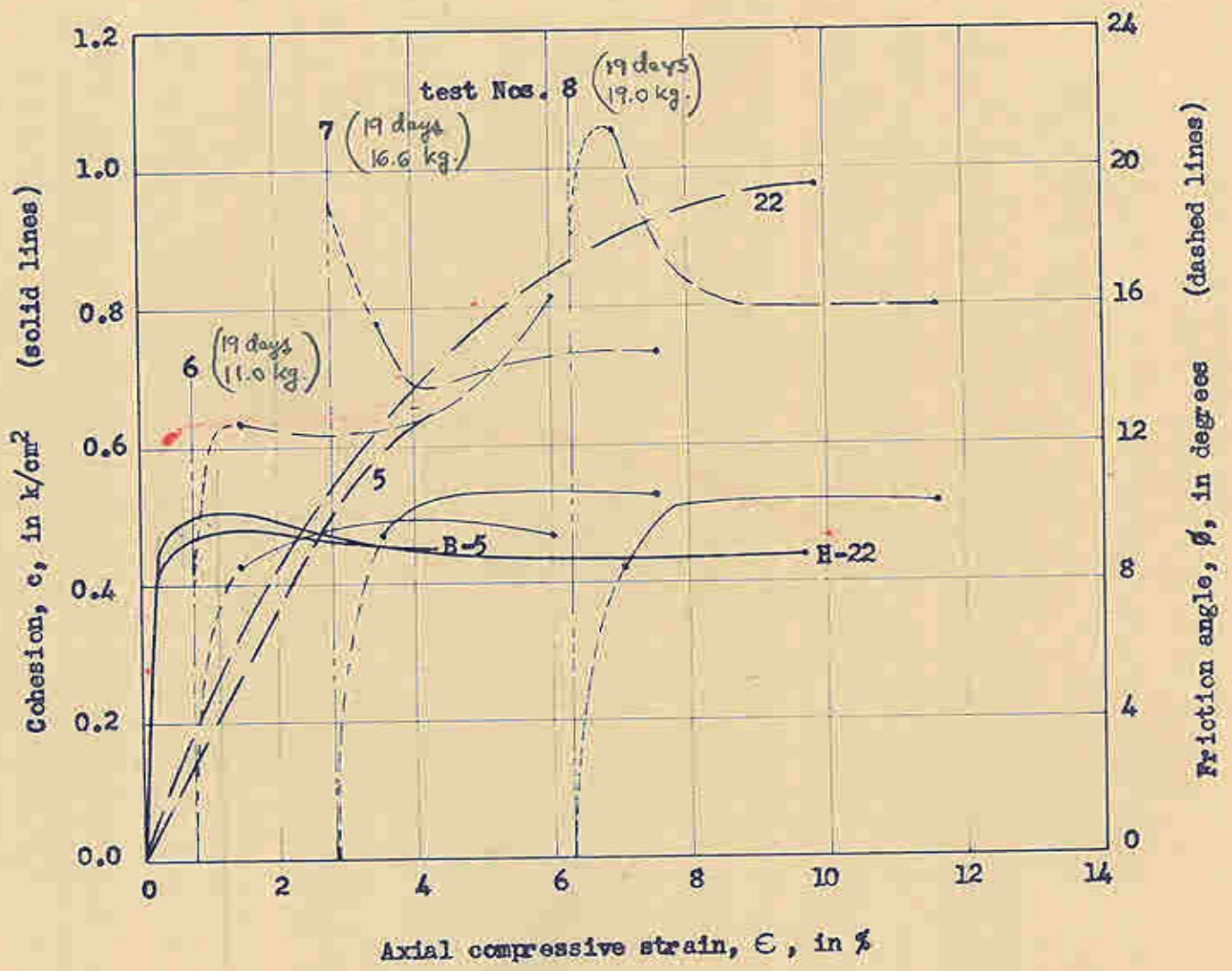

Figure 7.- Computed results of CFS-tests on BBC samples

test series. The absence of the tendency in these BBC samples for the friction angle to increase at the high CFS-test strains is probably due to the sample having reached a maximum frictional resistance at this strain rate.

Test Series C.- In this series of tests on remolded Boston Blue Clay, shown in Figure 8, the samples were allowed to stand, undrained, about 5,600 minutes longer than the series B samples before beginning the creep-strength test. Also the strain rate used in the CFS-tests was reduced for these and the remaining tests in order to be able to better define the cohesion-friction variations at low CFS-test strains.

The high initial build-up of friction in the CFS-test after creep is not so evident as in test series B, but the high initial friction and low initial cohesion are evident. Again there is the same general variation of cohesion and friction with the CFS-test strain, except in this BBC series there is a definite tendency for the friction to again increase after reaching a minimum value. This peak-and-dip variation is the same as that noted in test series A on the DWEPK samples.

Test Series D.- The CFS behavior of the undisturbed Boston Blue Clay series, shown in Figure 9, is somewhat different from that of the remolded soil. There is still the high initial build-up of friction, but there is now a definite cohesive strength exhibited initially. The cohesion quickly increases with the CFS-test strain while the friction remains essentially constant. As the CFS-test

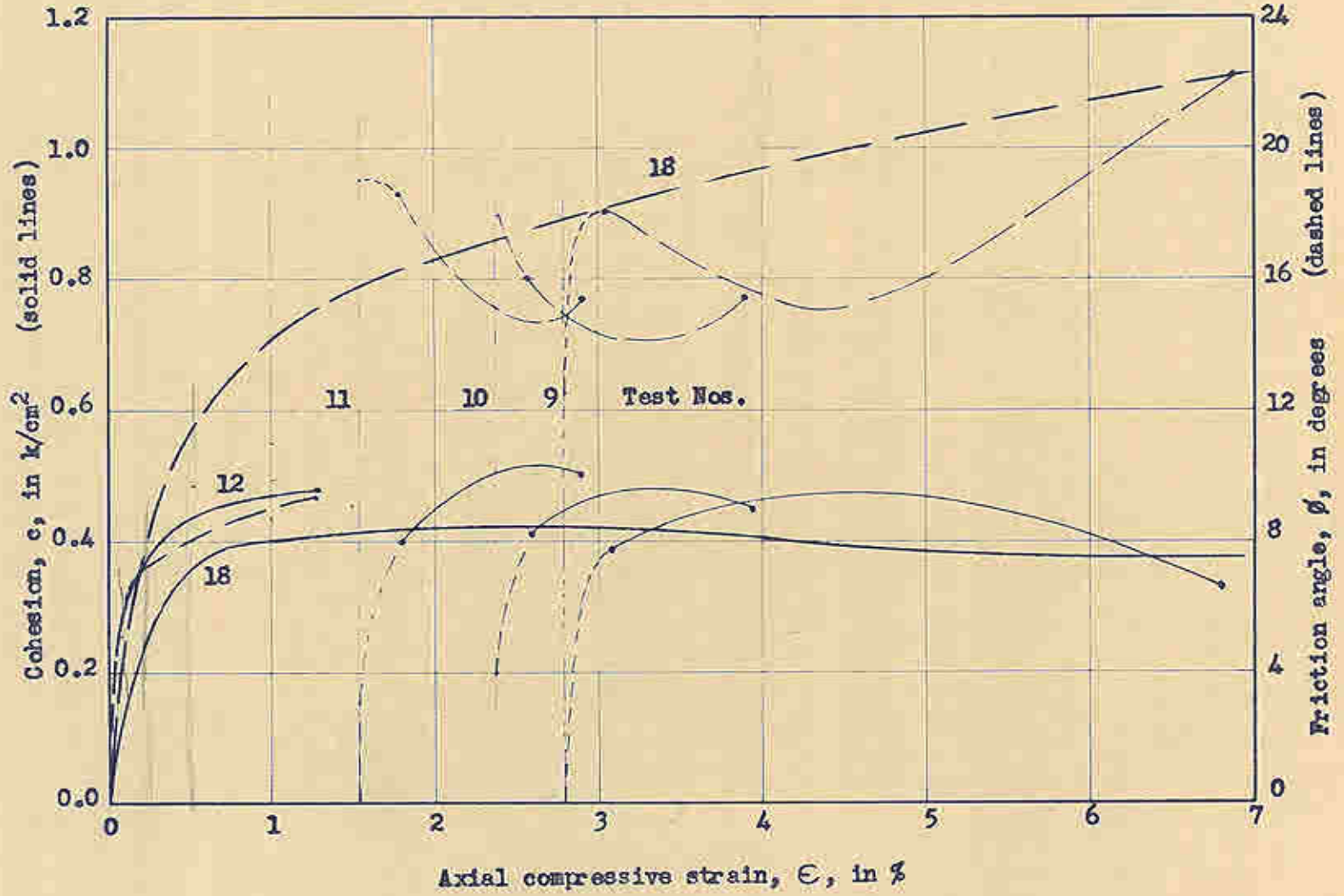

Figure 8.-Computed results of CFS-tests on EBC samples (t_c-6800 min.)

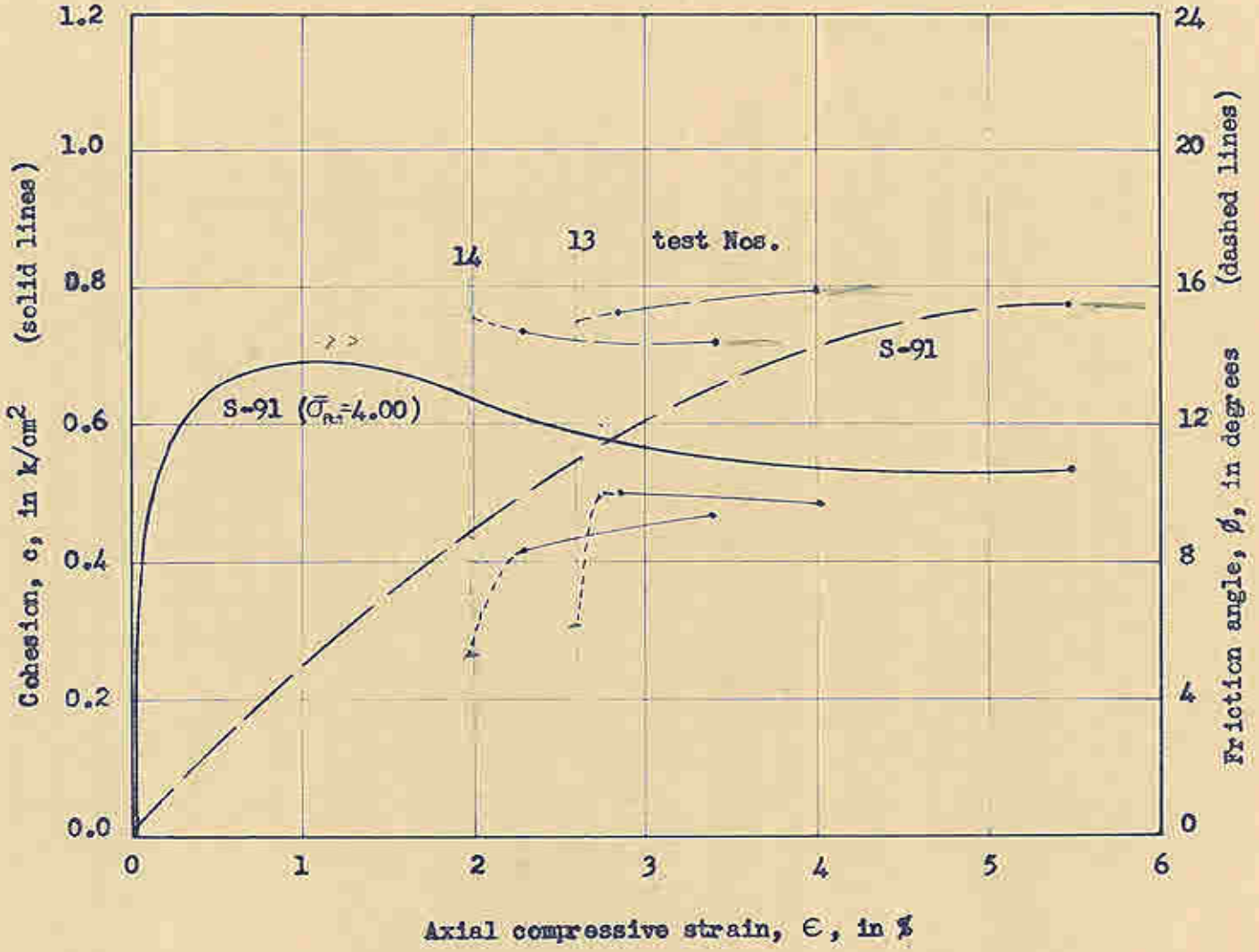

Figure 9.-Computed results of CFS-tests on U-BBC samples

strain is further increased the cohesion and friction remain essentially constant.

A comparison of the standard CFS-test, S-91, and the creep, strength tests, B-13 and B-14, clearly indicates that the absence of the tendency for the friction angle to increase with strains may be due to the possibility that the sample has already mobilized the maximum amount of friction. This would provide an explanation for the apparent high initial value of cohesion. If the sample could not mobilize any greater frictional resistance during the creep strains, the cohesion would be forced to carry the remainder of the stress if the load is to be sustained.

Test Series E.- This series of tests on both BBC and DWEPK samples are shown in Figure 10 and Figure 11, respectively. The loading procedure used in this series of tests was not the same as the zero to full load in 60 minutes procedure used in the other creep-strength tests. This procedure was used for the initial loading, but after the samples had almost stopped deforming under the initial load a series of loads were applied at daily intervals. The details of this test may be seen in Figure 40.

There was an extremely high build-up of friction in both the BBC and DWEPK samples under the high stresses. With the increased strain rate of the CFS-test there was the characteristic drop in friction and quick increase in cohesion. At the higher CFS-test strains both components tended to approach the values determined in the standard test.

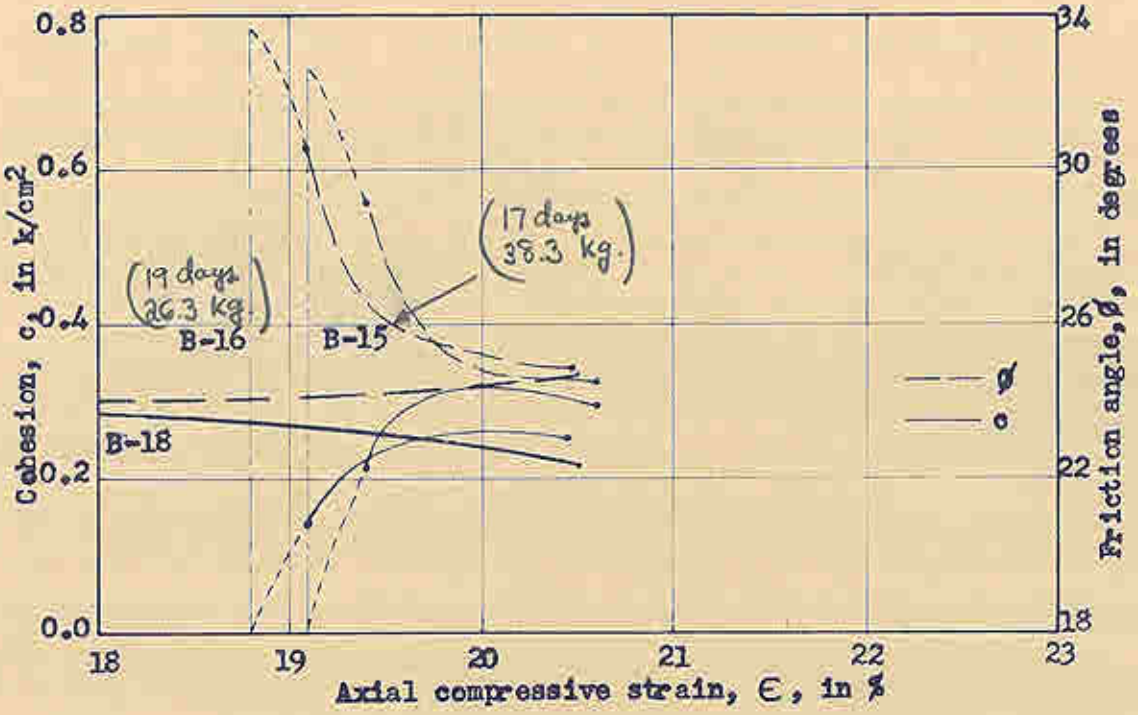

Figure 10.-Computed results of CFS-tests on BBC samples

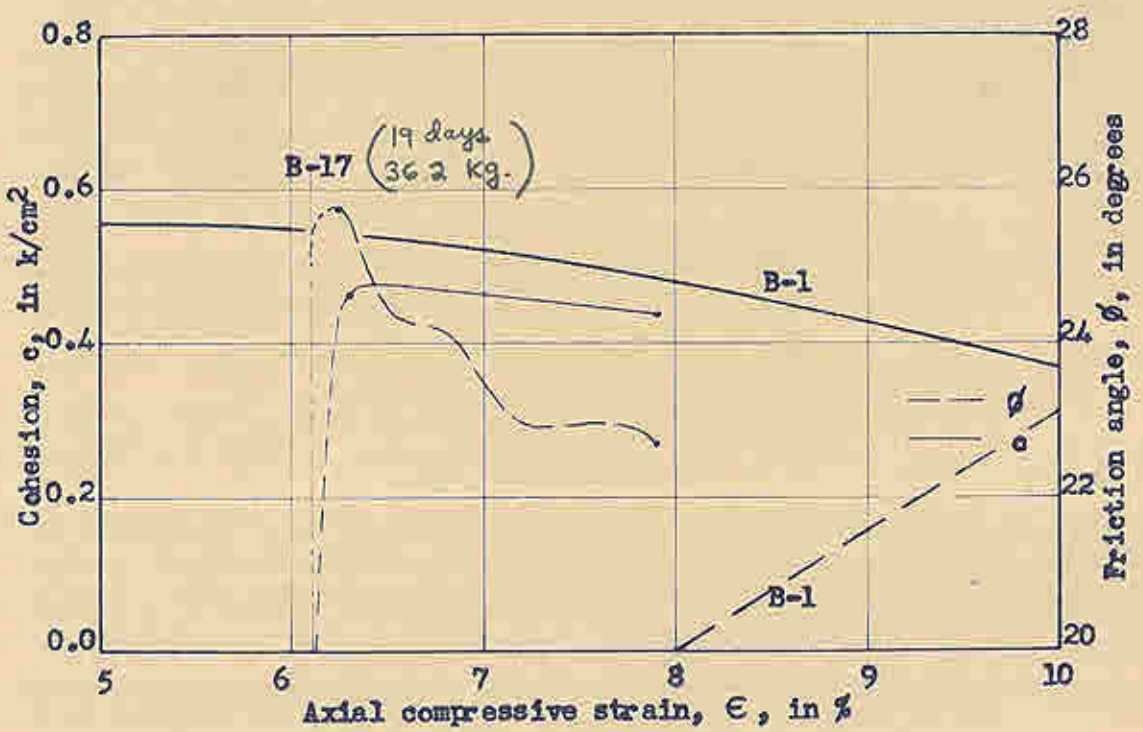

Figure 11.-Computed results of CFS-tests on DWEPK samples

Extrapolation of c and $\emptyset$ to Zero CFS-test Strain.- As was previously noted, the short dashed lines connecting the c and test curves with the zero CFS-test strain are the result of extrapolations based on computations using the Coulomb-Hvorslev failure criteria.

Since the axial load supported at the final creep strain (zero CFS-test strain) was known, as was the minor principal intergranular stress, this left c and $\emptyset$ as unknowns in equation 2. The equations for the extrapolation procedure to be discussed are shown in Figure 12. First $\emptyset$ was graphically extrapolated to zero CFS-test strain and then this value was used to compute the required initial cohesion as given by equation 5. Secondly it was assumed that the initial value of cohesion was zero and the initial value of friction was computed using equation 6.

Only tests B-10, B-13, and B-14 could be extrapolated using the first procedure. The remainder of the tests indicated that the initial value of cohesion was zero, or possibly negative, and that the total load was carried by the frictional component of strength. Table 6 presents the results of some of these computations.

The Possibility of an Apparent Negative Cohesion.- In the preceding discussion it was noted that in order to satisfy the Coulomb-Hvorslev failure criteria, it was found for 11 of 14 tests that to produce an extrapolation without abrupt discontinuities in the friction angle curve required that the initial cohesion be zero or negative. This conclusion was based on two computations; one

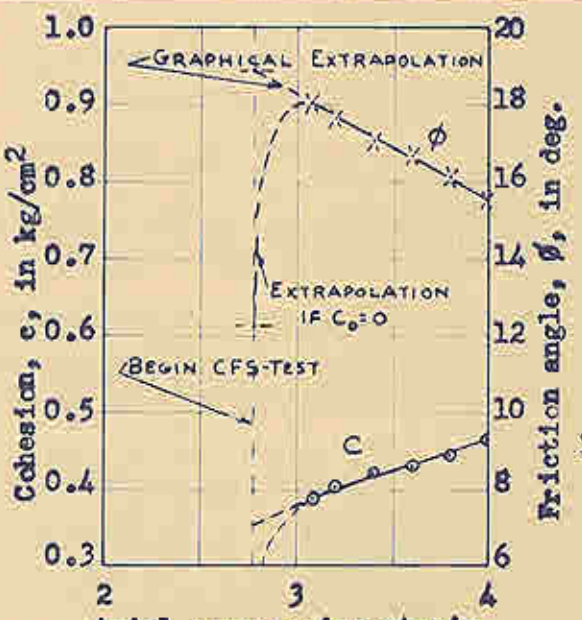

Test B-9

Equation (2) from Fig. :

$$\frac{\sigma_a}{2}=\left(\frac{\sin\phi_e}{1-\sin\phi_e}\right)\sigma_3+C_e\left(\frac{\cos\phi_e}{1-\sin\phi_e}\right)$$

Solving for the cohesion:

$$C_e=\left(\frac{1-\sin\phi}{\cos\phi}\right)\frac{\sigma_a}{2}-\tan\phi\ \sigma_3 \qquad (5)$$

Assuming the cohesion equal to zero and solving for ϕ:

$$\sin\phi_{\substack{e\\c=0}}=\frac{\sigma_a}{2\sigma_3+\sigma_a} \qquad (6)$$

The data at the end of the creep test for test B-9, shown to the left, was:

σ_a = 1.89 kg/cm²
u = 0.12 kg/cm²
σ_n = 3.65 kg/cm²
ϵ = 2.77 %
$\sigma_3=\sigma_n-u$ = 3.53 kg/cm²

Figure 12 - Cohesion - Friction Extrapolation To Zero CFS-Test Strain

TABLE 6

COHESION--FRICTION EXTRAPOLATION

Test. No.	Comp. Φ_o if $c_o = 0$ deg.	Graphical Extrap. Φ_o deg.	Comp. c_o for Extrap. kg/cm^2	σ'_{max} creep	σ'_{max} IOS	Graphical Extrap. c_o kg/cm^2
B-4	18.4 DW	22.0	-0.20	4.10	3.32	+0.47
B-6	8.0 BBC	13.0	-0.37	4.63	3.41	+0.38
B-9	12.2 DBC	19.0	-0.52	5.42	3.40	+0.36
B-10	21.7 DBC	19.0	+0.12	3.52	3.40	+0.25
B-13	21.5 UBBC	15.0	+0.31	3.77	3.51	+0.35
B-14	20.6 UDBC	15.0	+0.27	3.85	3.50	+0.40
B-15	29.5 DBC	32.5	-0.17	4.69	3.43	0.00

Obviously extrap $\phi \rightarrow$ c negative error with oc that occurred relative to creep test / IOS test ϕ_a

BNEOK	B-2		4.27	3.27
"	B-3 1.5%		3.54	3.42
BBC	B-7 ε_{creep} 2.7%		3.33	3.41
"	B-8 6.3%		3.90	3.40
"	B-11 1.6%		3.94	3.40
"	B-16		4.44	3.43

utilizing a graphically extrapolated value of friction angle; and the other utilizing the assumption of zero cohesion at zero CFS-test strain. The computations in the former case indicated negative values of cohesion except for the three cases noted. Since negative cohesion is not a conventional concept, the majority of extrapolations were made on the basis of zero initial cohesion.

The equations and CFS-coordinates for such a test, B-9, are shown in Figure 12. This test was performed at a strain rate less than 0.1 per cent axial strain per minute; thus, permitting good definition of the cohesion-friction variation at very low CFS-test strains. Performing a graphical extrapolation on the friction angle curve to zero CFS-test strain, a value of 18.8 degrees is obtained for the initial friction angle, ϕ_o. Using equation 5 to compute the value of cohesion gives:

$$c_o = \frac{1 - \sin 18.8^o}{\cos 18.8^o} \cdot \frac{1.89}{2} - 3.53 \tan 18.8^o$$

$$c_o = -0.52 \text{ kg/cm}^2$$

which is shown in Table 6. Thus, this extrapolation without abrupt variations in the friction angle curve requires that there be an negative value for the initial cohesion, c_o. If it is now assumed that the initial value of the cohesion is zero the required value of the friction angle is found from equation 6 as follows:

$$\sin \phi_o = \frac{1.89}{(2)\ (3.53)\ +\ 1.89} = 0.211$$

$$\phi_o = 12.2^o$$

as shown in Figure 12 as the value of the friction angle for the given conditions.

The question arises as to why there should be such an abrupt increase in friction with the small additional strains when the soil has already been highly strained. For there to be no abrupt change in friction over these small initial CFS-test strains requires a negative value of cohesion. Thus, this data suggests the possibility of the sample exhibiting an apparent negative cohesion.

Tests Indicating a Positive Value of Initial Cohesion.- In the preceding discussions it was noted that only three tests, B-10, B-13, and B-14, indicated some positive initial value of cohesion. A possible explanation for this may be obtained from the creep diagrams for these tests.

Test B-10 on BBC was tested two days from the time of initial loading at which time the sample was still in the transition period from initial adjustment to the visco-plastic portion (Figure 37). Tests B-13 and B-14 on U-BBC were tested in the visco-plastic portion of the creep diagram (Figure 38). It is interesting to note the high creep rates these specimens exhibited at the time of testing. These creep rates were on the order of two to ten times those noted in the other tests (Table 7). It was also noted in the CFS-tests on B-13 and B-14 following creep that it was not possible for the sample to mobilize any greater frictional resistance. These facts would suggest that the rate of creep may depend on the degree of mobilization

TABLE 7

COHESION--CREEP RATE

Test No.	Sample Type	Initial Cohesion kg/cm^2	Creep Rate mm/day
B-3	DWEPK	-0.12	0.005
B-6	BBC	-0.37	0.009
B-9	BBC	-0.52	0.006
B-10	BBC	+0.12	0.073
B-13	U-BBC	+0.31	0.022
B-14	U-BBC	+0.27	0.090

of the viscous cohesive component of strength.

Possible Creep-Failure Criterion.- On the basis of the foregoing evidence it seems possible that the creep deformations will reach a finite value only if the soil is able to mobilize enough frictional resistance to eventually carry the applied stresses. As long as part of the applied stress is carried by the viscous cohesional component of strength, the soil will creep. Thus, it may be possible to obtain creep failures when: (1) Any environmental conditions, such as an increase in pore water pressure, causes a decrease in the intergranular pressure and thus a decrease in the frictional resistance, and (2) if the soil cannot mobilize enough frictional resistance to withstand the applied stresses.

The Creep Characteristics of the Soils Used in This Study

General.- For the testing conditions and the soils used in this investigation the creep curves, shown in Figures 36 through 40, were generally divided into two characteristic stages. The first stage, commonly termed the initial elastic adjustment or initial adjustment stage, was characterized by a very high strain rate and large deformations. This initial adjustment was responsible for the greatest proportion of the total deformation. Within a short period of time, which varied from 1,000 to 4,000 minutes, there was a sharp decrease in strain rate. The strain rate hereafter remained essentially constant. Thus, the second stage of creep action, commonly termed the visco-plastic portion, was characterized by an

essentially constant creep rate. The third stage of creep action, increased strain rate to failure, was not obtained during this study. These creep characteristics were obtained for the zero to full loading period of one hour; for the remolded and undisturbed samples, and for creep periods up to nineteen days. A summary of the data obtained during the creep test is presented in Table 5.

Test Series A and B.- A comparison of these series of tests is shown in Figure 13. These tests were performed on DWEPK and BBC samples under the same testing and corresponding loading conditions. The results show that the DWEPK samples generally had less initial adjustment than the BBC samples. The creep rates at the same loads were approximately the same in those two soils (Table 5).

Test Series B, C, and D.- These tests were all performed on Boston Blue Clay remolded and undisturbed samples. A comparison of these tests is shown in Figure 14. This figure shows the influence of load, consolidation period, and structure of the soil on the creep characteristics of the same soil.

A comparison of tests B-8 and B-13, both subjected to about the same load, indicates the marked influence of structure on the creep characteristics of the sample. The U-BBC samples had an initial adjustment which was about 35 per cent of that for the BBC sample under the same conditions. Also the creep rate for the U-BBC was twice that for the BBC. A similar comparison of tests B-8 and B-10 will show the effect of the consolidation period. The BBC samples consolidated for 6,800 minutes had an initial adjustment which was

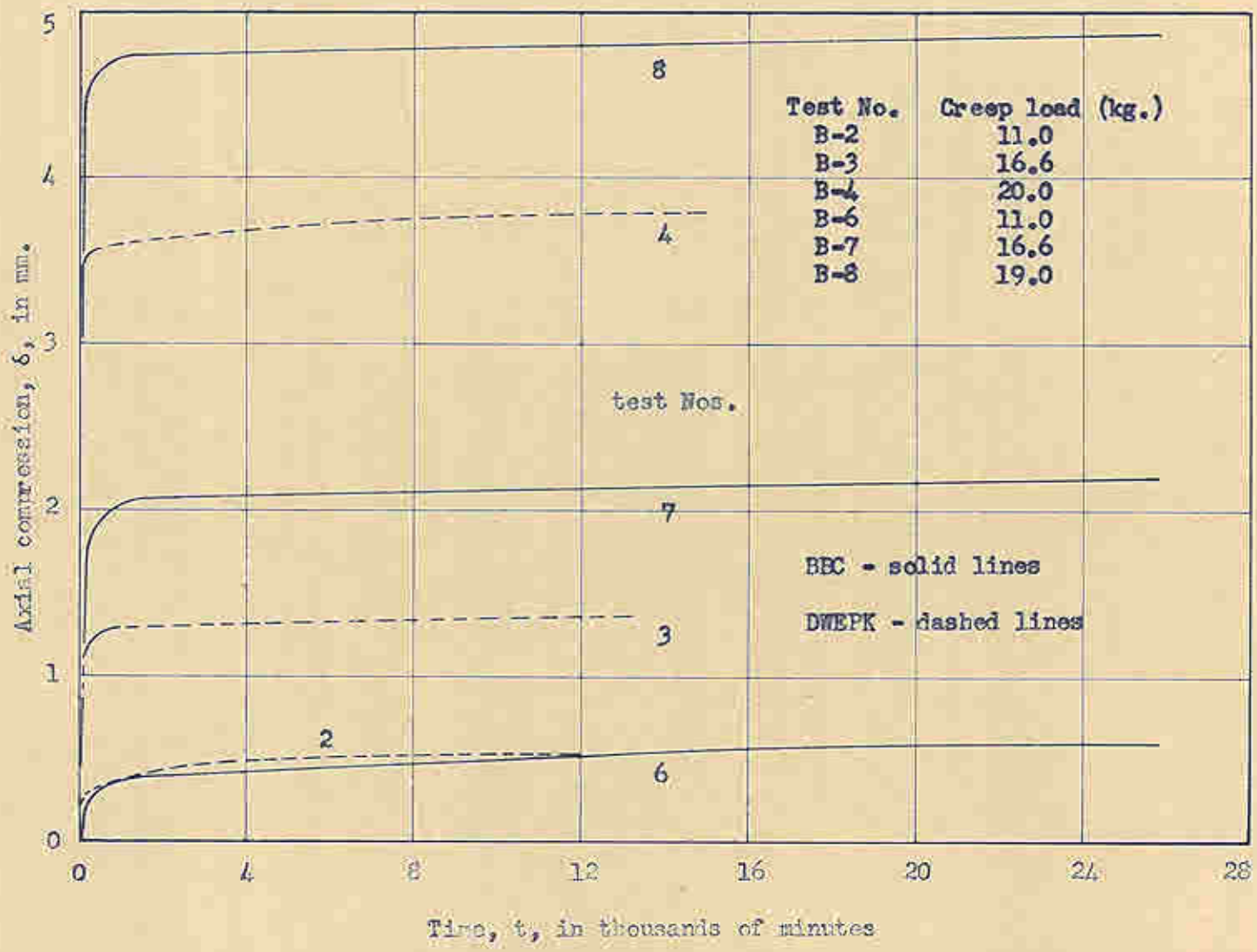

Figure 13.-Creep curves for BBC and DWEPK samples, test series A and B

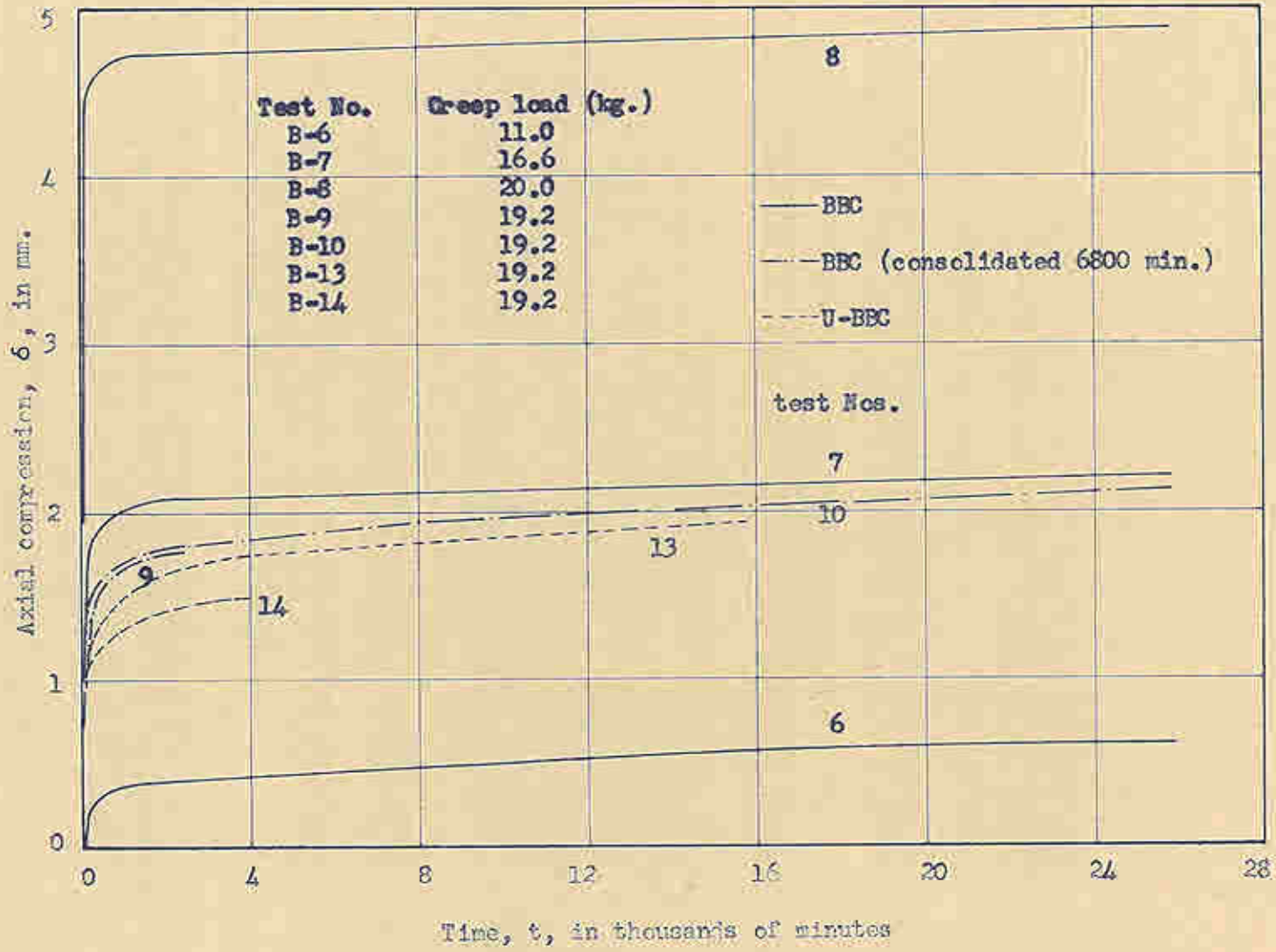

Figure 14.-Creep Curves for BBC and U-BBC samples, test series B, C, and D

about 35 per cent of that for the BBC samples consolidated 1,200 minutes.

A possible explanation of these widely different amounts of initial adjustment may be obtained from the standard CFS-tests on these samples before creep. For example, test B-8 (Figure 31) on BBC consolidated 1,200 minutes and subjected to a load of 19.0 kg showed an initial adjustment of 6.14 per cent axial strain; the standard CFS-test for this sample, Figure 20, shows a cohesion of 0.44 kg per cm^2 and a friction angle of 17.2 degrees at this strain. The test B-9 (Figure 38) on BBC consolidated 6,800 minutes and subjected to a load of 19.2 kg showed an initial adjustment of 2.30 per cent axial strain; the standard CFS-test for this sample (Figure 25) shows a cohesion of 0.41 kg per cm^2 and a friction angle of 17.0 degrees. Upon a comparison of these values it is seen that in the first case it took 6.14 per cent strain to mobilize the same strength shown in the second case at 2.30 per cent strain. A comparison of the other tests, which requires slightly more detailed calculations, will give similar results. Therefore, it appears likely that the magnitude of the initial adjustment, which comprises the greatest portion of the total deformations, will depend on the standard CFS characteristics of the soil before creep.

Test Series E.- The results of a previous investigation (6) indicated that a third stage, increased strain rate to failure, could be obtained in the creep diagram for a compression test on a soft clay soil. This is a characteristic behavior of a material tested in tension or in shear (60) but it is difficult to visualize such

a failure in compression.

In an attempt to produce such a failure by increased loading, an incremental loading procedure was applied to the specimens of test series E, shown in Figure 40. A high initial load was applied in the usual manner and the specimens allowed to deform for about ten days, after which time the creep rates had become very small. Increments of load, as shown in Figure 40, were applied thereafter.

It is noted for the tests on BBC that only "limited failures" were obtained; there would be a greatly increased strain rate for a period of about one day, after which time the deformations would almost cease. Failure planes were noted in these samples following the temporarily increased strain rate. The increased loading only slightly increased the strain rate of the DWEPK sample. Thus, for these very high loads and creep period up to nineteen days it was not possible to obtain the increased strain rate to failure portion of the creep diagram.

The Pore Water Characteristics During Creep

General.- The variation of the pore water pressure with time is shown for the various test series in Figures 40 through 44. For the majority of samples there was a peak in the pore water pressure in the early part of the creep test. This usually occurred a short time after the total load had been imposed and while the sample was in the transition from the first to second stage of creep. This peak pore water pressure, which was sustained for various lengths

of time, was generally followed by a decrease in pressure. The peak and final pore water pressures are tabulated in Table 5.

The Remolded Soils.- The general variation of the pore water pressure with time for BBC and DWEPK samples was the same as noted above. These tests indicate that there was a stress transfer occurring during the creep process; a transfer from the pore water to the soil structure as the creep period increased.

The Undisturbed Soil.- The behavior of the pore water pressure with time in the U-BBC samples, Figure 44, is seen to be somewhat different from that noted in the BBC samples, Figure 42. The pore water pressure quickly builds up to a maximum value which is then maintained throughout the remainder of the creep test. This would indicate that it was not possible for the U-BBC samples to effect such a transfer of stress with time as was noted in the BBC samples.

Comments on Pore Water Pressure Measurement.- In an interpretation of these results it is important to recognize the experimental conditions of the observations. The pore pressure was measured by means of a mercury manometer with an accuracy better than $\pm$ 0.01 kg per cm^2. Due to the coupled external-internal drainage system the measured values of the pore pressure are probably representative of that throughout the sample. The possibility of the decrease in pore water pressure due to the dissolving of the small (less than 2 per cent) amounts of air under the low (less than 2.5 kg per cm^2) pore

pressures seem slight, and any error due to leakage in the lines or membranes would be reflected as an increase in pore water pressure.

SECTION VII

CONCLUSIONS OF THIS INVESTIGATION

Conclusions Directly Supported by Experimental Data:

1. There is a transfer of stress to the frictional component of strength during creep in a near saturated clay soil.
2. In the remolded soils there is generally a decrease of pore water pressure with time. This decrease was not evident in the undisturbed soil.
3. For the conditions of this investigation, the soils exhibit the first and second stages of creep action.
4. The period allowed for consolidation of the sample will have a marked influence on both the cohesion-friction-strain characteristics and the creep characteristics.

Conclusions Suggested by Experimental Data:

5. There is a possibility that a near saturated clay soil may exhibit an apparent negative value of cohesion.
6. The creep rate in the visco-plastic or second stage of creep action may depend on the degree of mobilization of the viscous cohesive component of strength.
7. The magnitude of the initial adjustment during the creep process may depend on the cohesion-friction-strain characteristics of the soil before creep.

8. The experimental data suggests that it may be possible to obtain creep failures when : (1) Any environmental conditions cause a decrease in frictional strength, and (2) if the soil cannot mobilize enough frictional resistance to withstand the applied stresses.

APPENDIX

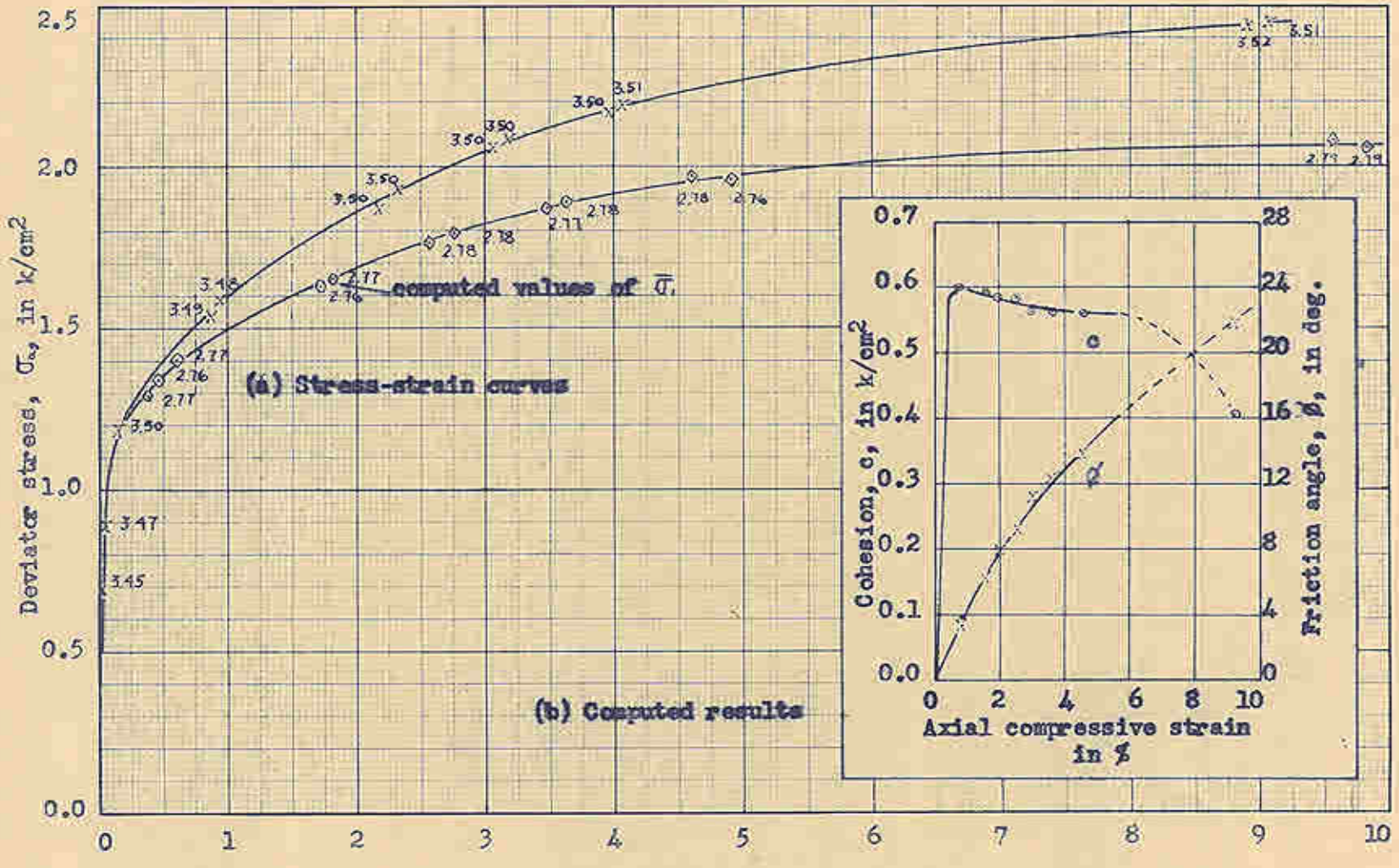

Figure 15.-CFS-test no. B-1, sample DWEPK 751

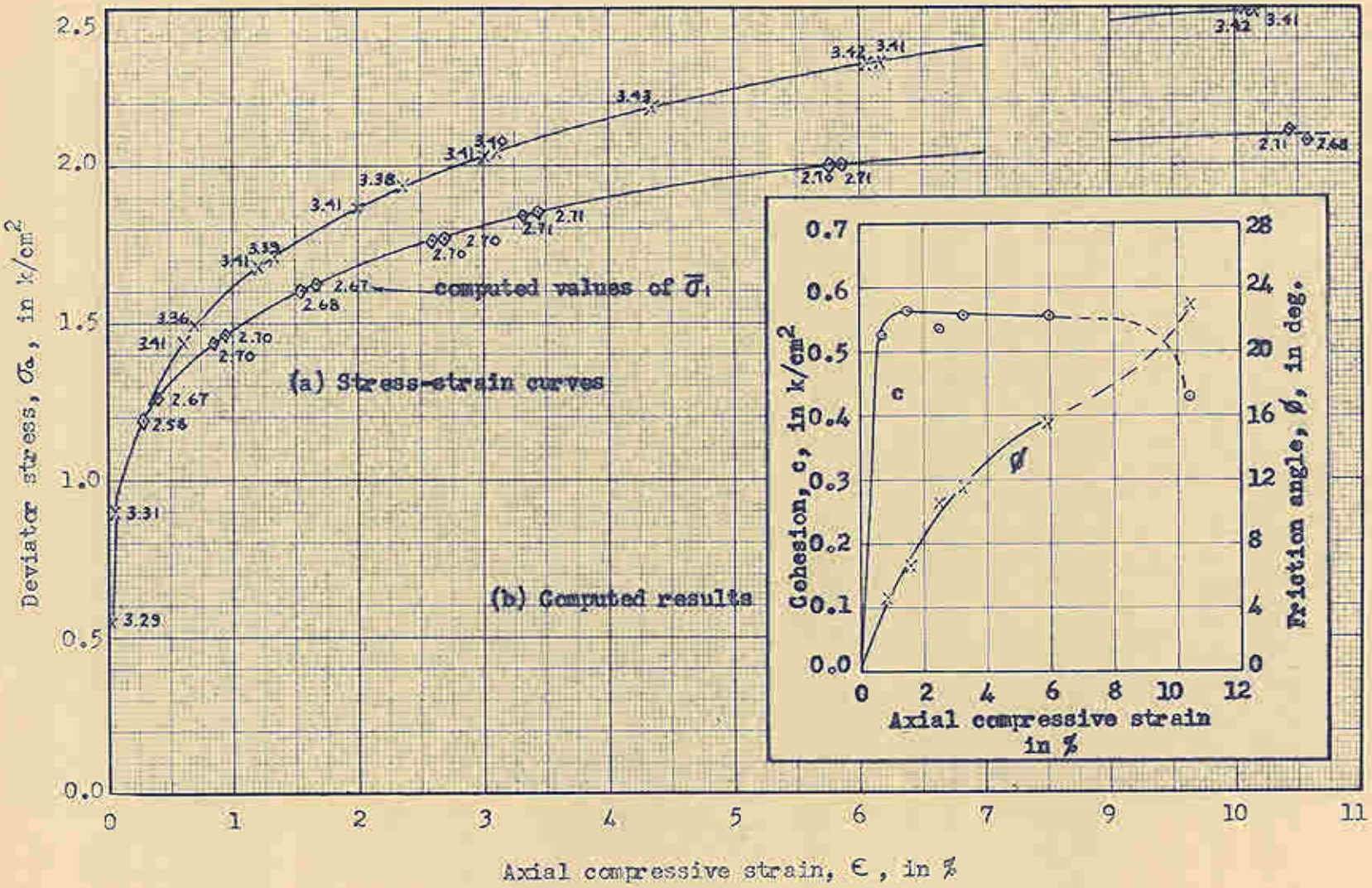

Figure 16. CFS-test no. H-13, sample DWEPK 799

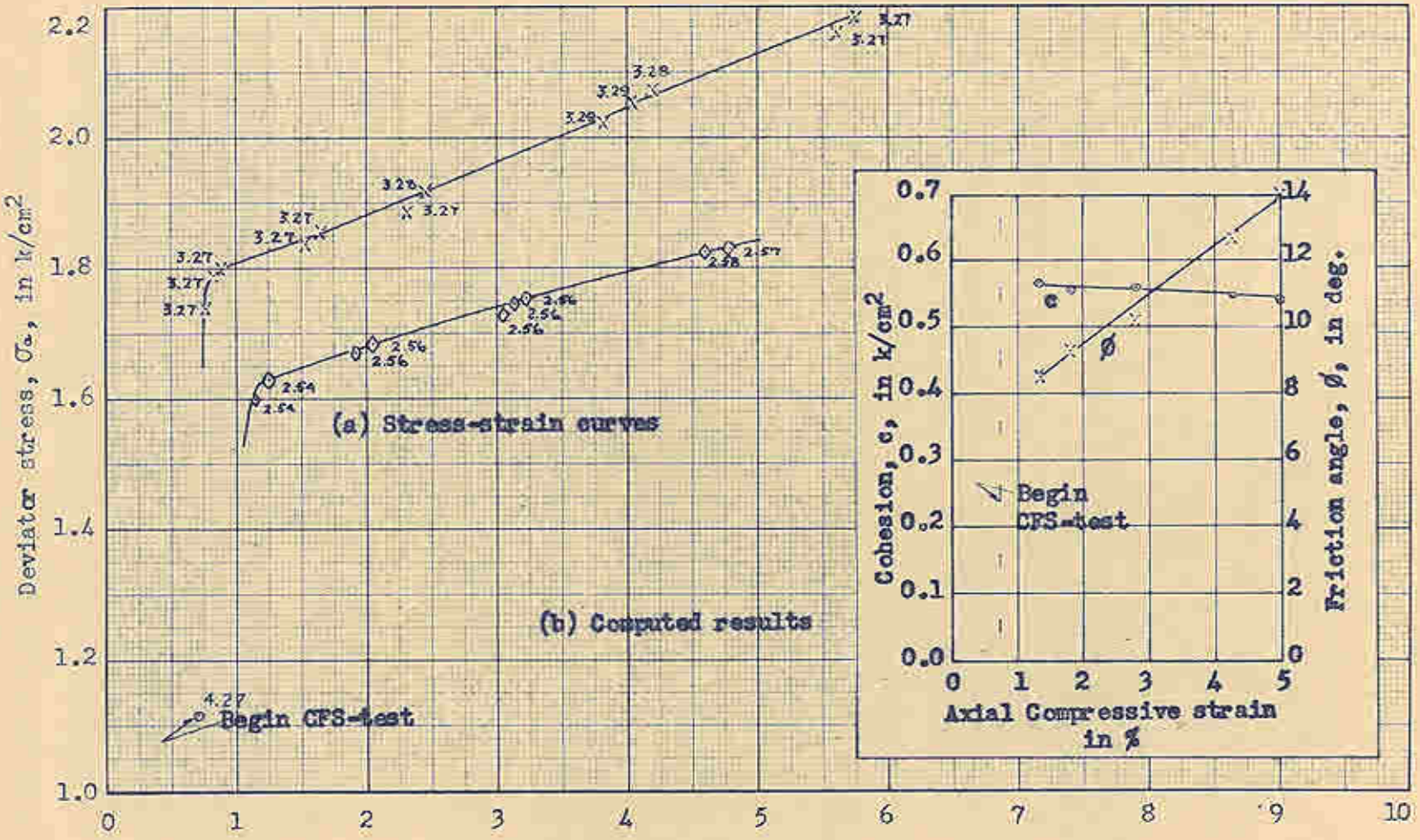

Axial compressive strain, ϵ, in %

Figure 17.-CFS-test no. B-2, sample DWEPK 752

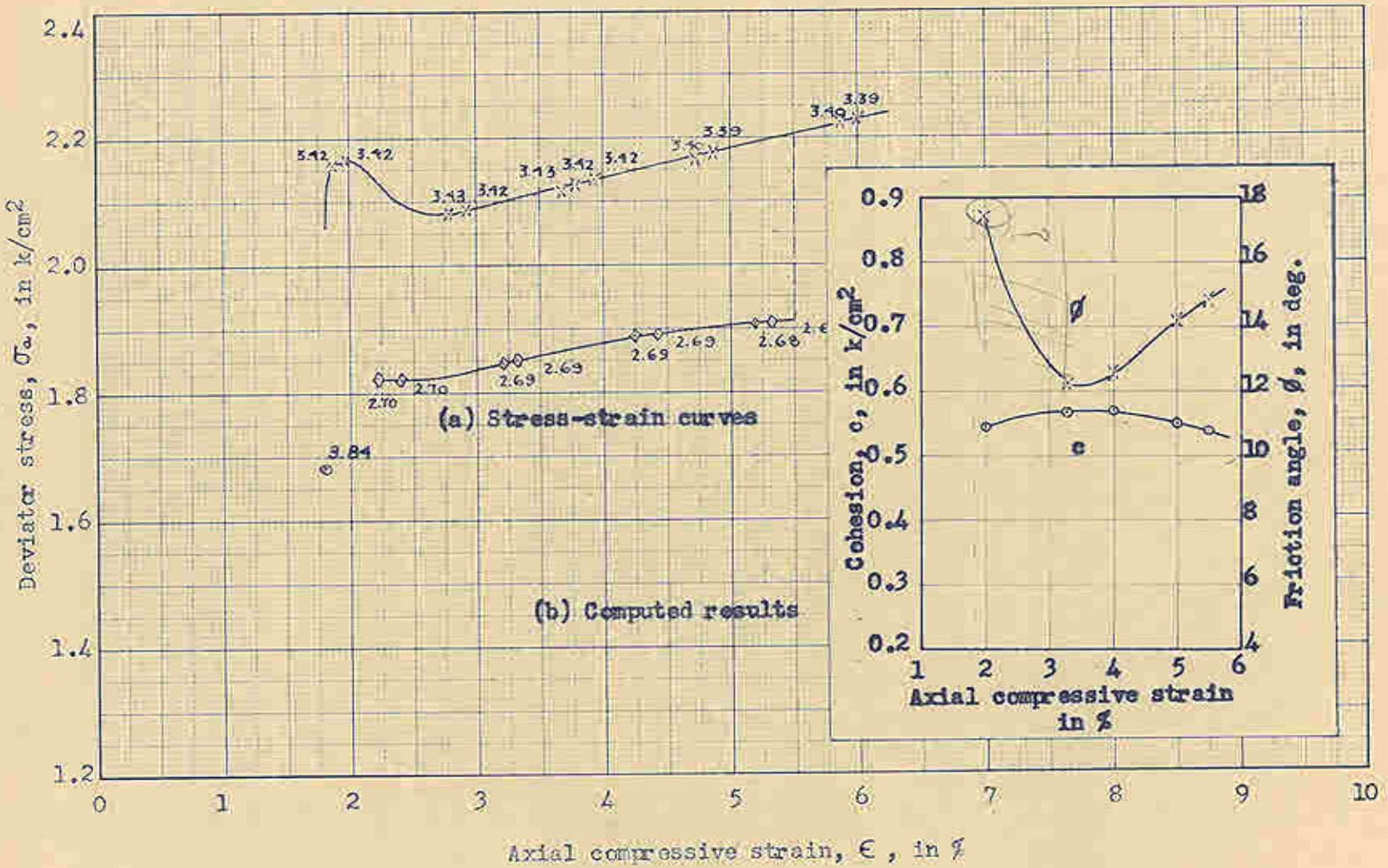

Figure 18.-CFS-test no. B-3, sample DWEPK 755

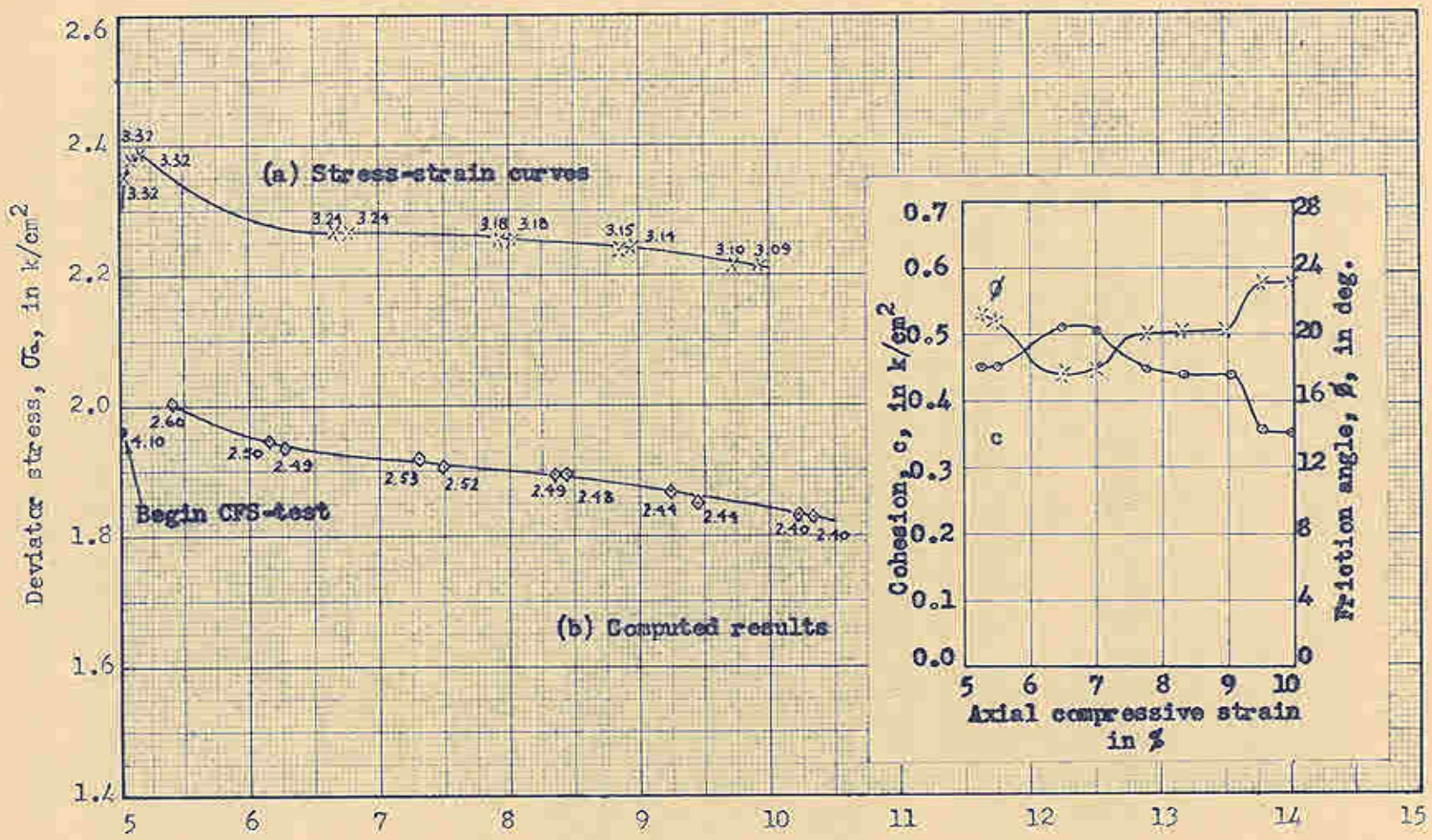

Figure 19.-CFS-test no. B-4, sample DWEPK 757

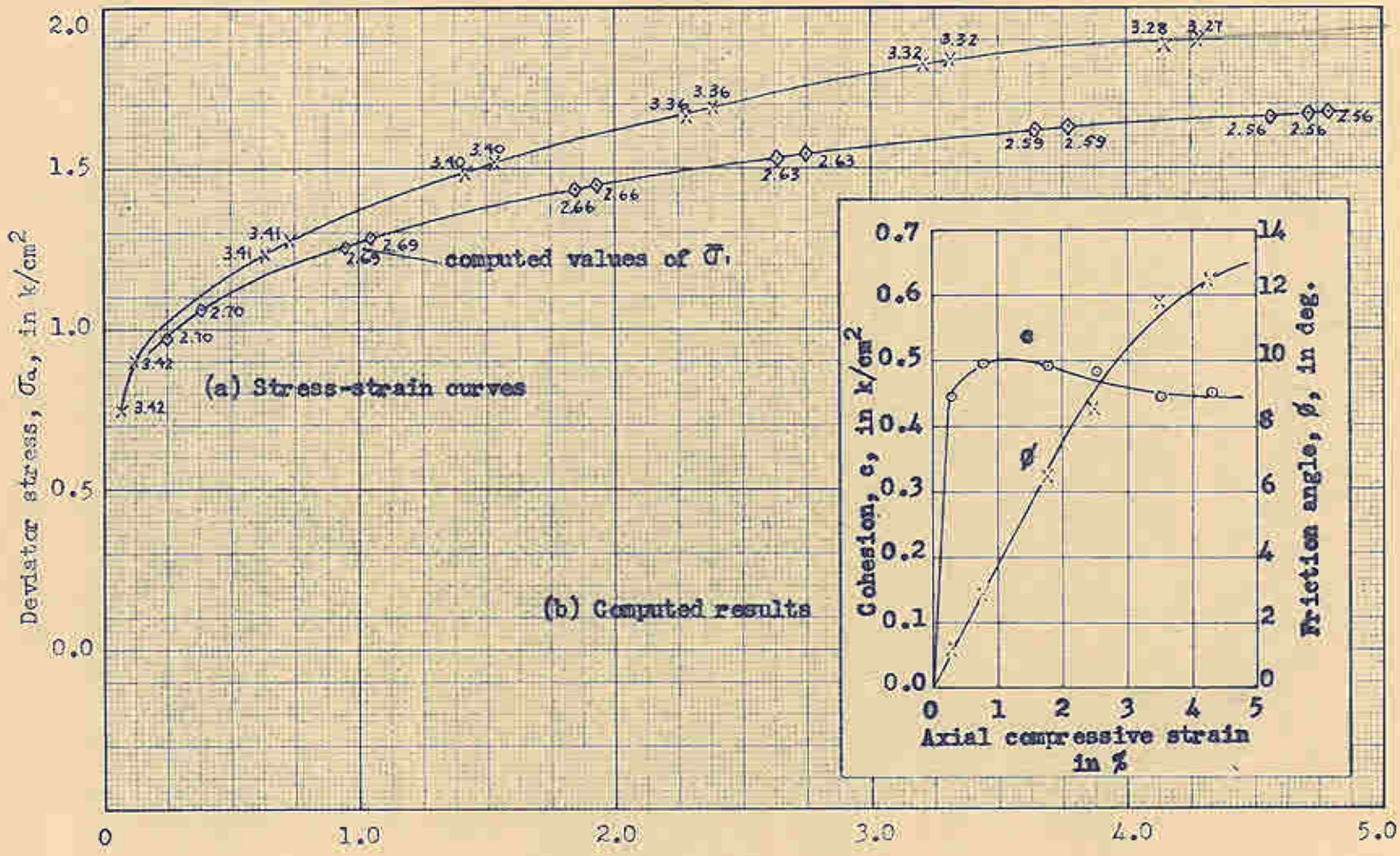

Figure 20.-CFS-test no. B-5, sample BBC 521

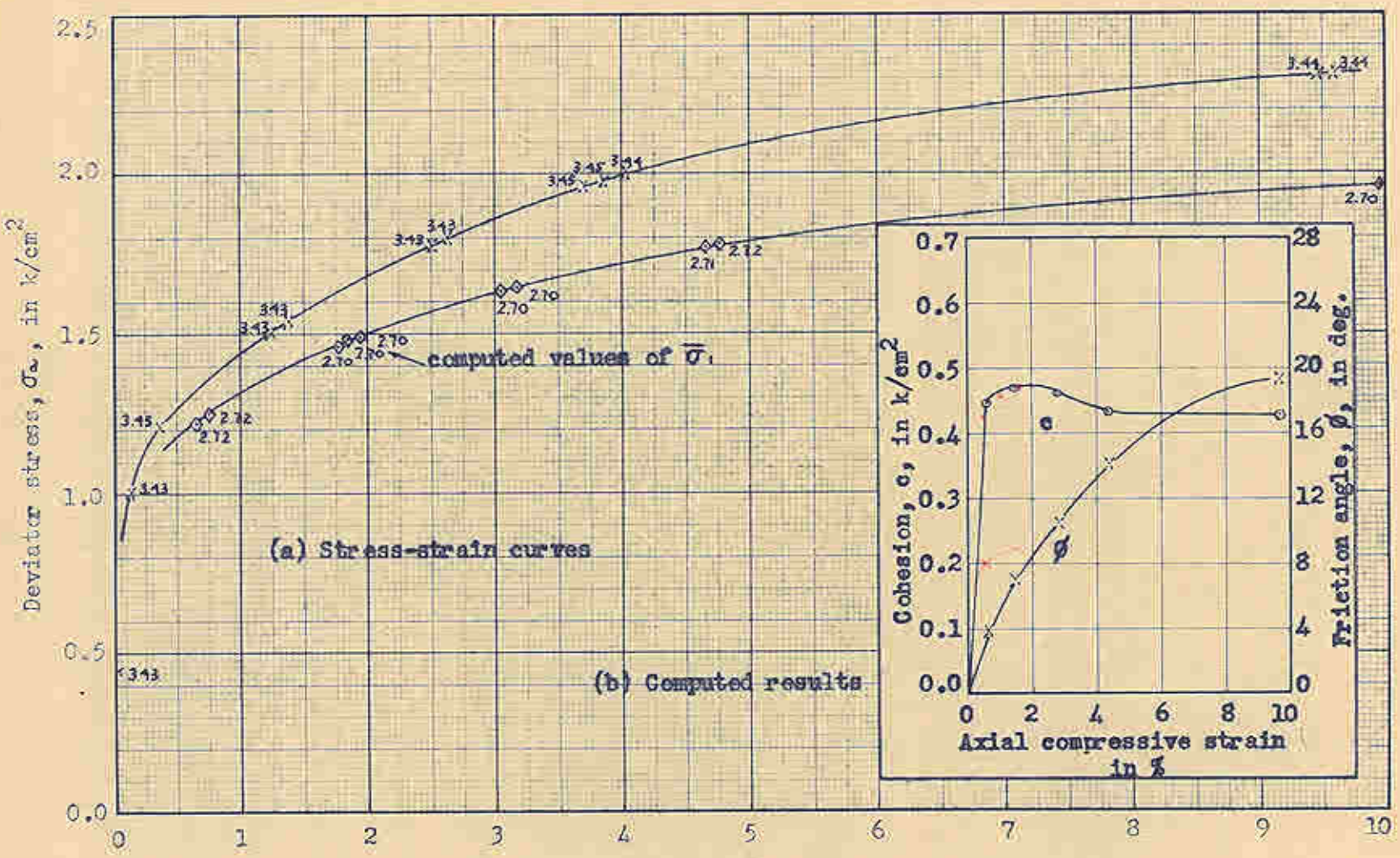

Figure 21.-CFS-test no. H-22, sample BBC 539

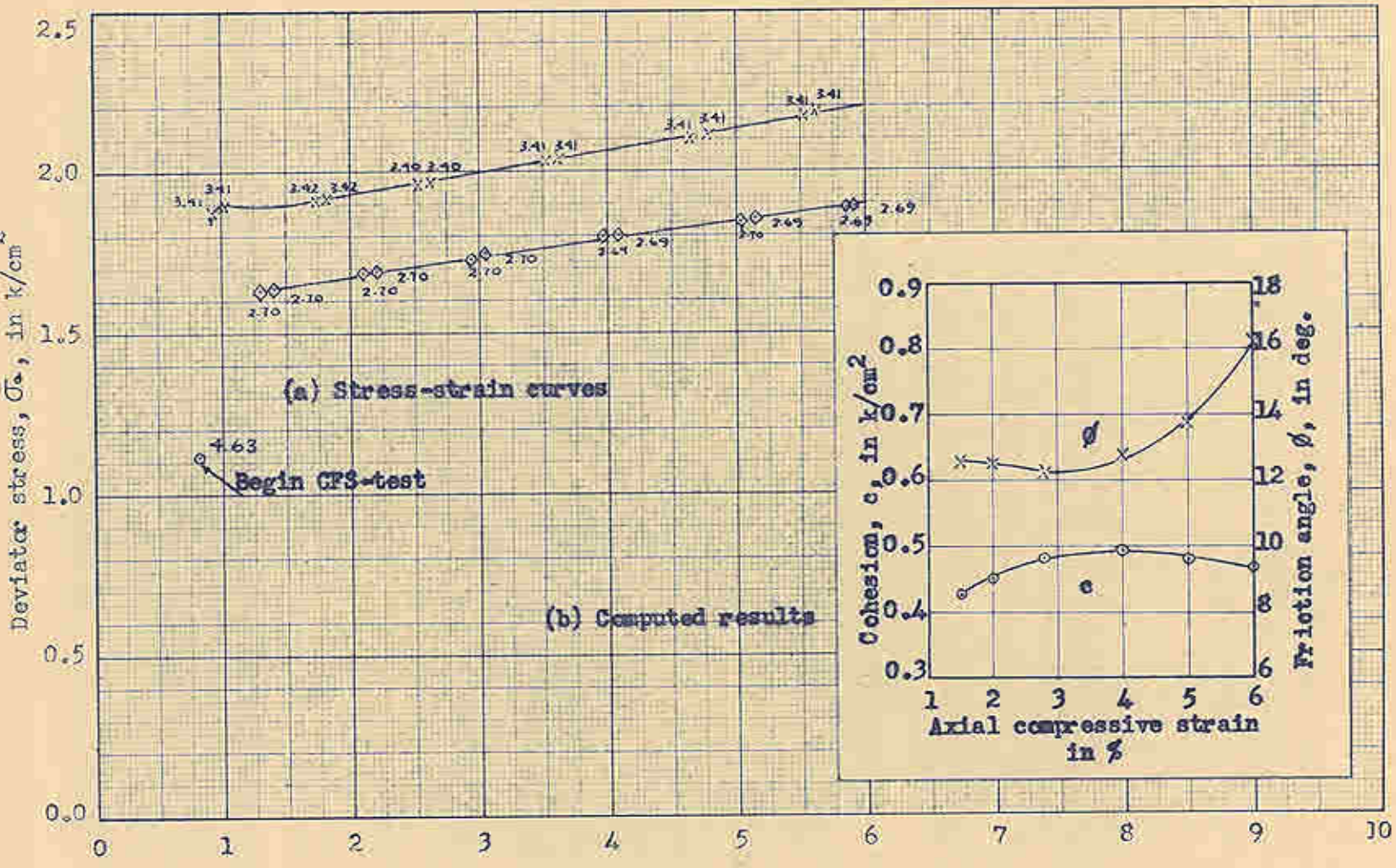

Figure 22.-CFS-test no. B-6, sample BBC 519

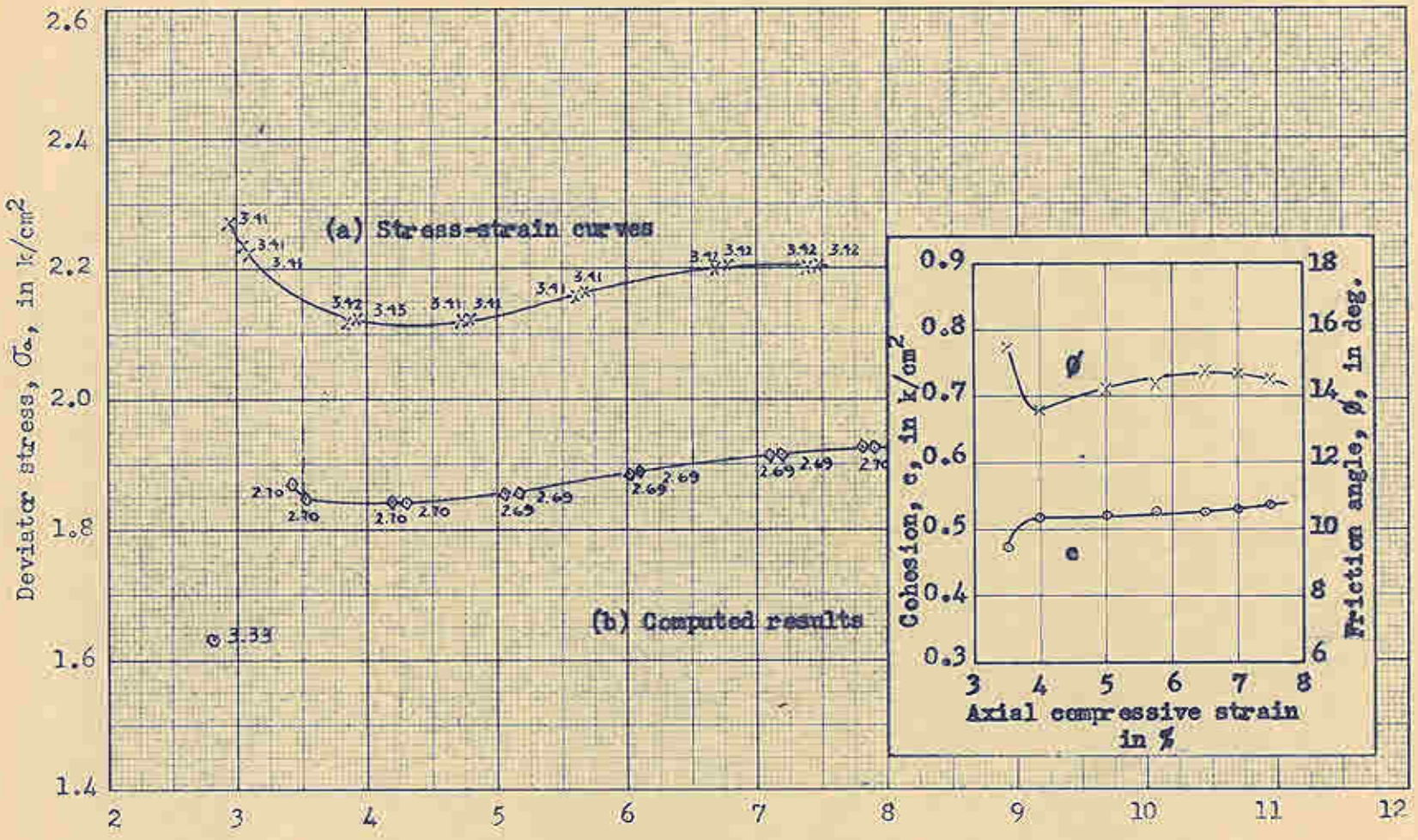

Figure 23.-CFS-test no. B-7, sample BBC 520

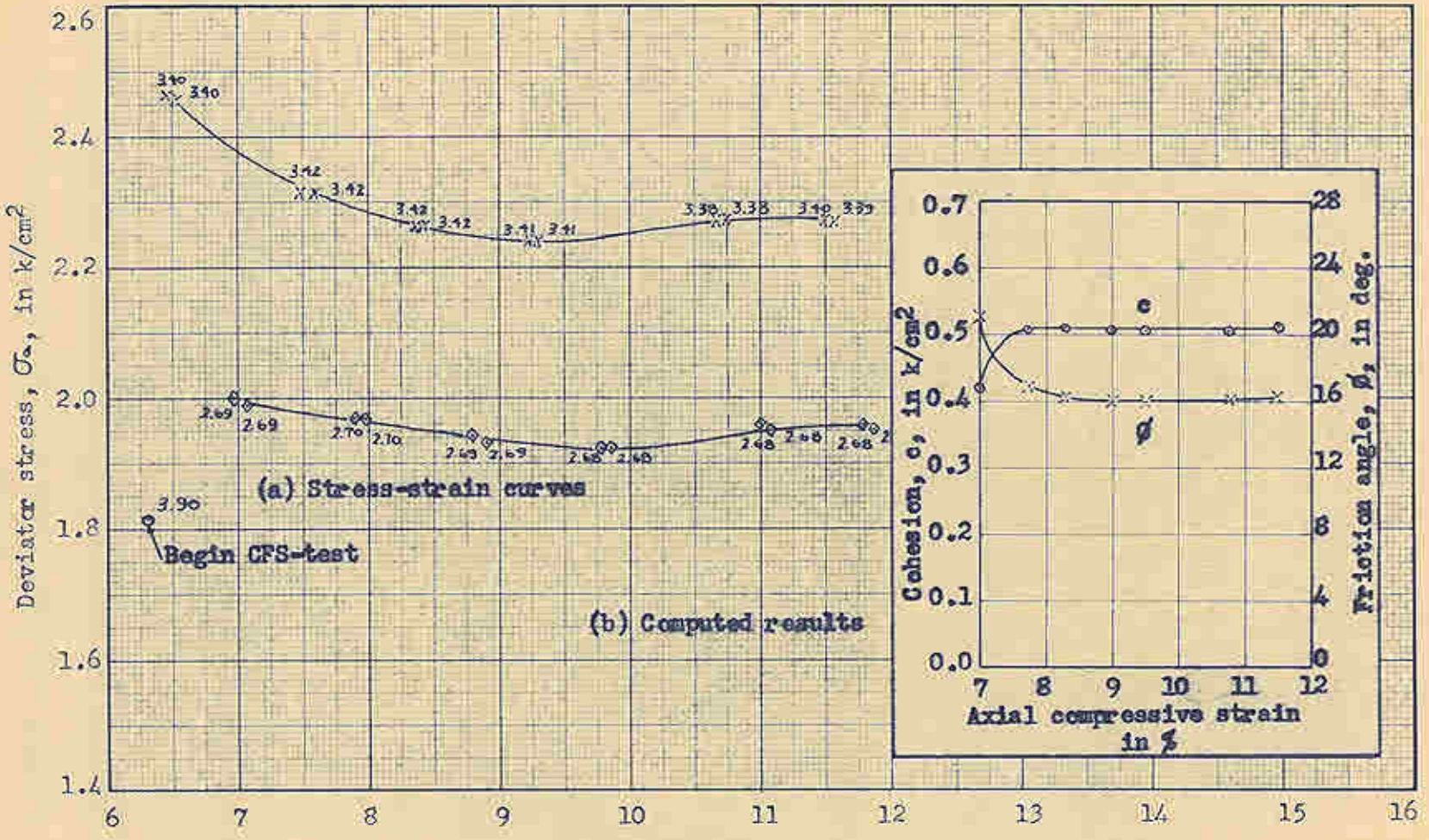

Figure 24.-CFS-test no. B-8, sample BBC 521

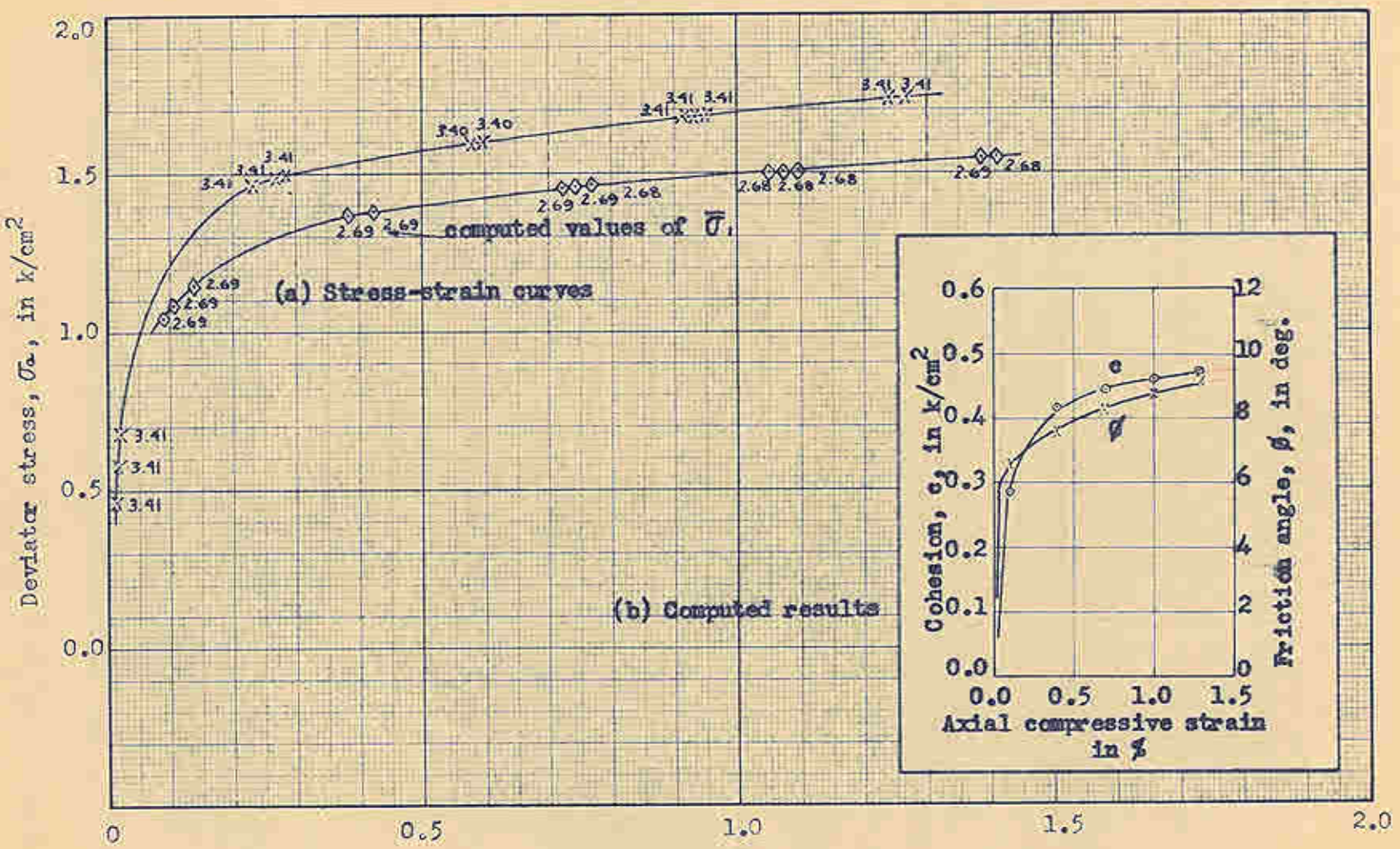

Figure 25.-CFS-test no. B-12, sample BBC 528

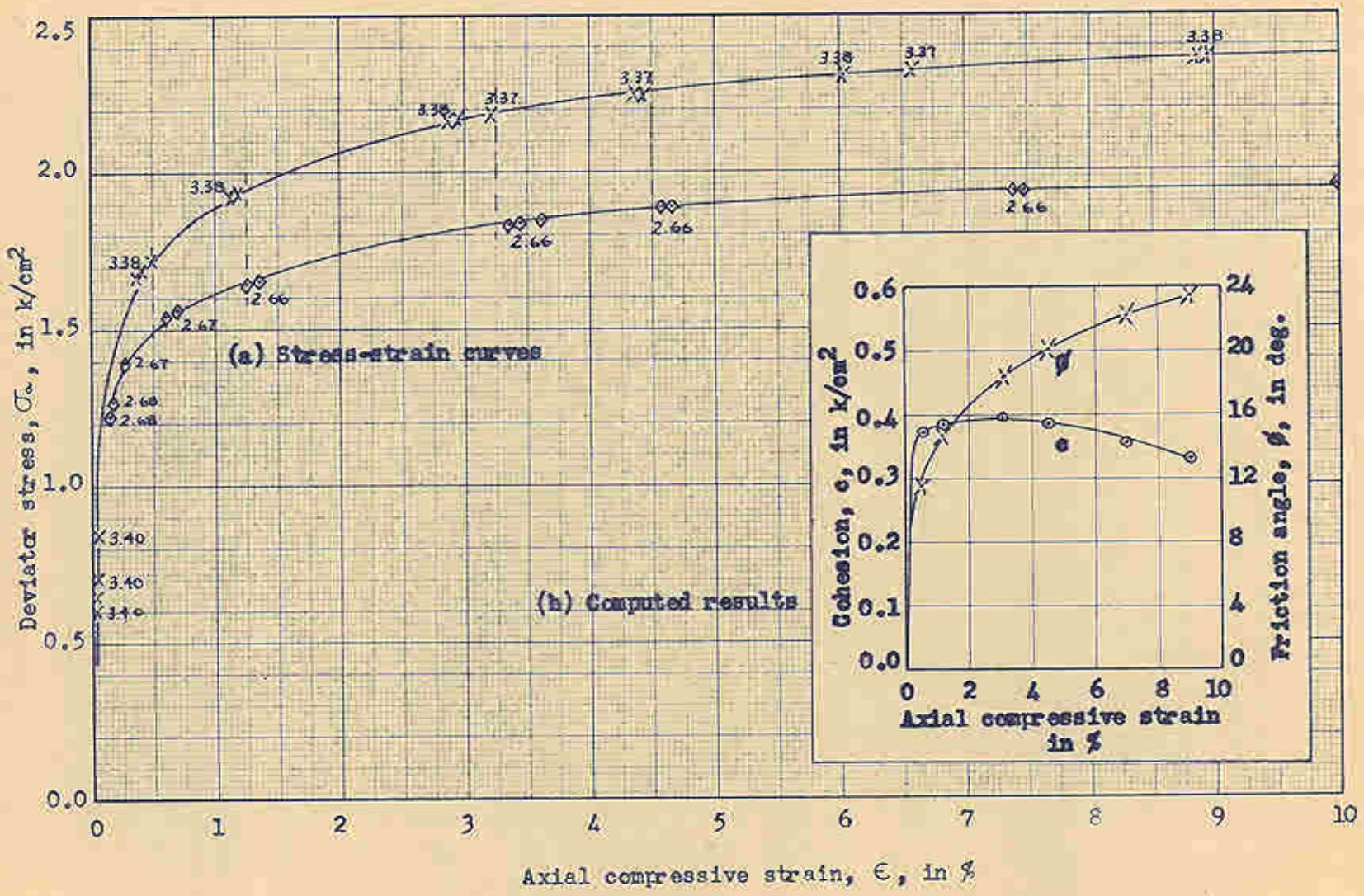

Figure 26.-CFS-test no. B-18, sample BBC 532

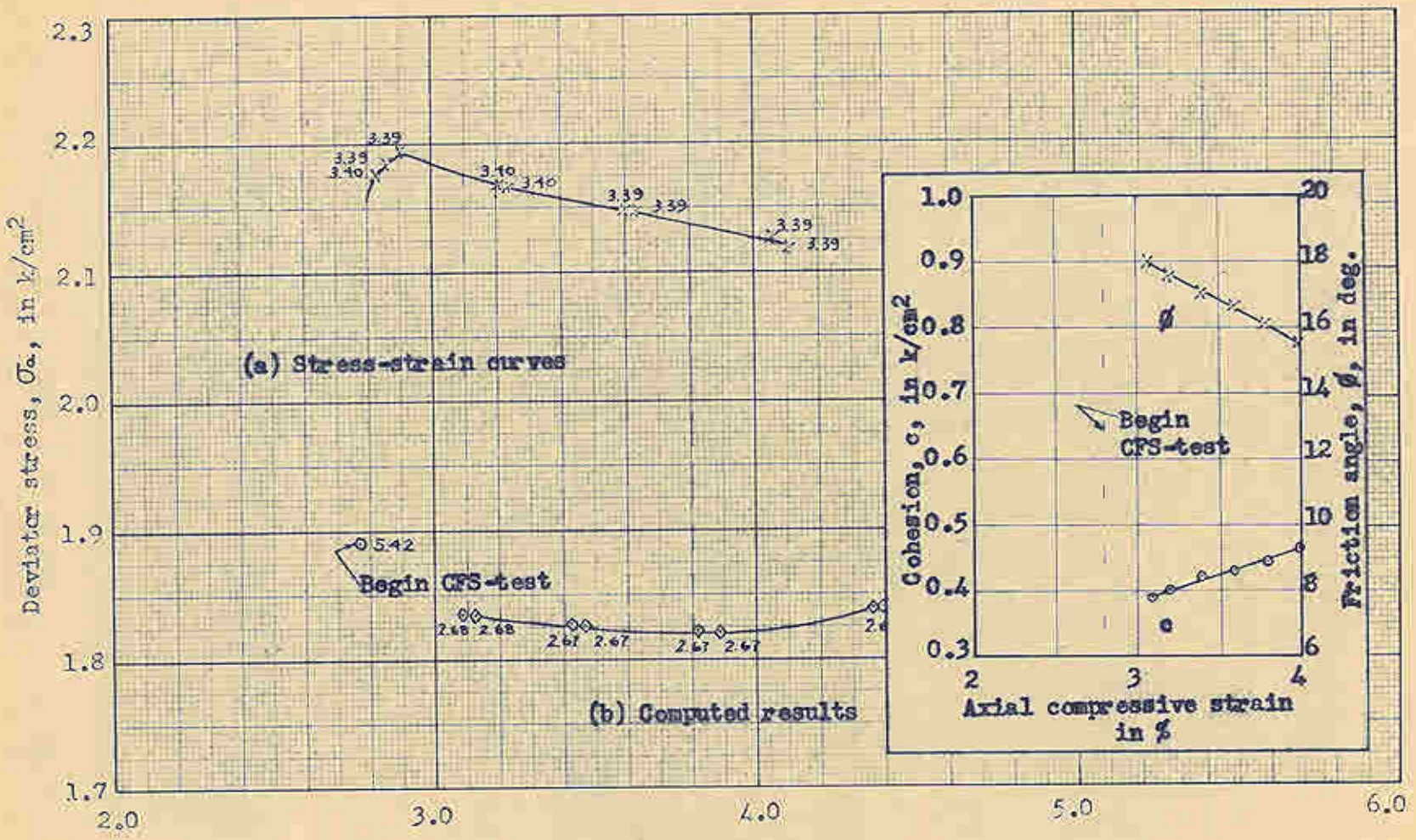

Axial compressive strain, ϵ, in %

Figure 27.-CFS-test no. B-9, sample BEC 525

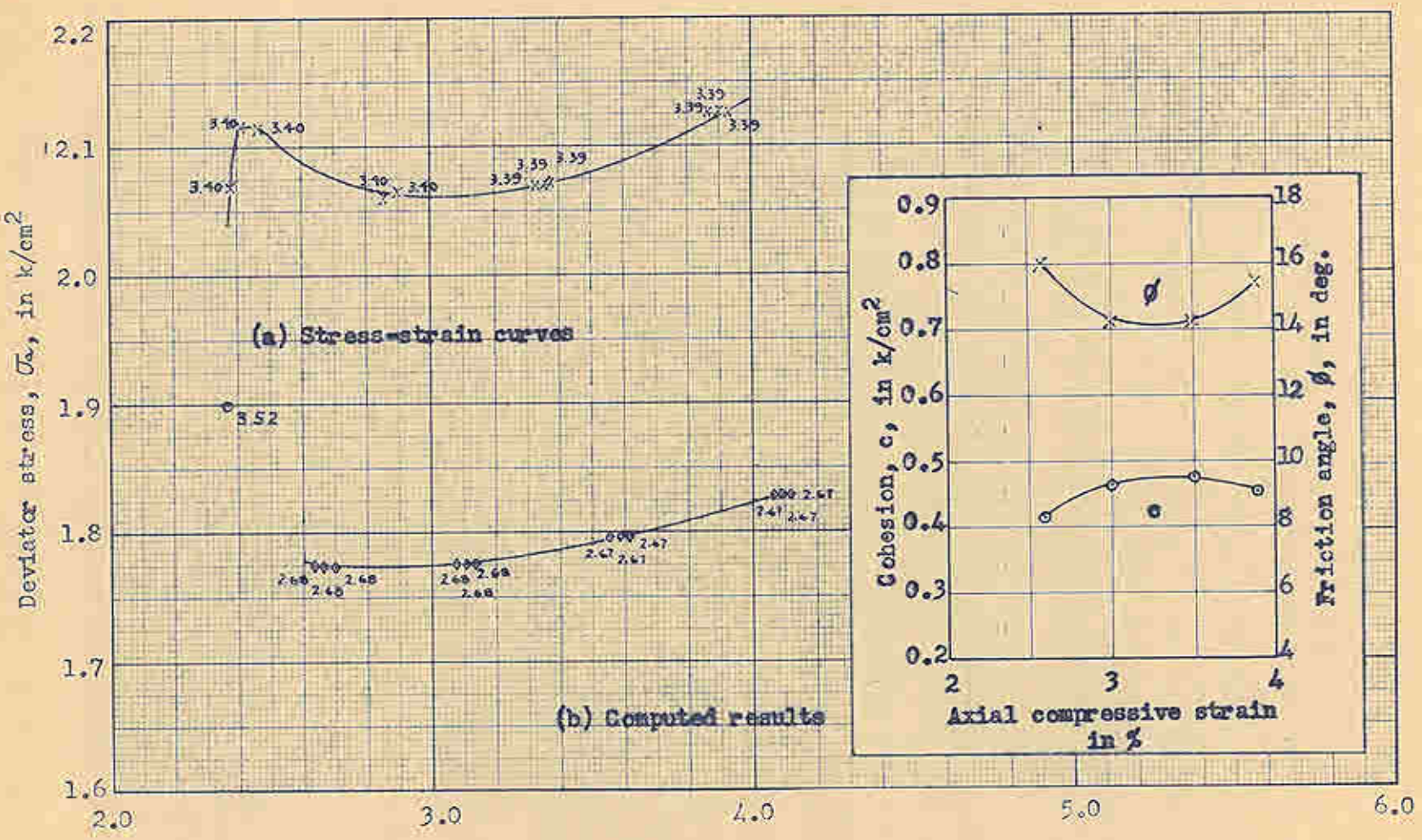

Axial compressive strain, ϵ, in %

Figure 28.-CFS-test no. B-10, sample BBC 526

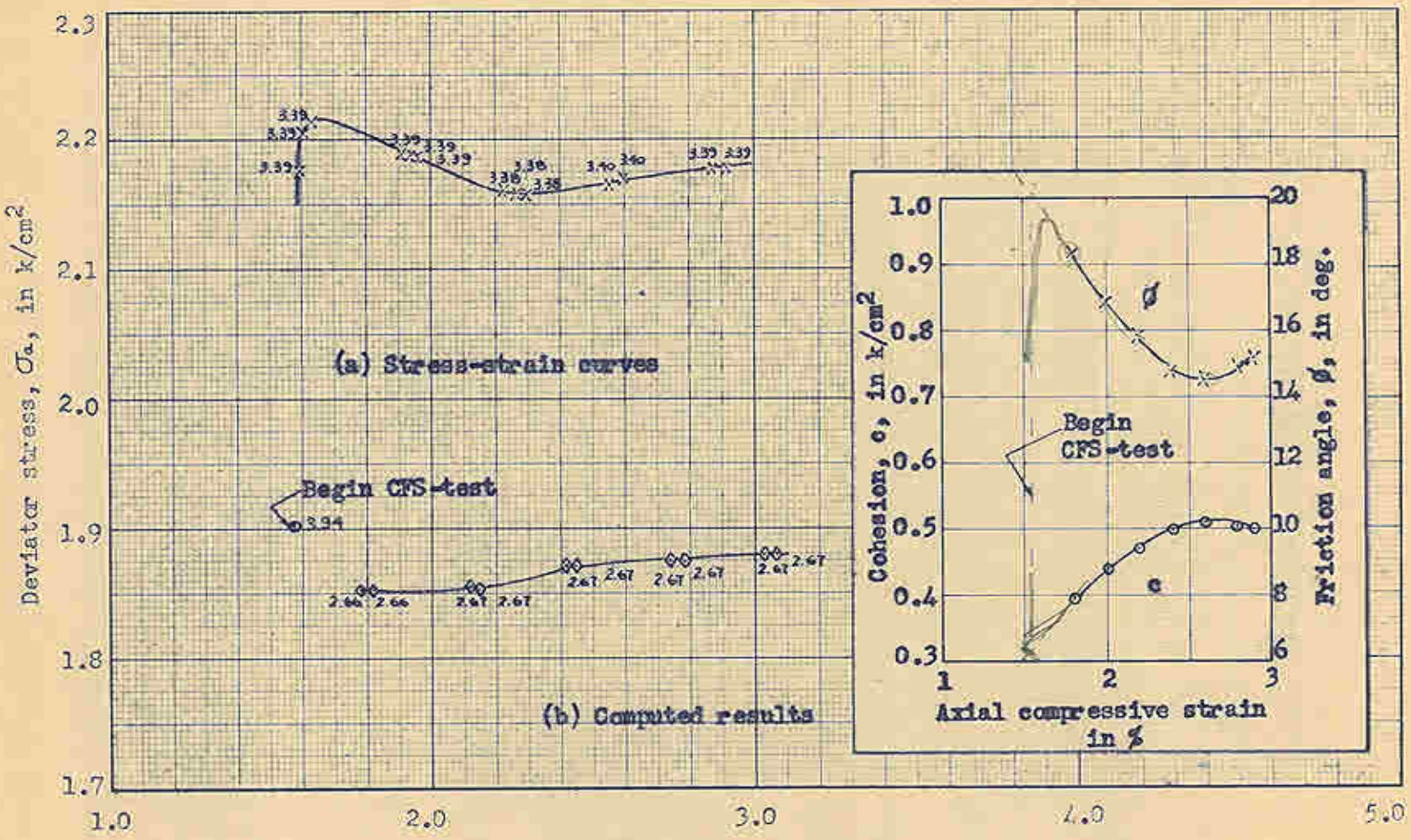

Figure 29.-CFS-test no. B-11, sample BBC 527

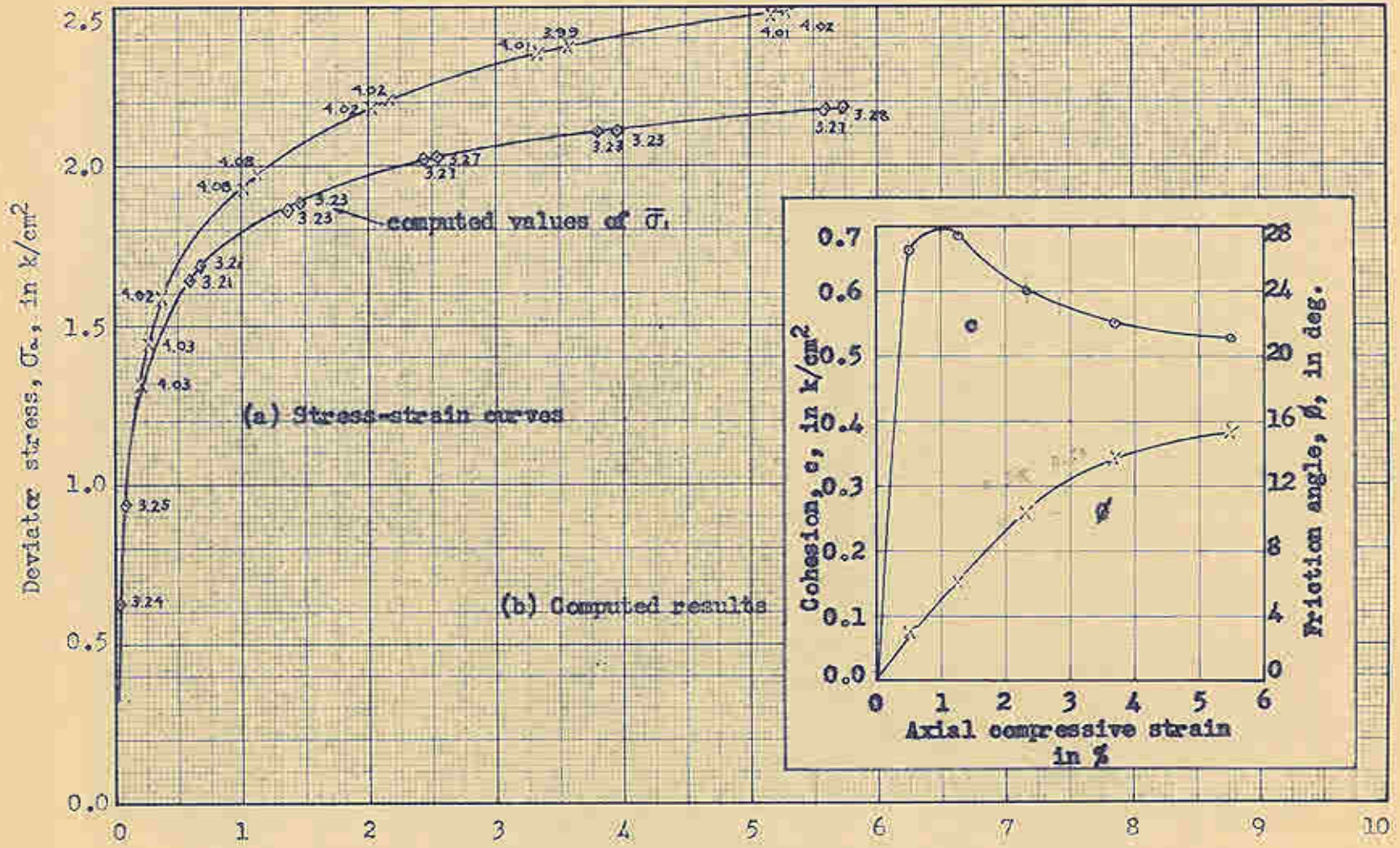

Figure 30.-CFS-test no. S-91, sample U-SBC R4

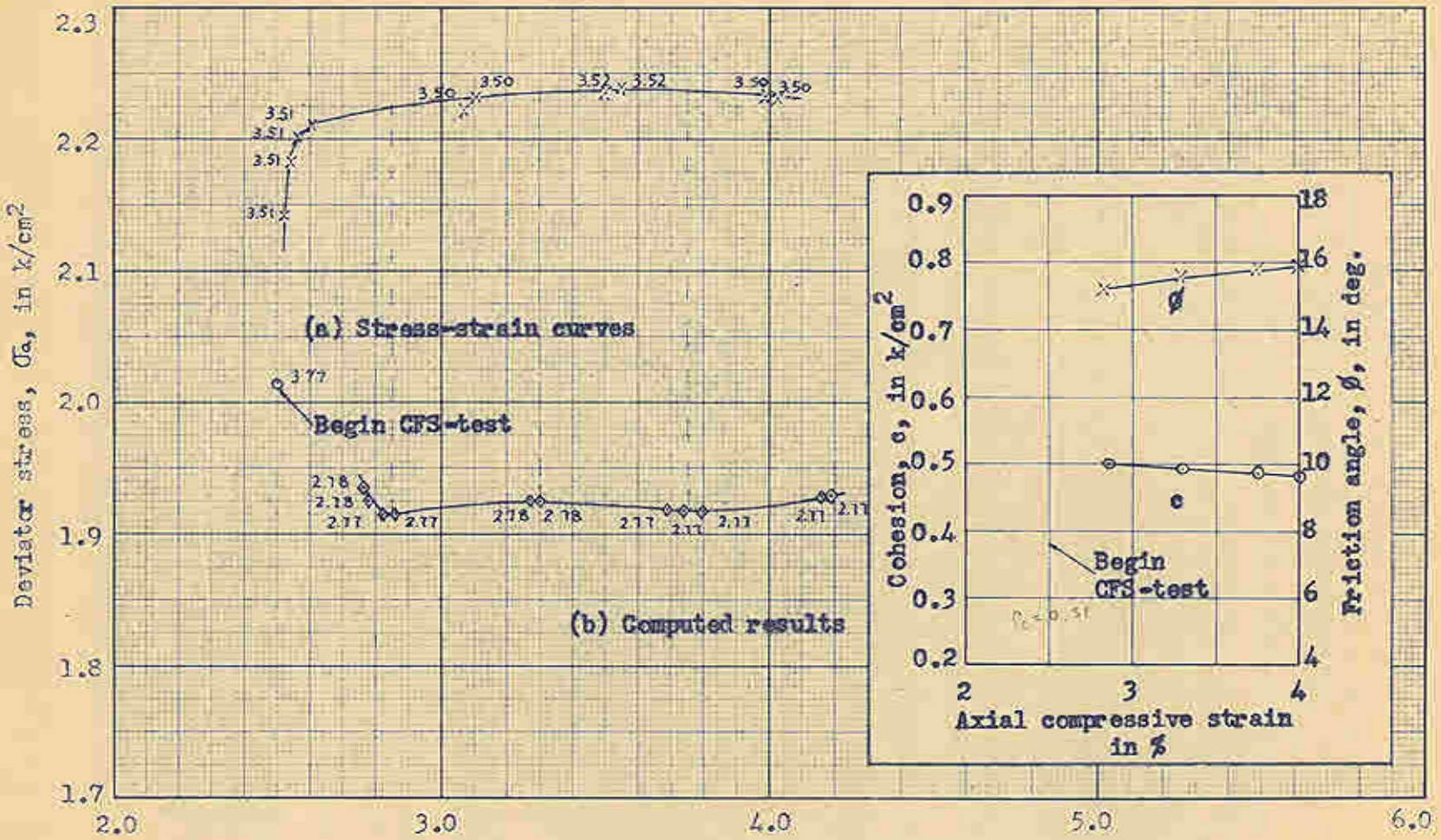

Axial compressive strain, ϵ, in %

Figure 31.-CFS-test no. B-13, sample U-BBC 32

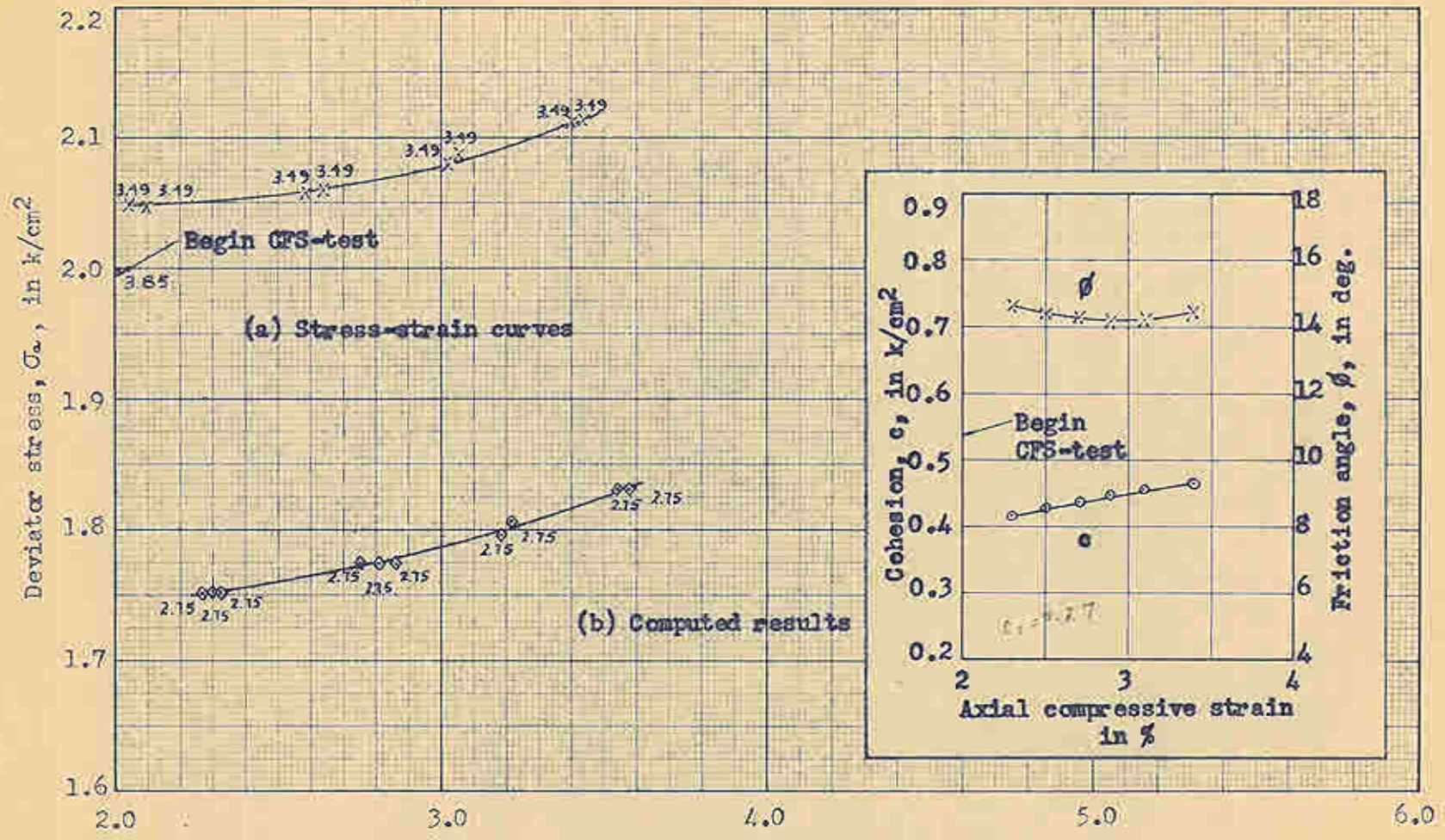

Figure 32.-CFS-test no. B-14, sample U-BRC R3

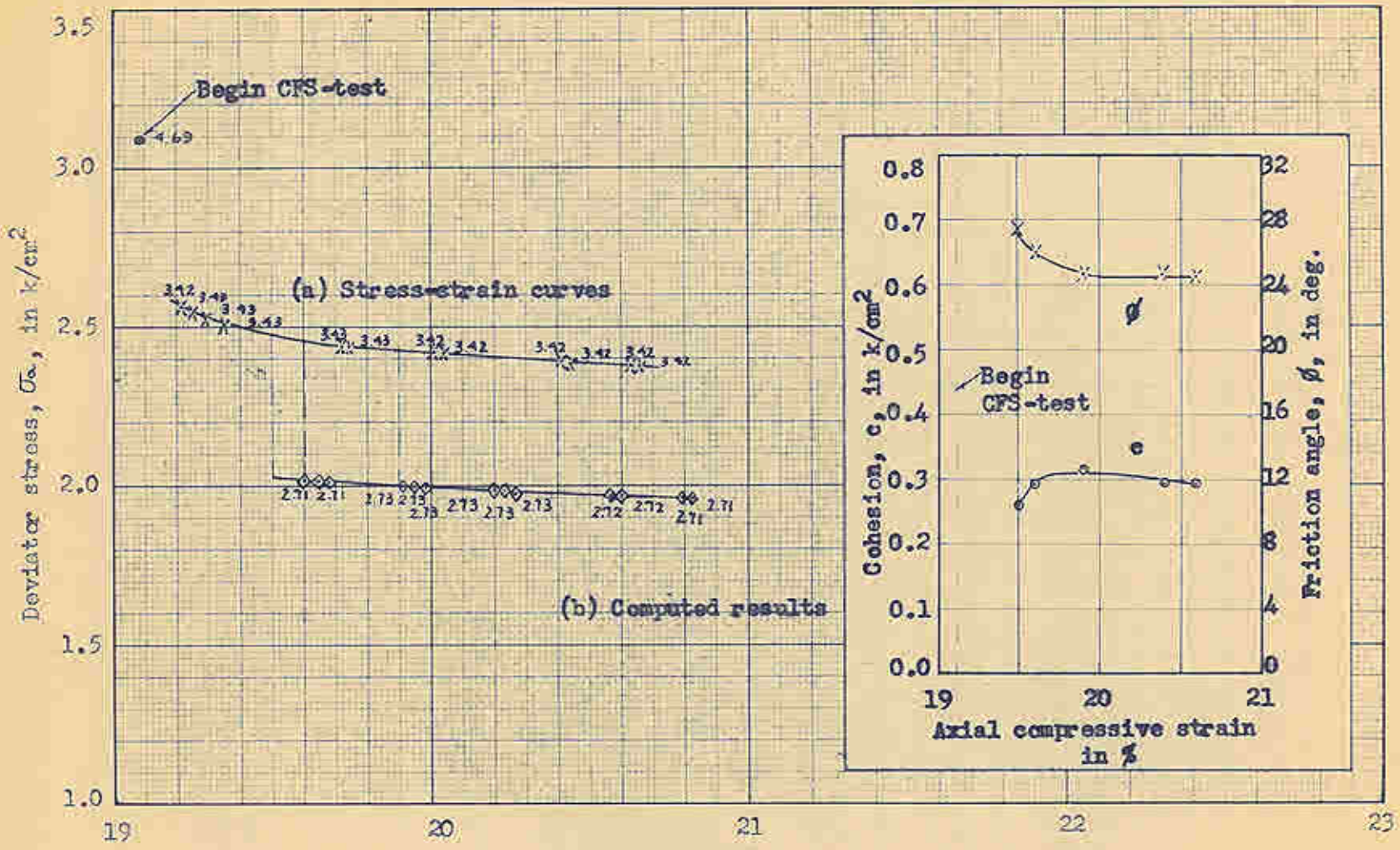

Figure 33.-CFS-test no. B-15, sample BBC 529

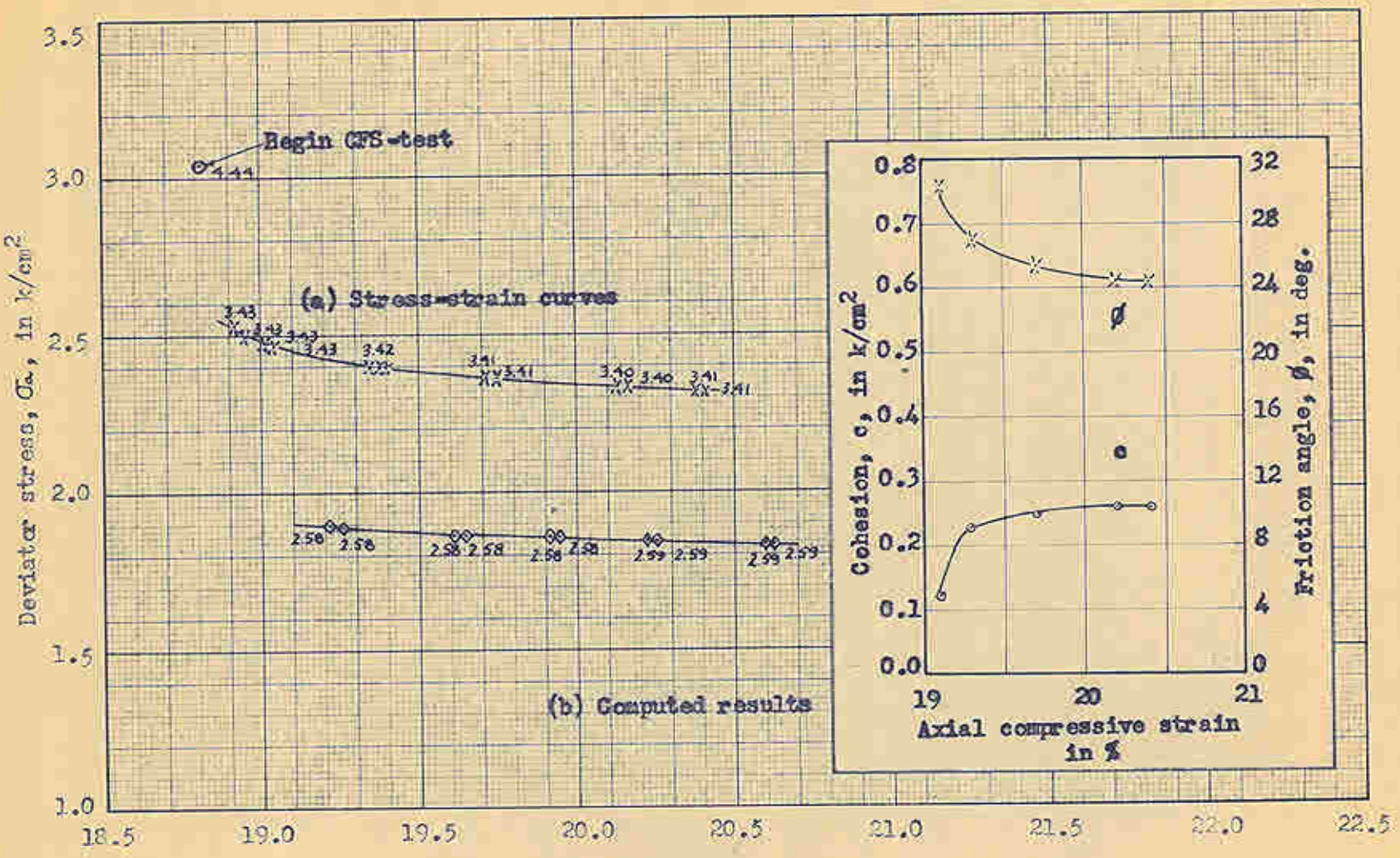

Figure 34.-CRS-test no. B-16, sample BBC 530

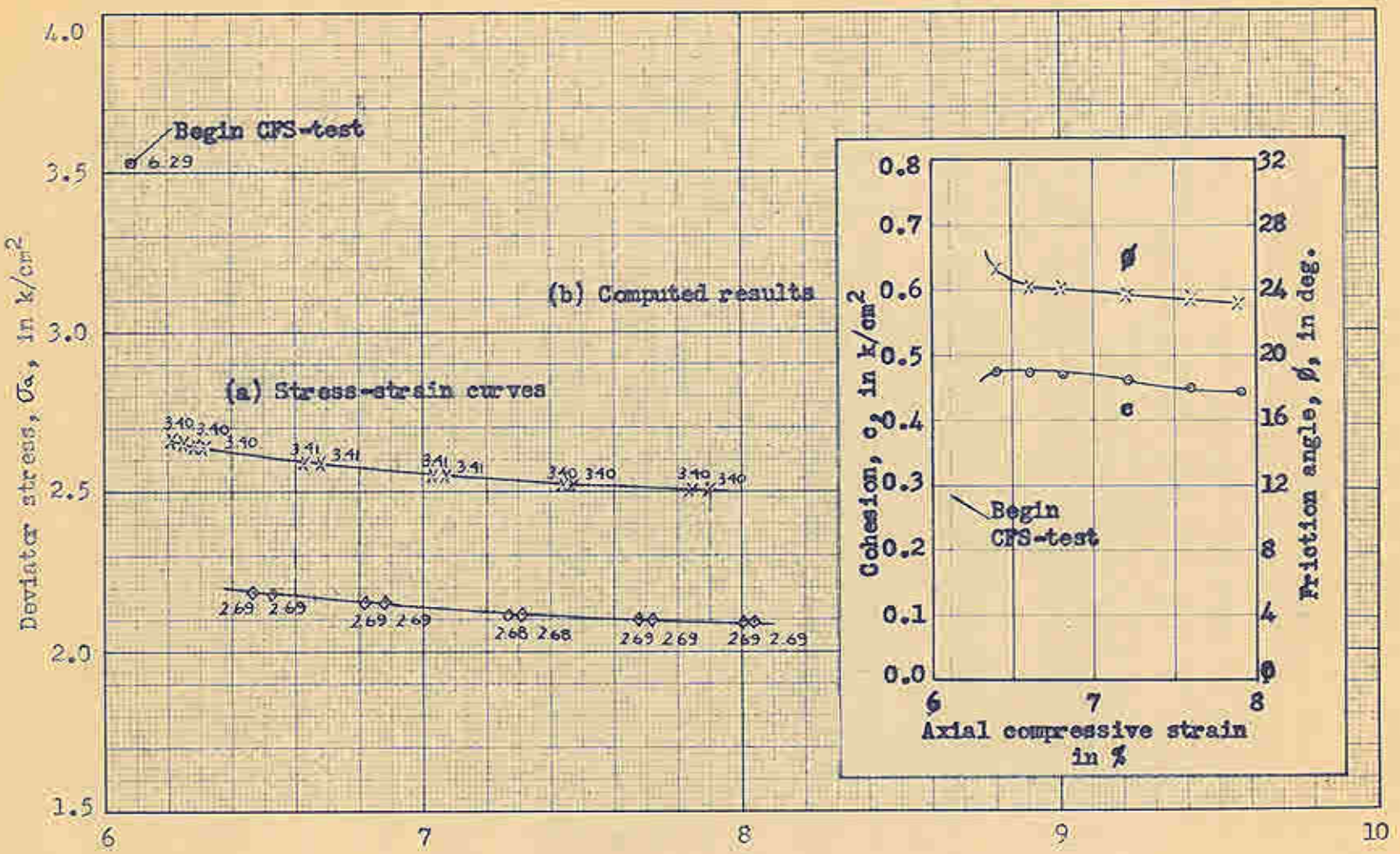

Figure 35.-CFS-test no. B-17, sample DWEPK 759

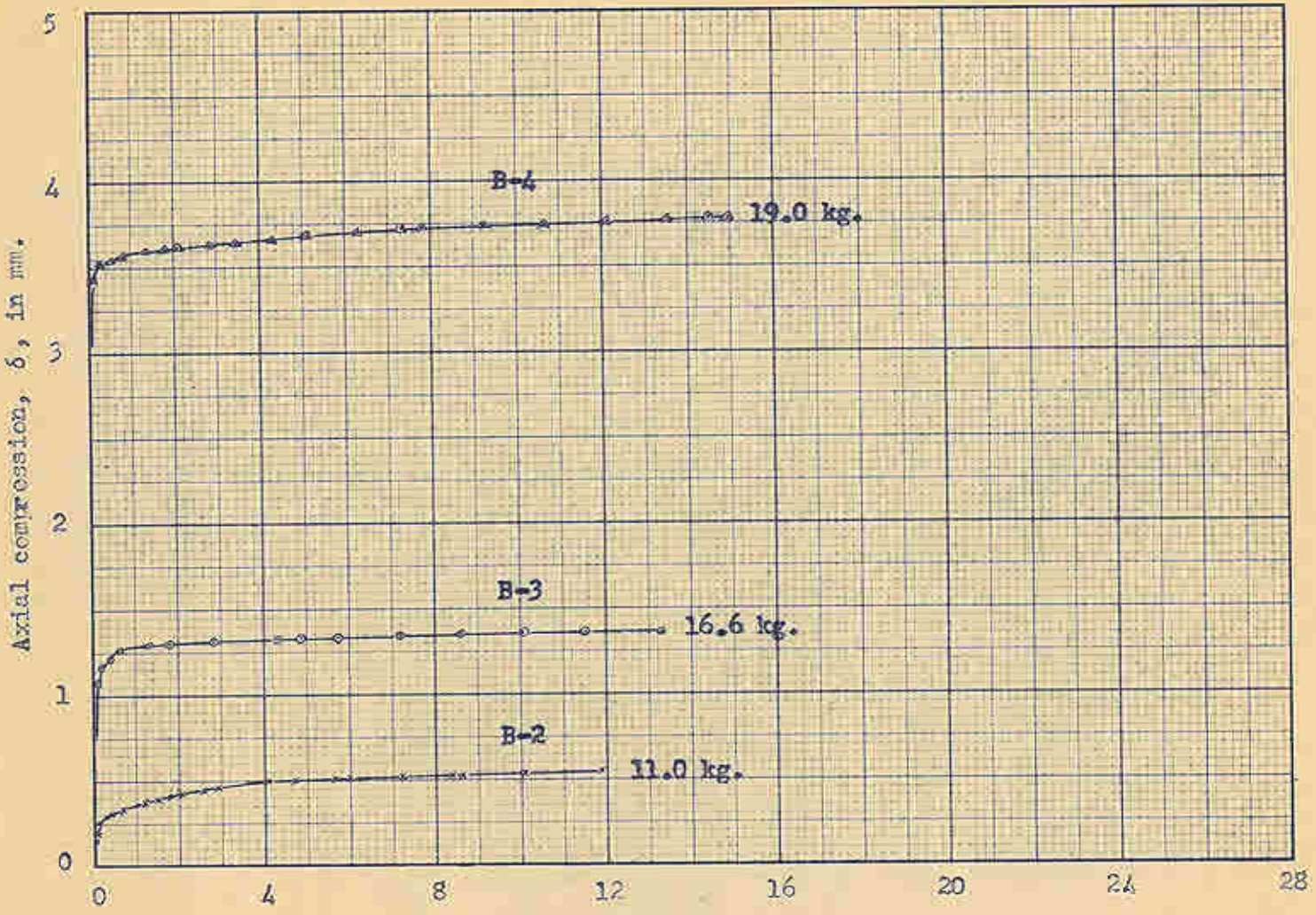

Figure 36.-Creep curves for DWEPK samples, test series A

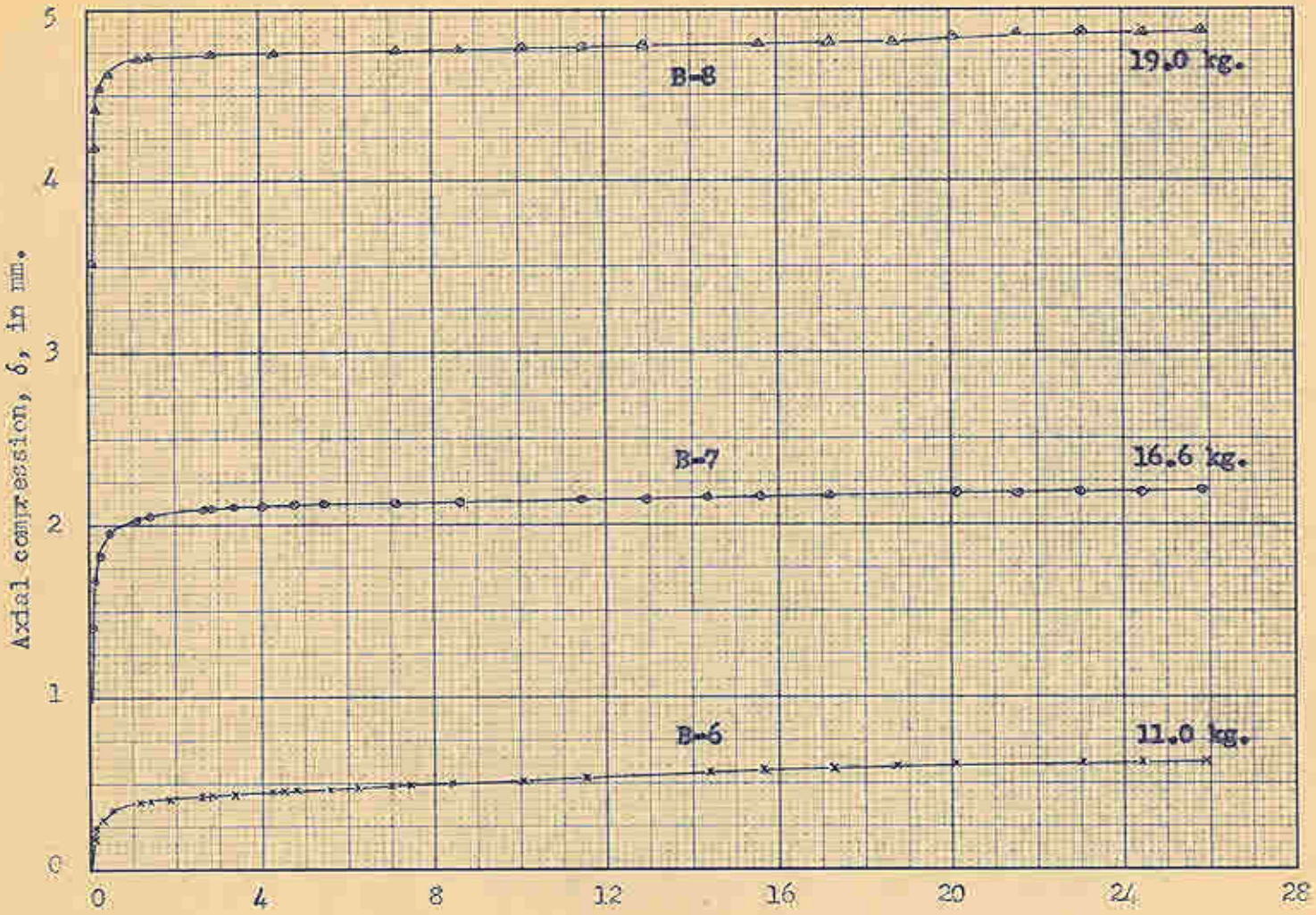

Figure 37.-Creep curves for BBC samples, test series B

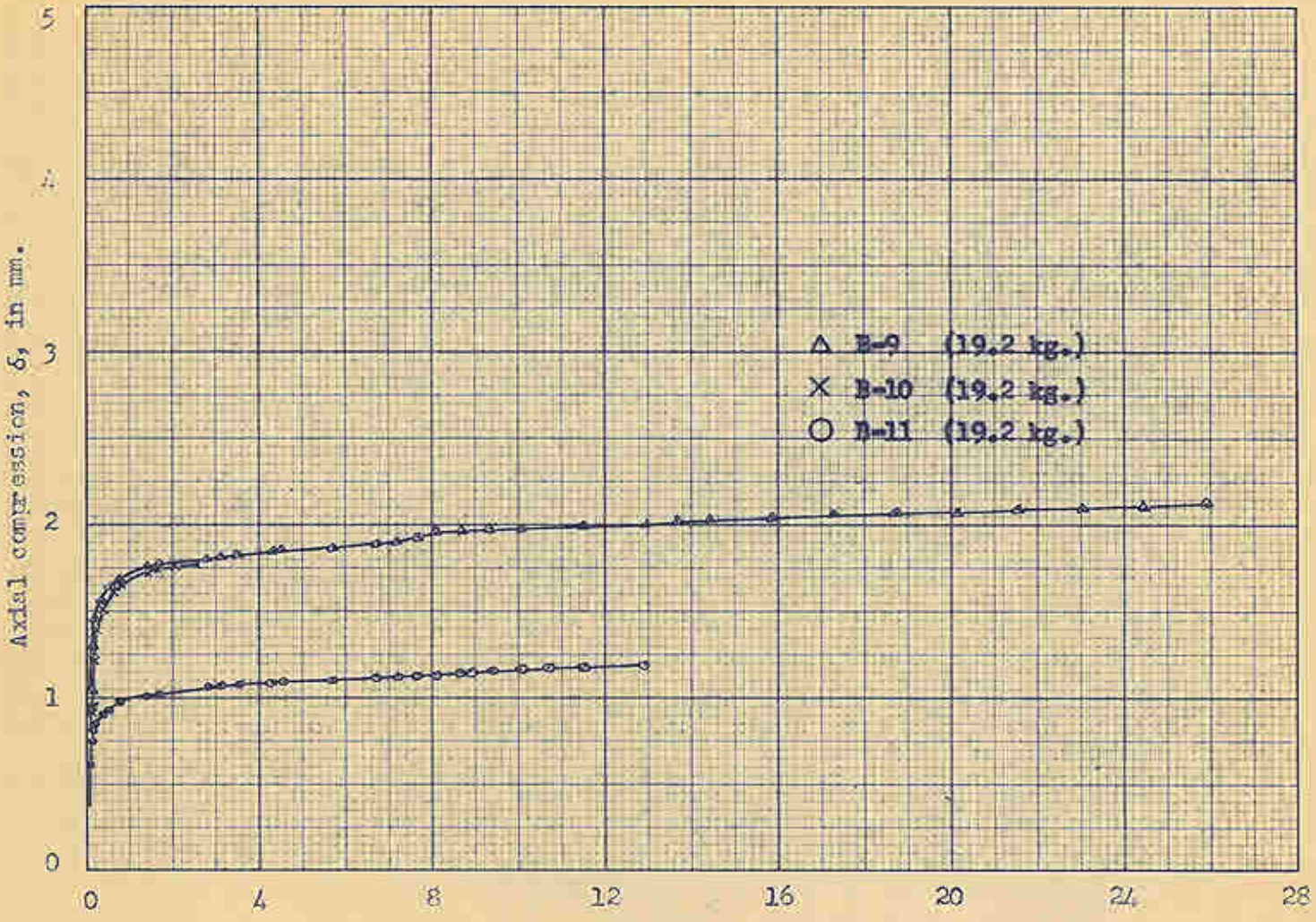

Figure 38.-Creep curves for BBC samples, test series C (t_c=6800 min.)

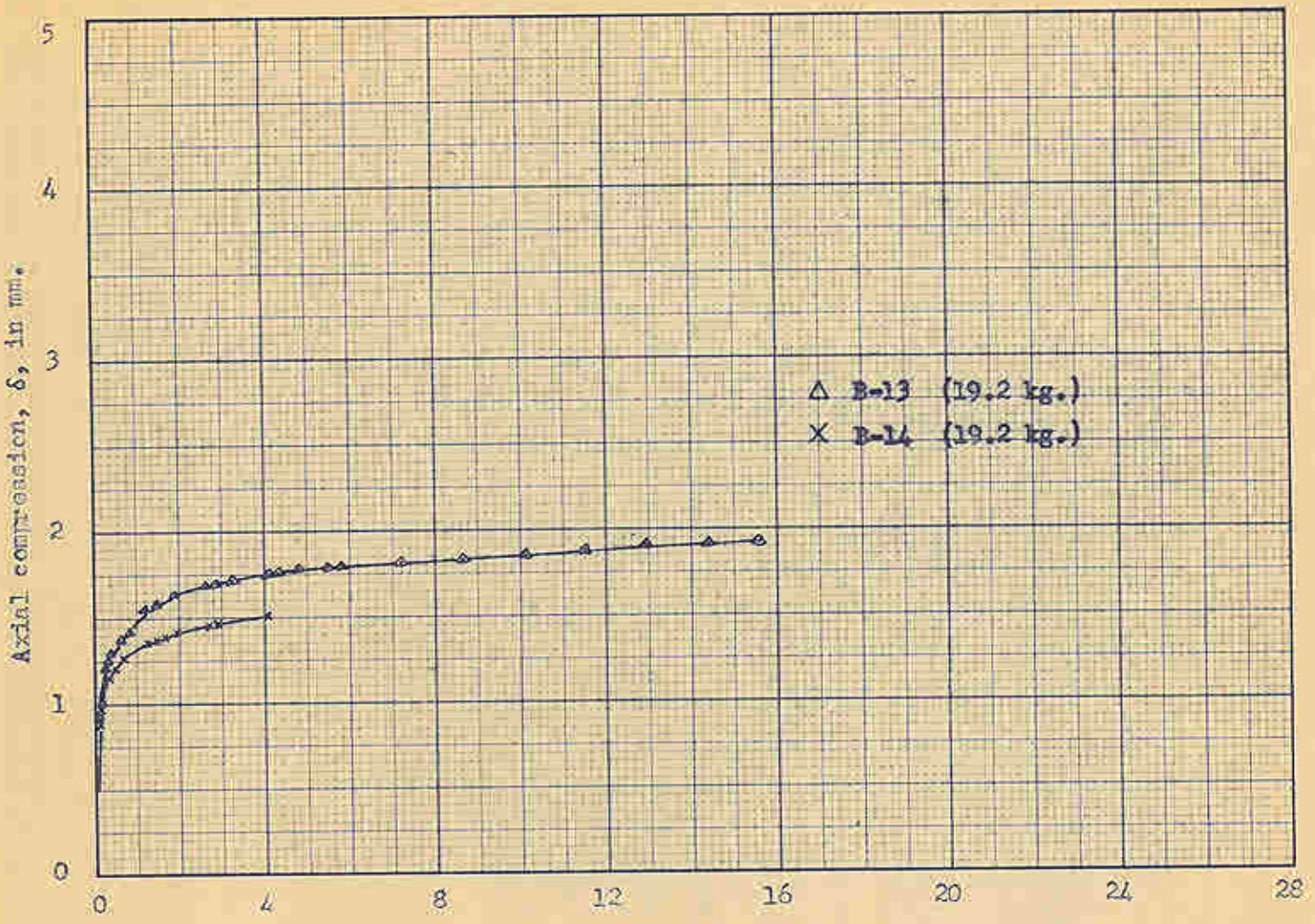

Figure 39.-Creep curves for U-BBC samples, test series D

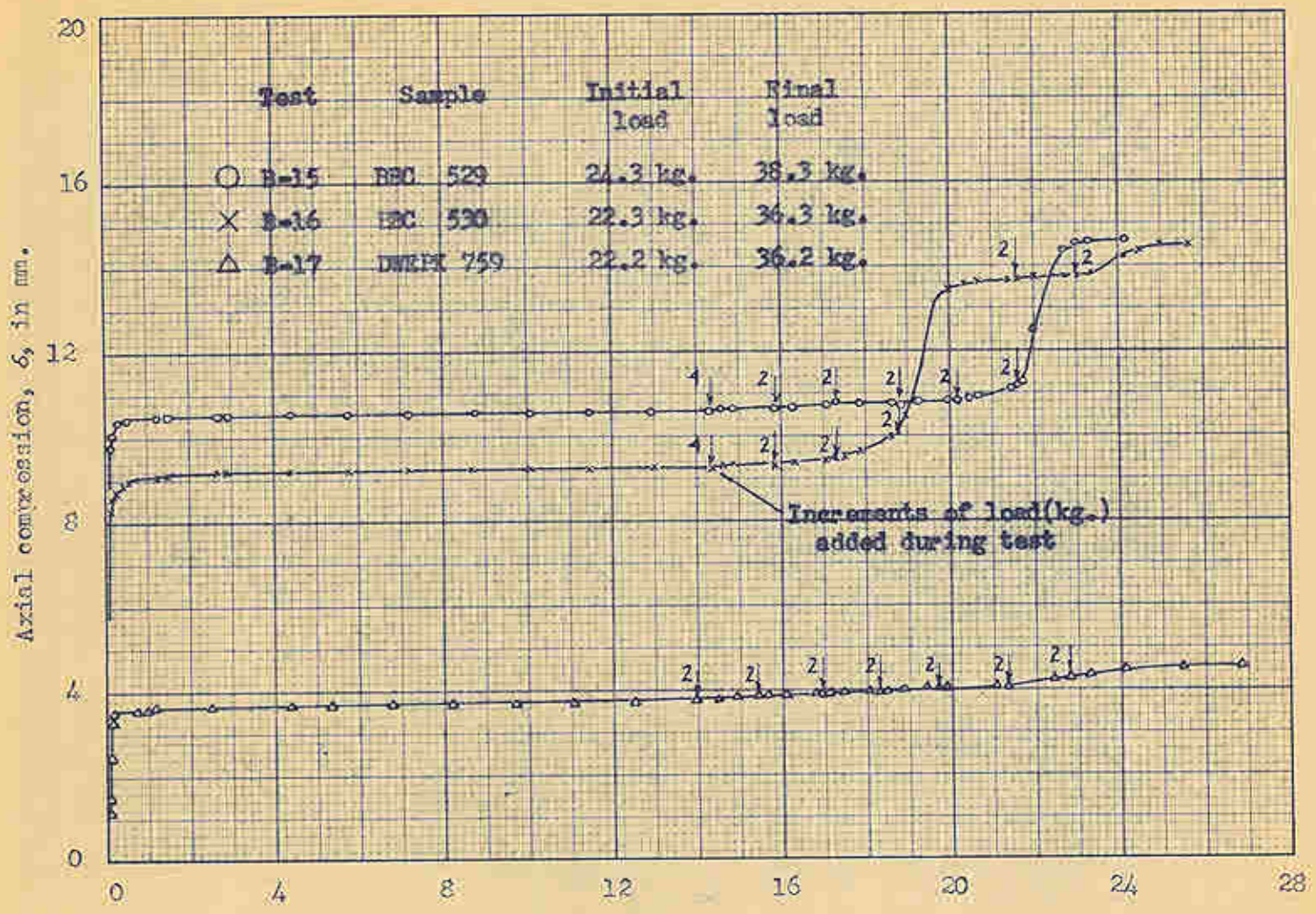

Figure 10.-Creep Curves for BBC and DWEPK samples, test series E

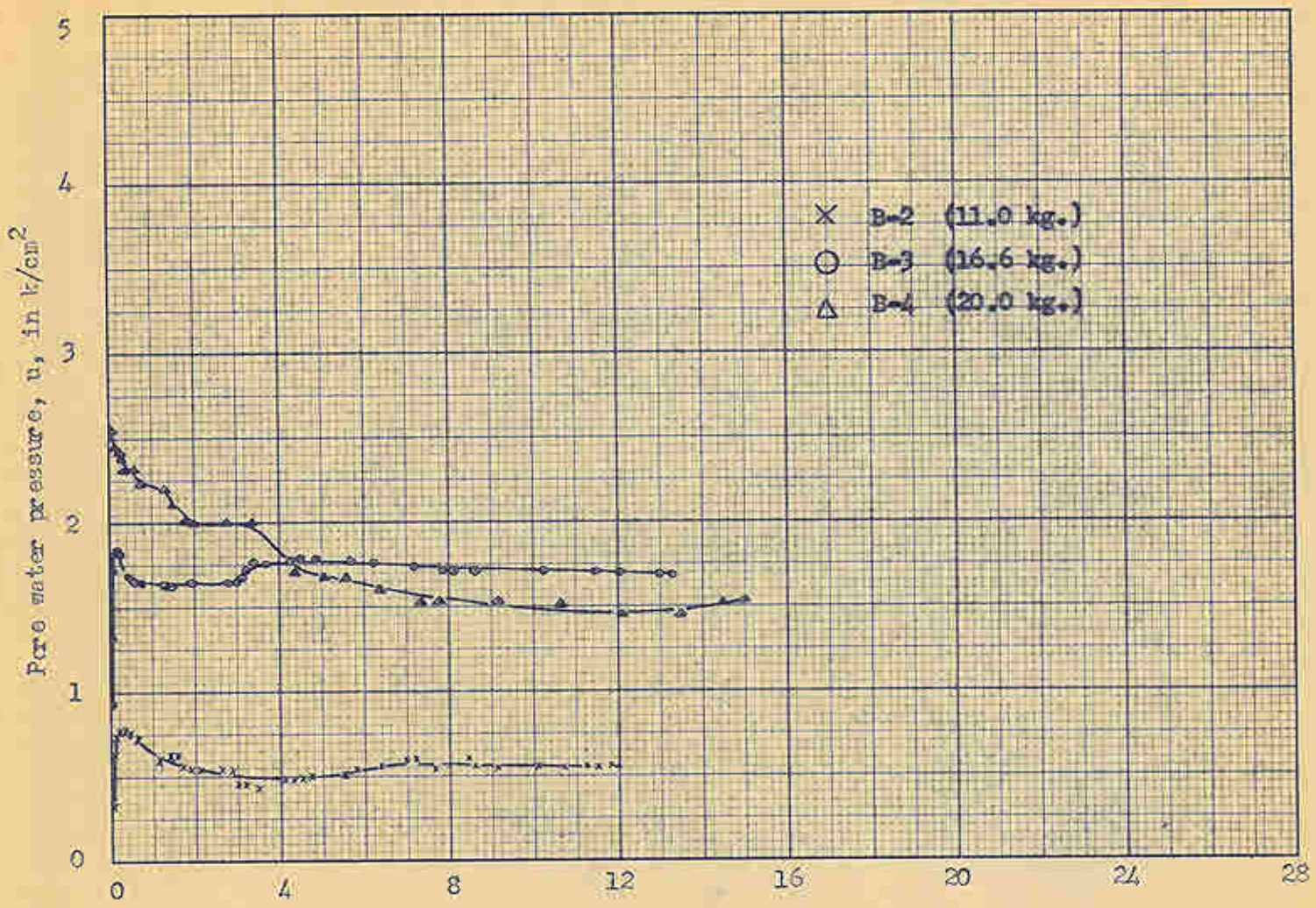

Figure 41.-Pore water pressure/time curves for DWEPK samples, test series A

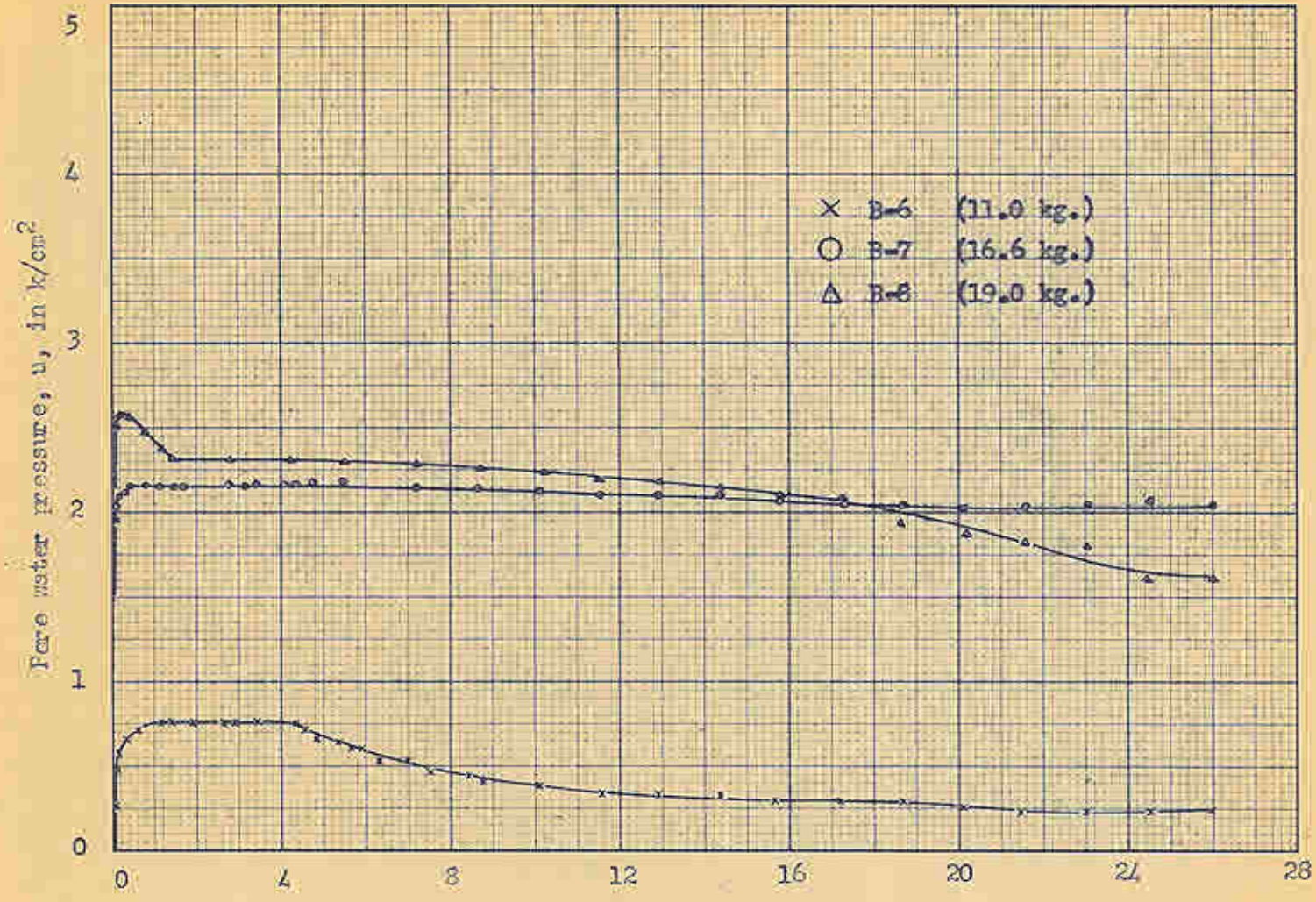

Figure 42.-Pore water pressure/time curves for BBC samples, test series B

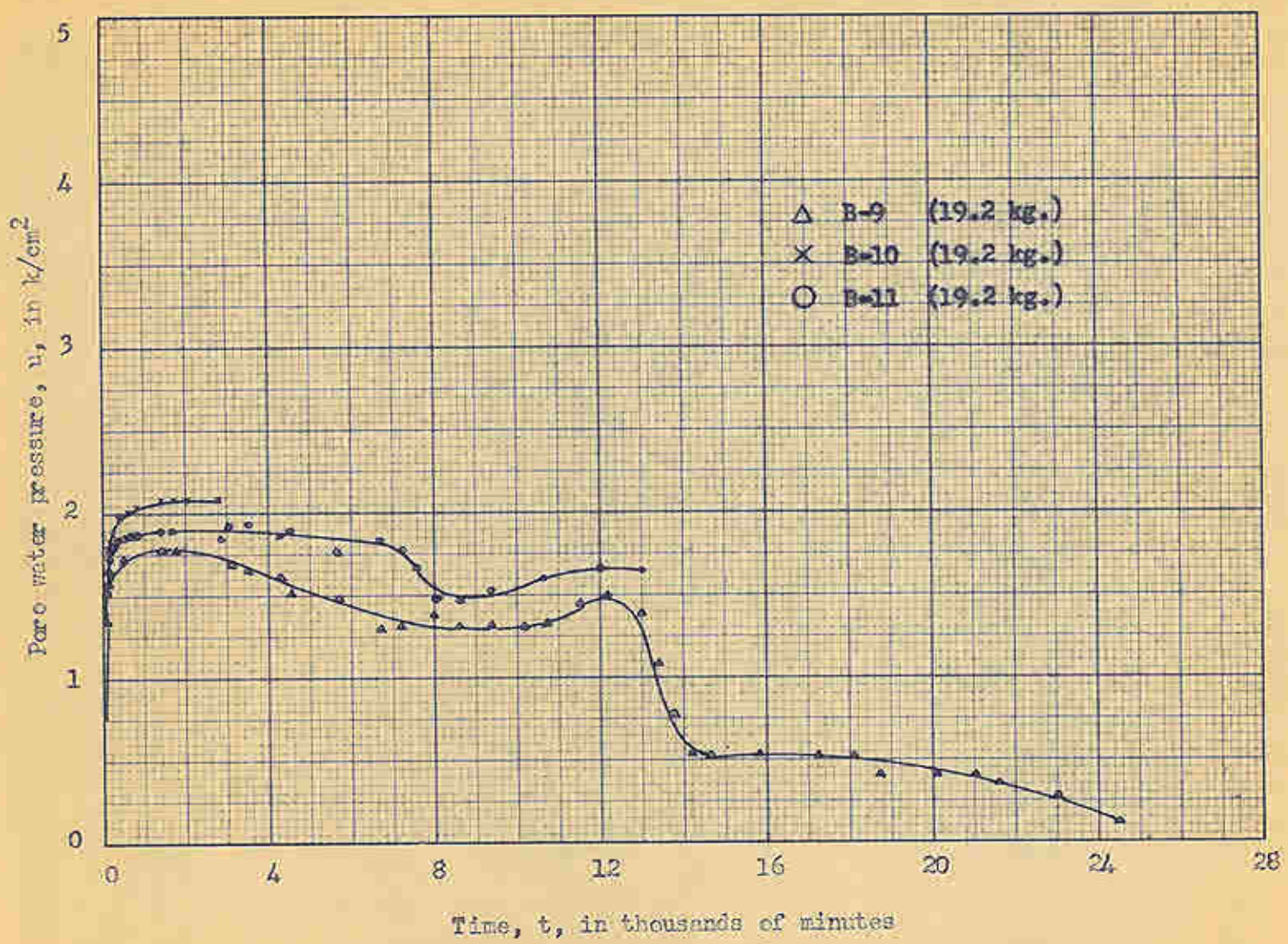

Figure 43.-Pore water pressure/time curves for BBC samples, test series C (t_c-6800 min.)

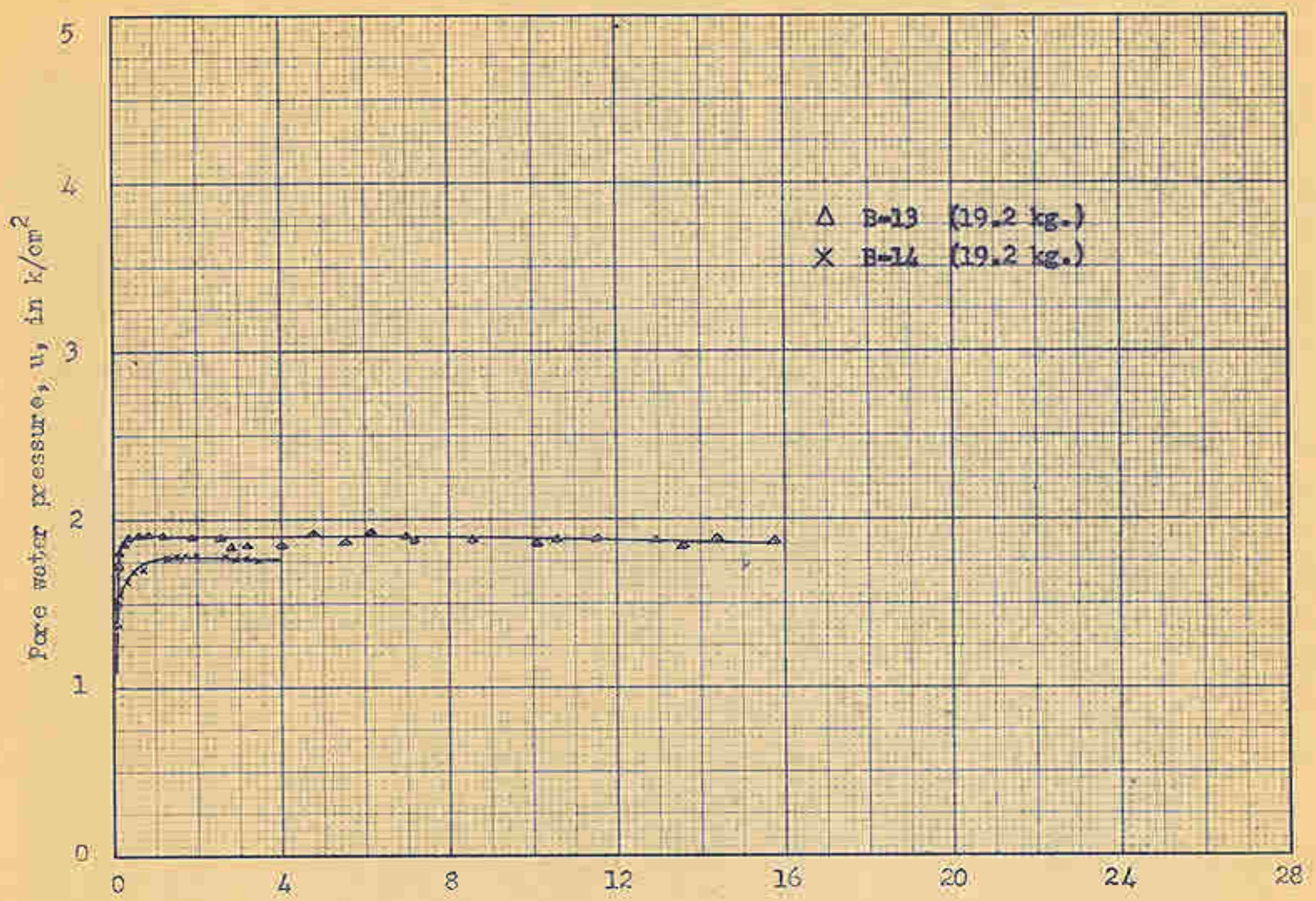

Figure 44.-Pore water pressure/time curves for U-BBC samples, test series D

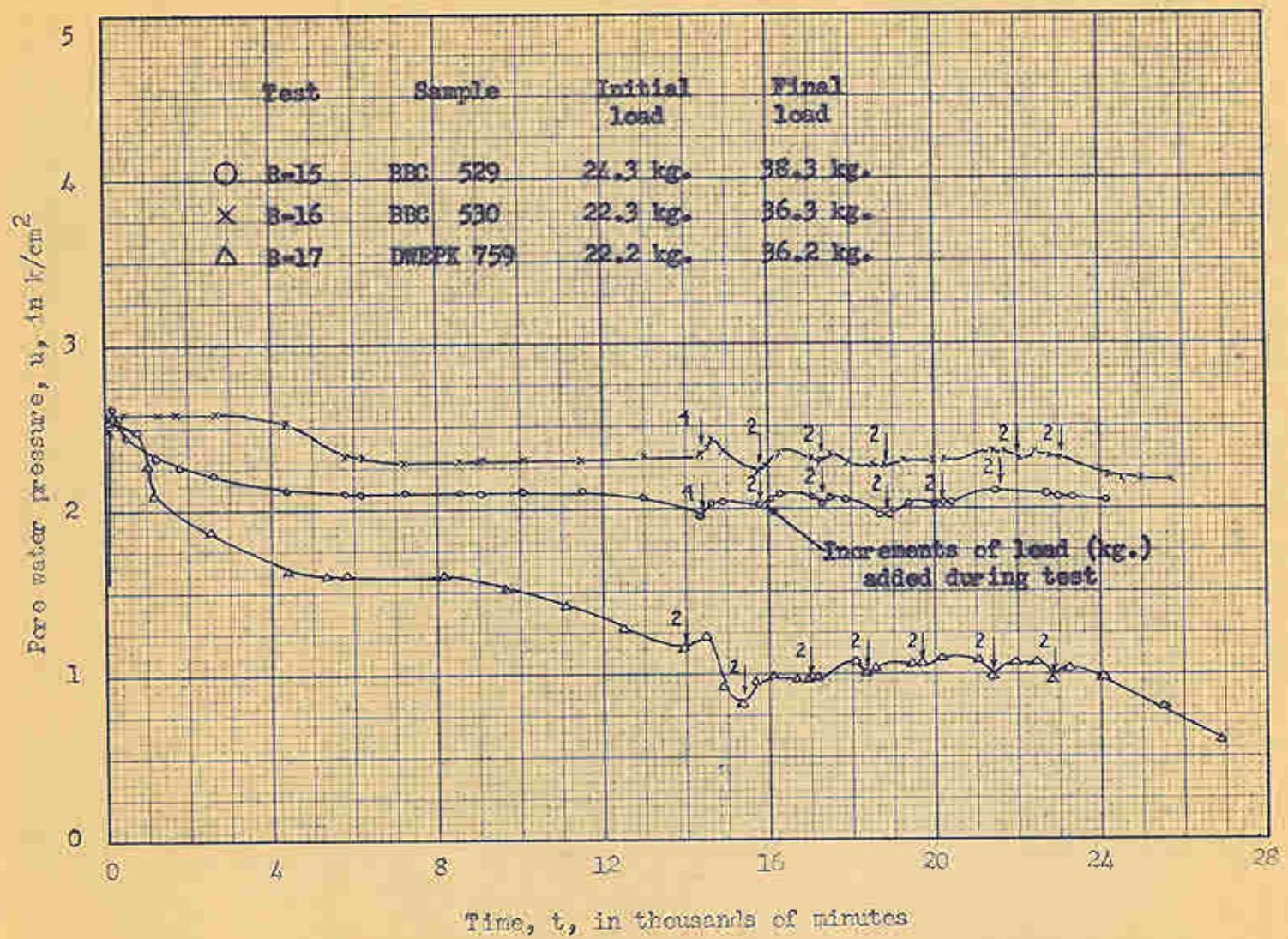

Figure 45.-Pore water pressure/time for BBC and DWEPK samples, test series E

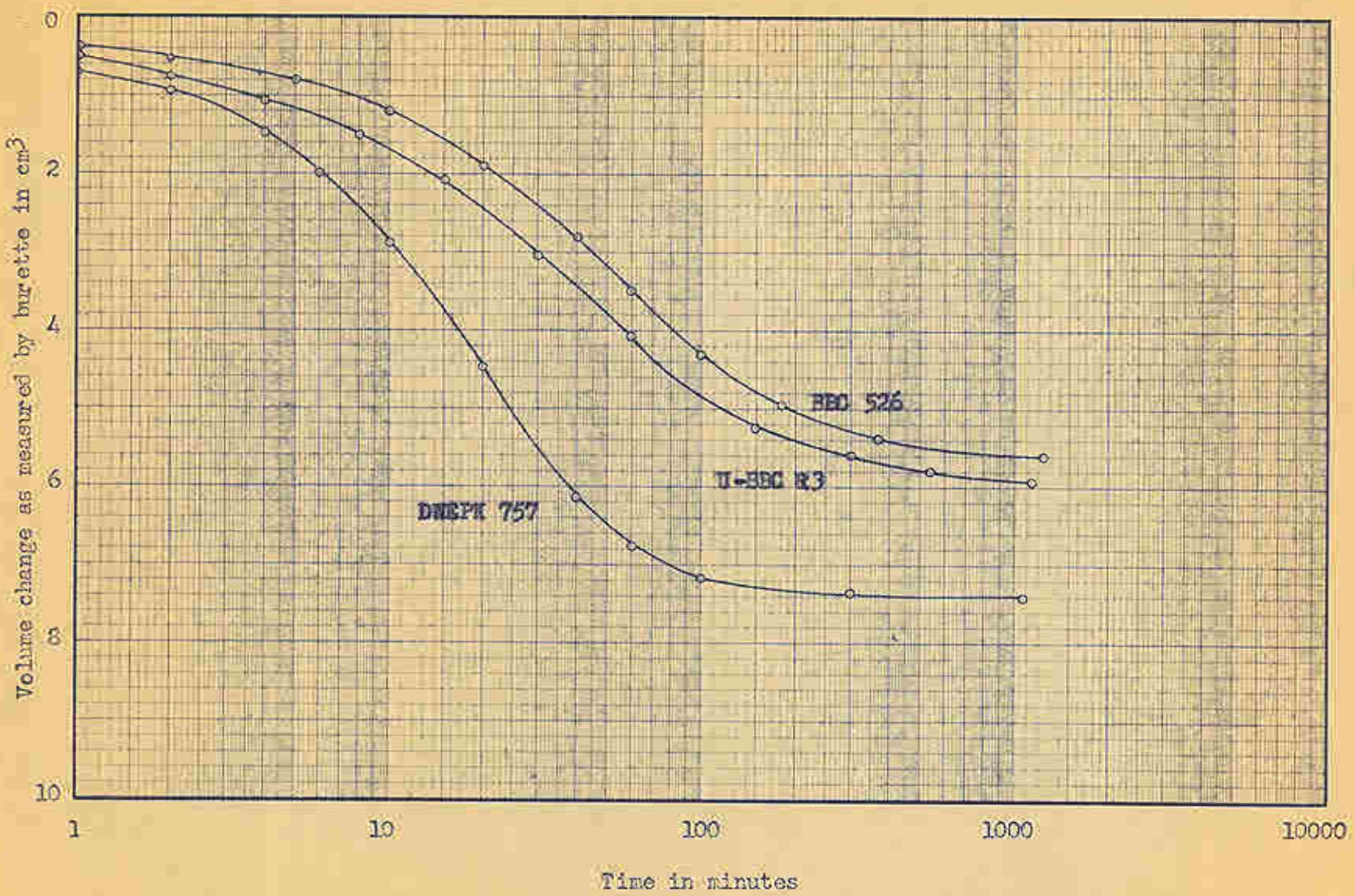

Figure 46.-Typical Hydrostatic Consolidation Curves for DWEPK, BBC, and U-BBC

BIBLIOGRAPHY

1. Andresen, A., Bjerrum, L., Dibiago, E., and Kjaersli, B. "Triaxial Equipment Developed at the Norwegian Geotechnical Institute," Norwegian Geotechnical Institute Publication No. 21, Oslo, 1957.

2. ASTM Committee. "Symposium on the Effect of Temperature on the Properties of Metals," Proceedings, ASTM, vol. 31, 1931.

3. Berger, L., and Gnaedinger, J. "Thixotropic Strength Regain of Clays," ASTM Bulletin, No. 160, 1949.

4. Bloor, E. C. "Plasticity: A Critical Survey," British Ceramic Society Transactions, vol. 56, 1957.

5. Blair, G.W.S. A Survey of General and Applied Rheology. London, 1949.

6. Casagrande, A., and Wilson, S. D. "Effect of Rate of Loading on the Strength of Clays and Shales at Constant Water Content," Harvard Soil Mechanics Series, No. 39, 1951.

7. Department of the Army. "Control of Soils in Military Construction," Technical Manual, TM 5-541, 1951.

8. Eirich, F. R. Rheology: Theory and Applications. Vol. 1, 1956.

9. Findley, W. N. "Effect of Crystallinity and Crazing, Aging, and Residual Stress on Creep of Monochlorotrifluoroethylene Canvas Laminate and Polyvinyl Chloride Respectively," Proceedings, ASTM, vol. 58, 1958.

10. Findley, W. N., and Peterson, D. B. "Prediction of Long-Time Creep With Ten-Year Creep Data on Four Plastic Laminates," Proceedings, ASTM, vol. 51, 1951.

11. Geuze, E.C.W.A., and Tan Tjong-Kie. "The Mechanical Behavior of Clays," Rheology, Proceedings of the Second International Congress on Rheology, London, 1953.

12. Haefelli, R. "Creep Problems in Soils, Snow, and Ice," Proceedings of the Third International Conference on Soil Mechanics and Foundation Engineering, vol. III, 1953.

13. Hall, J. R., Jr. "An Experimental Study of the Effect of Anisotropical Consolidation on Cohesion and Friction in Saturated Clay," unpublished master's thesis, University of Florida, June, 1960.

14. Hough, B. K. Basic Soils Engineering. New York: The Ronald Press Co., 1957.

15. Housel, W. S. "Earth Pressure on Tunnels," Transactions, ASCE vol. 108, 1943.

16. Houser, E. A., and Johnson, A. L. "Plasticity of Clays," Journal, American Ceramic Society, vol. 25, 1942.

17. Hvorslev, J. M. "Torsion Shear Tests and Their Place in the Determination of the Shearing Resistance of Soils," Harvard Soil Mechanics Series, No. 13, 1939.

18. Krynine, D. P., and Judd, W. R. Principles of Engineering Geology and Geotechnics. New York: John Wiley and Sons, 1957.

19. Lambe, T. W. "The Structure of Compacted Clay," Journal of the Soil Mechanics and Foundations Division, ASCE, May, 1958.

20. Lambe, T. W. "The Engineering Behavior of Compacted Clay," Journal of the Soil Mechanics and Foundations Division, ASCE, May, 1958.

21. Loewer, Eney, Semour, and Pascoe. "Physical Properties of Plasticized Sulfur Cements," Proceedings, ASTM, vol. 51, 1951.

22. Lommitz, C. "Linear Dissipation in Solids," Journal of Applied Physics, vol. 28, 1957.

23. Lorman, W. R. "The Theory of Concrete Creep," Proceedings, ASTM, vol. 40, 1940.

24. Macey, H. H. "Experiments on Plasticity," Transactions, The Ceramic Society, vol. 43-44, 1944.

25. Macey, H. H. "Rheology of Clay," Journal of Scientific Instruments, vol. 18, 1941.

26. Martin, J., and Yoh-Han Pao. "Creep Relaxation Relations for Styrene and Acrylic Plastics," Proceedings, ASTM, vol. 51, 1951.

27. Matlock, H., Fenske, C. A., and Dawson, R. F. "De-aired, Extruded Soil Specimens for Research and Evaluation of Test Procedures," Bulletin, ASTM, No. 177, October, 1951.

28. MacFarlane, J. W. "Effect of Structure on Secondary Compression Kaolinite," unpublished master's thesis, University of Florida, January, 1959.

29. McVetty, P. G. "The Interpretation of Creep Tests," Proceedings, ASTM, vol. 34, Part II, 1934.

30. Moore, H. F. The Creep and Fracture of Lead and Lead Alloys. New York, 1935.

31. Nadai, A. Theory of Flow and Fracture of Solids. New York: McGraw-Hill Book Co., vol. 1, 1950.

32. Nadai, A. "The Creep of Metals," Transactions, ASME, vol. 55, 1933.

33. Nadai, A. "The Phenomenon of Slip in Plastic Materials," Proceedings, ASTM, vol. 31, 1931.

34. Neville, A. M. "Theories of Creep in Concrete," Journal, ACI, vol. 27, Sept., 1955.

35. Norton, F. H. "The Flow of Ceramic Bodies at Elevated Temperatures," Journal, American Ceramic Society, vol. 19, 1936.

36. Norton, F. H. "Fundamental Study of Clay VIII: A New Theory for Plasticity of Clay-Water Masses," Journal, American Ceramic Society, vol. 31, 1948.

37. Norton, F. H., Johnson, A. L., and Lawrence, W. G. "Fundamental Study of Clay V: Nature of Water Film in Plastic Clay," Journal, American Ceramic Society, vol. 27, 1944.

38. Odqvist, F.K.G. "Recent Advances in Theories of Creep in Engineering Materials," Applied Mechanics Review, vol. 7, Dec., 1954.

39. Parker, E. F. "Creep of Metals," High Temperature Properties of Metals, American Society for Metals, 1950.

40. Partridge, J. H. "Creep of Refactory Materials," Transactions, British Ceramic Society, vol. 53, 1954.

41. Peck, R. B., Hanson, W. E., and Thornburn, T. H. Foundation Engineering. New York: John Wiley & Sons, 1957.

42. Peck, R. B., Ireland, H. I., and Teng, C. Y. "A Study of Retaining Wall Failures," Proceedings of the Second International Conference on Soil Mechanics and Foundation Engineering, vol. 3, 1948.

43. Ries, H., and Watson, T. L. Elements of Engineering Geology. New York: John Wiley & Sons, 1949.

44. Rosenqvist, I. T. "Physico-Chemical Properties of Soils: Soil Water Systems," Journal of the Soil Mechanics and Foundations Division, ASCE, April, 1959.

45. Rowe, P. W. "Hypothesis for Normally Loaded Clays at Equilibrium," Proceedings of the Fourth International Conference on Soil Mechanics and Foundation Engineering, vol. 1, 1957.

46. Russell, R., and Hanks, C. F. "Stress Strain Characteristics of Plastic Clay Masses," Journal, American Ceramic Society, vol. 25, 1942.

47. Schmertmann, J. H., and Osterberg, J. O. "An Experimental Study of the Development of Cohesion and Friction with Axial Strain in Saturated Cohesive Soils," pre-print of paper to be presented before the Conference on Shear Testing of Soils, ASCE, 1960.

48. Skempton, A. W. "The Colloidal Activity of Clays," Proceedings of the Third International Conference on Soil Mechanics and Foundation Engineering, vol. 1, 1953.

49. Soderbert, C. R. "Interpretation of Creep Tests for Machine Design," Transactions, ASME, 1936.

50. Taylor, D. W. Fundamentals of Soil Mechanics. New York: John Wiley and Sons, 1948.

51. Terzaghi, K. "Mechanics of Landslides," Application of Geology to Engineering Practice, "Berkey Volume," edited by Sidney Paige, 1950.

52. Terzaghi, K., and Peck, R. B. Soil Mechanics in Engineering Practice. New York: John Wiley & Sons, 1948.

53. Terzaghi, K. "Discussion," Proceedings of the Third International Conference on Soil Mechanics and Foundation Engineering, vol. III, 1953.

54. Terzaghi, K. "Undisturbed Clay Samples and Undisturbed Clays," Harvard Soil Mechanics Series, No. 16, 1941.

55. Terzaghi, K. "Influence of Geological Factors on Engineering Properties of Sediments," Harvard Soil Mechanics Series, No. 50, 1955.

56. Timoshenko, S. Strength of Materials. Part II, Advanced Theory and Problems, New York: D. Van Nostrand Co., 1956.

57. Tschebotarioff, G. P. Soil Mechanics, Foundations, and Earth Structures. New York: McGraw-Hill, 1956.

58. Vialov, S. S., and Skibitsky, A. M. "Rheological Processes in Frozen Soils and Dense Clays," Proceedings of the Fourth International Conference on Soil Mechanics and Foundation Engineering, vol. 1, 1957.

59. Ward, A. G., and Freeman, P. R. "Rheology of Stiff Pastes," Journal of Scientific Instruments, vol. 25, 1948.

60. Whittaker, H. "Effect of Particle Size on Plasticity of Kaolinite," Journal, American Ceramic Society, vol. 22, 1939.

61. Williamson, W. O. "Oriented Aggregation, Differential Drying Shrinkage, and Recovery from Deformation of a Kaolinite-Illite Clay," Transactions, British Ceramic Society, vol. 54, 1955.

BIOGRAPHICAL SKETCH

Robert Glenn Bea was born in Mineral Wells, Texas, January 14, 1937. He received his elementary and high school education in the public schools of Jacksonville, Florida. After graduation from Landon High School in 1954 he entered Jacksonville University and received an Associate of Arts degree in June, 1956.

He then entered the University of Florida and received the degree of Bachelor of Civil Engineering, with High Honors, in January, 1959. Following his graduation, he entered the Graduate School at the University of Florida to begin studies leading to the degree of Master of Science in Engineering, majoring in Civil Engineering.

He has worked as an engineer-in-training for the U.S. Army Corps of Engineers and as an estimator for the S. S. Jacobs Company, both of Jacksonville, Florida.

He is an Associate Member of the American Society of Civil Engineers, an EIT Member of the Florida Engineering Society, and an alumnus member of Jacksonville University. He is a member of the honorary fraternities of Sigma Tau and Phi Kappa Phi and is a charter member of Iota Pi Sigma.

While at the University of Florida he received the J. Hillis Miller Memorial Scholarship, the Rayonier Scholarship, a Graduate Research Assistantship, and a National Science Foundation Cooperative Fellowship.